3.0 How Is the Gulf Coast Climate Changing?

Lead Authors: Barry D. Keim, Thomas W. Doyle, and Virginia R. Burkett

Contributing Authors: Claudia Tebaldi, Ivor Van Heerden, S. Ahmet Binselam, Michael F. Wehner, Tamara G. Houston, and Daniel M. Beagan

The central Gulf Coast is one of warmest, wettest regions in the United States, where annual rainfall averages over 150 cm (60 inches) per year (Christopherson, 2000). Since there is very little topographic relief, changes in precipitation and runoff could have a dramatic impact on fragile Gulf Coast ecosystems and coastal communities by changing the hydroclimatology of the region. Changes in runoff are important to virtually all transportation modes in the Gulf Coast region. Interstate highways in Houston and New Orleans, for example, are occasionally flooded by locally intense rainfall, and several State and local highways are closed due to high rainfall at least once every five years. Even ports can be affected by high rainfall and runoff to shallow coastal waterways. Changes in temperature and moisture regime also are relevant to many aspects of transportation planning, construction, and maintenance. Airport runway length requirements, for example, are determined by mean maximum temperature for the hottest month of the year. As the climate and sea surface warm, we can anticipate an increase in the intensity of hurricanes making landfall along the Gulf of Mexico coastline. As the ocean warms and ice sheets decline, sea level rise is likely to accelerate, which has serious implications for the Gulf Coast region where much of the land is sinking (subsiding) due to local geological processes and human development activity.

This chapter summarizes the direct and indirect effects of climate change that are most likely to affect transportation in the Gulf Coast region. The key climate "drivers" examined in the study region are:

- Temperature;
- Precipitation;
- Sea level rise; and
- Hurricanes and less intense tropical storms.

The interactive effects of these drivers, coupled with ongoing environmental processes in the region, are discussed in the following sections. This chapter presents scenarios of future climate change in addition to analysis of historical trends. While the environmental trend information for the study area is compiled from region-specific data sources, a regional model of future climate was not available for the Gulf Coast study area. One

approach that is widely used to identify plausible changes in climate at a regional scale is to extract output from general circulation models run at a global scale. This approach was used in this study and is described in the following sections of the report. Specific implications of the scenarios of future climate for each mode of transportation are discussed in the subsequent chapter of this report.

Intended Use of Climate and Emissions Scenarios in the Context of This Report

A "scenario" is a plausible description of possible future conditions and is generally developed to inform decision making under uncertainty. Building and using scenarios can help people explore what the future might look like and the likely challenges of living in it (Shell International, 2003). Scenarios are distinct from assessments, models, and similar decision-support activities, although they can provide important inputs to these activities. Scenarios also can be distinguished from precise statements about future conditions, which may be referred to as "forecasts" or "predictions." Compared to these, scenarios tend to presume lower predictive confidence, because they pertain to processes for which weaker causal understanding or longer time horizons increase uncertainties (Parson et al., 2007).

Climate scenarios describe potential future climate conditions and are used to inform decision making relative to adaptation and mitigation. Scenarios can be constructed for higher order aspects of climate change and its impacts, such as future changes in sea level, drought and storm intensity, or vegetation distribution. Scenarios of relative sea level rise, for example, in a subsequent section of this report were constructed by combining climate-change scenarios with information about coastal subsidence and other specific regional characteristics. The climate and sea level rise scenarios discussed in this report identify plausible potential future conditions for the Gulf Coast region. They are intended to frame the analysis of potential risks and vulnerability within the transportation sector.

The Earth's climate is determined, in part, by the concentration of atmospheric greenhouse gases and particulates that absorb infrared radiation (heat) reflected from the Earth's surface. Human activity is increasing greenhouse gas and particulate emissions, which has resulted in an increase in the Earth's temperature (Intergovernmental Panel on Climate Change [IPCC], 2001, 2007). In order to assess how the climate may change in the future, future emissions must be specified. The Intergovernmental Panel on Climate Change (IPCC) has conducted three exercises to generate scenarios of 21st century greenhouse-gas emissions, the most recent being the IPCC Special Report on Emissions Scenarios (SRES) (Nakicenovic and Swart, 2000). To explore the potential effects on transportation, we selected a range of emissions futures from the SRES report, including the low-emissions B1 scenario, the mid-range A1B scenario, and the high-emissions A2 scenario. The AIFI scenario, which assumes the highest reliance on fossil fuels during this century, also was added to the SRES scenarios used to assess the effects of sea level rise.

The SRES A1B scenario assumes a balance across all energy sources, meaning it does not rely too heavily on any one particular source, including fossil fuels. It is, therefore, based on the assumption that improvement rates apply to all energy sources and end-use technologies. The A2 scenario assumes that economic development is primarily regionally

oriented and that per capita economic growth and technological change are more fragmented and slower than for the other emission scenarios. The B1 scenario assumes a high level of social and environmental awareness with an eye toward sustainability. It includes an increase in resource efficiency and diffusion of cleaner technologies (IPCC, 2001). These three emission scenarios are among the six "marker/illustrative scenarios" selected for climate model simulations in the IPCC's Third and Fourth Assessment Reports (IPCC, 2001, 2007) (figure 3.1). The B1 scenario lies at the lower extreme end of the potential changes in atmospheric CO_2 concentrations during this century, while the A1B emission scenario is considered a middle-of-the-range scenario in terms of the hypothesized rate of greenhouse gas emissions. The A2 scenario is among the higher end of the SRES scenarios in terms of both CO_2 and SO_2 emissions. The influence of SRES emission scenarios on global temperature simulations is presented in table 3.1.

3.1 Temperature, Precipitation, and Runoff

The climate of the study area is influenced by remote global factors, including the El Niño Southern Oscillation, and regional factors such as solar insolation. Due to the influence of the nearby Gulf of Mexico, the region is warmer and moister than most other continental regions at this latitude. Rainfall across the study area has little seasonality, with slightly higher rainfall values in spring and summer relative to fall and winter. The region enjoys mild winters, which are occasionally interrupted by cold air masses extending far south from the northern pacific or the Arctic, which brings low temperatures and freezing conditions. Rainfall in the region is dependent upon a variety of processes, including frontal passages in the winter and spring (Twilley et al., 2001). Short-lived, unorganized thunderstorms fueled by afternoon heating and moisture are common in the study area and associated, in part, with a prominent sea/land breeze (Ahijevych et al., 2003).

The Gulf Coast, like much of the world, has experienced significant changes in climate over the past century. With continued increases in atmospheric greenhouse gases and their radiative forcing, the Earth's climate is expected to change even more rapidly during the 21st century (IPCC, 2007). Computer-based climate simulation models are used to study the present climate and its responses to past perturbations like variation in the sun's output or major volcanic eruptions. They also are used to assess how the future climate would change under any specified scenario of greenhouse-gas emissions or other human activity (Parson et al., 2007).

3.1.1 Historical Data Sources

Changes in the historical climatology of the study area were investigated from an empirical perspective relying on instrumental records. The assessment of the present climate and 20th-century trends was built around climatic data from the United States Climate Division Datasets (CDD) (Guttman and Quayle, 1996) and the United States Historical Climate Network (USHCN) (Karl et al., 1990; Easterling et al., 1996). Since CDD were used in a portion of this analysis, caution needs to be taken with data from 1905 to 1930, which are

synthesized from statewide data as described by Guttman and Quayle (1996) and therefore are not true averages of data from within a climate division.

Empirical trends and variability were analyzed for temperature and precipitation at the CDD level for the climate divisions along the Gulf Coast from Galveston, TX, to Mobile, AL, including Texas Climate Division 8, Louisiana Divisions 6-9, Mississippi Division 10, and Alabama Division 8 (figure 3.2).

Keim and others (2003) showed that CDD can have spurious temperature trends. Our analysis synthesized CDD consisting of averages of stations within each division from the USHCN (table 3.2). The Filnet data have undergone numerous quality assurances and adjustments to best characterize the actual variability in climate. These adjustments take into consideration the validity of extreme outliers, time of observation bias (Karl et al., 1986), changes in instrumentation (Quayle et al., 1991), random relocations of stations (Karl and Williams, 1987), and urban warming biases (Karl et al., 1988). Furthermore, missing data were estimated from surrounding stations to produce a nearly continuous dataset for each station.

Monthly averages from the USHCN stations from 1905 to 2003 within each climate division were then averaged annually, thereby constructing an alternative "divisional data" annual time series. The year 1905 was selected as a starting point because it represents a common period of record for all but one of the USHCN stations utilized in the study – the exception is Fairhope, AL, beginning in 1919. Fairhope was maintained because it is the only USHCN station available in Alabama Climate Division 8. Only USHCN FILNET stations with a continuous monthly record of temperature from January 1905 through December 2003 were included in the analysis, with the exception of Fairhope. USHCN precipitation data were not as serially complete as temperature, and there were fewer stations available. As a result, this study incorporated the original CDD for precipitation, which seems reasonable given results of Keim and others (2005).

3.1.2 General Circulation Model Applications for the Study Area

The scenarios of future climate referenced in this report were extracted from an ensemble of up to 21 different atmosphere-ocean general circulation model (GCM) efforts, which contributed the results of their simulations in support of the IPCC's Fourth Assessment Report, and are labeled "Coupled Model Intercomparison Project 3" (CMIP3). Gridded output limited to the study area was extracted from each GCM. Figure 3.3 shows the study region and the boundaries used to subset the global grid of a typical GCM output. Results are presented as spatial averages across the entire area. The GCMs were run under three forcings, the low-emissions B1, the high-emissions A2, and the mid-range A1B scenarios from the IPCC's SRES (Nakicenovic and Swart, 2000).

Scenarios of future temperature and precipitation change for the middle of the 21st century were derived from the regional GCM runs. Scatter diagrams were produced to convey the range of output of the models with respect to present conditions following the procedures of Ruosteenoja et al. (2003) (figure 3.4). Probability density (or distribution) functions

(PDF) were developed by applying the method of Tebaldi and others (2004, 2005). Data forming the basis of the PDF estimation is an ensemble of historical and future climate simulations (from which temperature and precipitation are extracted). Output of temperature and precipitation (averaged for area l and seasonal fluctuations) from up to 21 different GCMs under the three different scenarios was considered for two 20-year periods, one representative of recent climatology (1980-1999) and one representative of the future mid-century time slice (2040-2059). Thus scenarios of "climate change" are to be interpreted with respect to these two time periods and conditional on the SRES A1B, A2, and B1 scenarios (Nakicenovic and Swart, 2000). While the results from the GCM runs are indeed plausible, they should be interpreted as mid-, high-, and low-range results, respectively, among the SRES scenarios of the potential changes in temperature and precipitation.

The statistical procedure synthesizes the multimodel ensemble of projections into a continuous PDF by applying a Bayesian method of estimation. At the core of the method is the idea that both observed and modeled temperature and precipitation contribute information to the estimate, so that different models will be differently "weighted" in the final probabilistic projections on the basis of their differential skill in reproducing observed climate. The method used also considered the convergence of different models when producing future trajectories, rewarding models that agree with one another and downweighting outliers. In the version of the statistical procedure applied here, the latter criterion is discounted, ensuring that even model projections that disagree with the consensus inform the shape of the final PDFs. This choice is made as a result of two considerations: the ensemble of GCMs at our disposal is not made of independent models (there are components and algorithms in common, for example), so rewarding agreement is somewhat questionable when one can argue that the agreement is not independently created. The second consideration has to do with the width of the PDFs produced, since enforcing the convergence criterion has the effect of narrowing the width of the PDFs to a range even smaller than the original ensemble range. It is well understood that the range of uncertainty addressed by this particular ensemble of models is limited when compared to the whole range of sources of uncertainty that can be listed, when examining climate change projections. Thus we preferred to produce conservative estimates of the uncertainty (i.e., larger rather than smaller). The result of applying the statistical analysis to the GCM output are PDFs of temperature and precipitation change (the latter as absolute values or percent change with respect to historical precipitation averages) from which any percentile can be derived.

3.1.3 Water-Balance Model

The primary tool used to investigate the hydroclimatology of the study area was a modified Thornthwaite Water Balance Model as described by Dingman (2002). The Thornthwaite model is simply an accounting of hydroclimatological inputs and outputs. Monthly values of temperature, precipitation, and potential evapotranspiration – called reference evapotranspiration – were entered into the budget, and parameters such as rain/snow ratios, soil moisture, soil moisture deficits, and runoff were calculated. The water balance was

modified slightly by using an alternative reference evapotranspiration (ETo) term than that originally used by Thornthwaite to provide a better estimate of ETo in the central Gulf Coast region. As with any monthly water balance, atmospheric and terrestrial variables (such as ET_o, soil moisture, runoff, etc.) were parameterized by using bulk terms. A description of the procedures used to estimate evapotranspiration, soil moisture, and other components of the water balance model are presented in appendix D.

3.1.4 Temperature and Runoff Trends

Results from our analysis of temperature variability during 1905 to 2003 indicate that the 1920s or 1930s was generally the warmest decade for the various Gulf Coast climate divisions (figure 3.5). After a step down in the temperature in the late 1950s, the coolest period occurs in the 1960s, while a warming trend is evident for all seven climate divisions beginning in the 1970s and extending through 2003. Of the seven climate divisions, LA6, LA8, and MS10 have slight but significant cooling trends at an $\alpha \leq .05$ over the 98-year period of record. Precipitation variability shows that the 1940s and 1990s were the wettest decades, while the 1950s was generally the driest (figure 3.6). Although all of the climate divisions at least suggest long-term patterns of increasing rainfall, only MS10 and AL8 have trends that are significant at an $\alpha \leq .05$.

Data for each of the seven climate divisions were amalgamated into a regional dataset, by month, and the continuous monthly water balance model was run. In a typical year, ET_o is low in winter and early spring, and most rainfall is converted to runoff because soil moisture storage remains at, or near, capacity. As temperatures rise in late spring and early summer and the number of hours of daylight increases, ET_o also increases. Evapotranspiration will often exceed rainfall in July, August, and September, which leads to soil moisture utilization, on the average. Then in late fall, precipitation often exceeds ET_o leading to recharge of soil moisture. Regional trends in model-derived runoff shows large inter-annual variability with the high values in the 1940s and from 1975 to 2003 (figure 3.7). Despite the variability, a long-term trend was detected in the data at an $\alpha \leq .05$, and the trend line indicates a 36 percent increase in runoff over the time period. Moisture deficits show high values from the mid-1940s through the mid-1960s, with 1998 to 2000 also high (figure 3.7) but without any long-term trends during that period.

Historical monthly extremes of precipitation, runoff, and deficit in the Gulf Coast Region were analyzed to provide a focus for this portion of the analysis. In the empirical record, there is some evidence of an increase in precipitation extremes in the United States and in the Gulf south. Karl et al. (1995) shows that one-day extreme rainfall events have increased in portions of the United States, and Keim (1997) shows heavy rainfall events have increased in the south-central United States. These heavy rainfall events have very likely contributed the increases in runoff found in this study.

The period 1971 to 2000 serves as the baseline climatology for this analysis. Using water balance output for this 30-year period, partial duration series (PDS) are generated for the three variables. A PDS includes the number of events (monthly extremes) equal to the number of years under examination, which is 30 in this case. As such, the 30 largest

monthly totals of precipitation, runoff, and deficit were extracted and then fit to the beta-p distribution, as recommended by Wilks (1993), and the 2-, 5-, 10-, 25-, 50-, and 100-year quantile estimates are determined for each. These data serve as a baseline for assessing potential future changes in extremes of precipitation, runoff, and deficit.

3.1.5 General Circulation Model Results and Future Climate Scenarios

To explore how the regional climate may change over the next 50 years, output from an ensemble of GCM runs used by IPCC for the Fourth Assessment Report (2007) was analyzed. Scatterplots and probability density functions of average temperature and precipitation change were derived from the GCM ensemble output for the IPCC SRES greenhouse gas emissions scenarios labeled A1B, A2, and B1. The results presented in the following discussion are based on GCMs (table 3.3) that contributed runs to the IPCC archive used in the IPCC's Fourth Assessment Report and are consistent with the temperature and precipitation projections reflected in IPCC Fourth Assessment Report (2007).

The GCM results run with the A1B, A2, and B1 emissions scenarios suggest a warmer Gulf Coast region, with the greatest increase in temperature occurring in summer and lowest increases in winter (tables 3.4, 3.6, and 3.8). This is consistent with another analysis of historical data that shows a significant increase in summer minimum temperature across the Gulf Coast study area between 1950 and 2002 (Groisman et al., 2004).

Although the climate model output for the A1B, A2, and B1 emissions scenarios demonstrate a large degree of similarity, the A1B scenario was retained for more detailed analysis since it is considered "mid-range" of the IPCC emissions scenarios. Also, we note that the major differences in CO_2 concentrations under the IPCC SRES scenarios occur after 2040 (figure 3.1), which helps explain why temperature and precipitation do not vary widely among the GCM experiments with the high-, low-, and mid-range emissions scenarios (tables 3.4 to 3.9). Stated another way, the climate scenarios presented in these tables are not likely to change significantly during the next three to four decades by mitigation measures that would reduce emissions, although mitigation measures could substantially affect the climate in the latter half of this century. Probability density functions for seasonal temperature and precipitation change through 2050 are presented in figures 3.8 and 3.9, respectively.

Hourly or daily precipitation extremes cannot be reliably simulated by current GCM experiments. The percentiles (i.e., the 5th, 50th, and 95th percentiles) from the A1B PDFs were used as a proxy for assessing potential changes to hydrological extremes across the region. These percentiles stretch the range of output from all 21 GCMs, while also providing the middle of the PDF, or region under the curve where there is most agreement between the models (i.e., 50th percentile). The 1971-2000 temperature and precipitation data therefore were modified seasonally according to the predicted changes presented in tables 3.5, 3.7, and 3.9 for each of the three quartiles. The water-balance model was then rerun using the three quartile datasets to simulate the hydrology under these altered climate

conditions. These datasets provided the means necessary to produce new PDS of precipitation, runoff, and deficit for additional extreme value statistical testing.

The 2-, 5-, 10-, 25-, 50-, and 100-year return periods for mean monthly precipitation show only modest differences between the current climate and the projected climate in 2050 at the three PDF percentiles (figure 3.10). As expected, there is a decrease in monthly precipitation extremes at the 5th percentile for the less rare return periods (2- to 25-year), relative to the current climate, which would be expected given the reduction in precipitation by up to 36 percent in summer. However, given the shape of the beta-p distribution, the 100-year precipitation event is slightly larger than the baseline. Results for the 50th percentile indicate that the less rare return periods are on par with current climate patterns, but that the rare return periods may have modestly larger storms. At the 95th percentile, storms are generally larger across the board.

Monthly runoff extremes show a very different relationship to the current climate. At both the 5th and 50th percentiles, there is a dramatic reduction in projected runoff (figure 3.11). The mid-range of the GCMs suggests a decline in runoff relative to the 1971-2000 baseline period. Runoff rates are lower because precipitation is somewhat reduced, but perhaps more importantly, the projected increases in temperature also lead to increases in potential and actual evapotranspiration, and evapotranspiration rates are highest in the Gulf and southeastern United States compared to other regions (Hanson, 1991). An increase in actual evapotranspiration, without any increase in precipitation, translates into a reduction in runoff rates. However, at the 95th percentile, precipitation increases anywhere from 9 to 26 percent, depending on season.

Extremes in monthly deficit show a more complex pattern between the quartiles and over the various return periods (figure 3.12). The 5th percentile shows much larger deficits occurring relative to the 1971-2000 baseline. This is especially relevant at the two-year return period, which is nearly 30 percent larger in magnitude/intensity than in the current climate. This observation makes sense because as temperatures become somewhat warmer, thereby increasing potential evapotranspiration, there also are substantial reductions in precipitation. The net effect of this combination would be an increase in deficits (and drought intensity). Smaller reductions in precipitation at the 50th percentile dampen the increases in deficits. At the 95th percentile, increases in temperature are more than offset by the dramatic increases in precipitation, with deficits substantially reduced in their intensity.

3.1.6 Changes in Daily Temperature

To examine trends in extreme temperature for the study area, daily maximum temperature, and minimum temperature were analyzed from 1950 through 2005. The historical analysis presented uses a dataset and tools developed for an analysis of North American extremes based on the daily data set from the USHCN (National Oceanic and Atmospheric Administration [NOAA], 2006). Temperature indices of transportation sensitive parameters were created on a station basis and then averaged together. For localized analyses, anomalies of the indices for all stations within 500 km of the target location were

averaged together. For the U.S. time series, anomalies of station-level indices were first averaged into 2.5° latitude by 2.5° longitude grid boxes. Where a grid box did not have any stations, the values of the indices from neighboring grid boxes were interpolated into that grid box in order to make the averaging area more spatially representative. The grid box values were then averaged on an area-weighted basis to create U.S. time series. The time series figures show the annual values and a smoothed line derived from a locally weighted regression (Lowess filter; Cleveland et al., 1988). An advantage of a Lowess filter is that it is not impacted very much by one extreme annual value that might occur in an El Niño year, and therefore it depicts the underlying long-term changes quite well.

The number of very hot days has been increasing on average across the United States. Figure 3.13 shows the average change since 1950 in the warmest 10 percent of July maximum and minimum temperatures at each station. The positive trend in minimum temperatures implies significantly warmer nights. The maximum temperature decreased after a period of south-central U.S. droughts in the 1950s and has been increasing ever since.

Temperature trends across the Gulf States region are not as pronounced as they are nationally due to the moderating effect of the proximate Gulf of Mexico waters. Figure 3.14 shows the anomaly in the number of days above 100 °F averaged over stations within 500 km of Dallas, TX. Although centered outside the Gulf States region considered in this report, many of the stations are well within it, and this figure is certainly representative of the behavior of Gulf States extreme temperatures in the recent past. Note the cooling following the 1950s droughts. Also, note that the magnitude of interannual variations is considerably larger than any trend.

Notwithstanding this absence of a detectible trend in the number of days exceeding a high threshold temperature, it is very likely that in the future the number of very hot days will substantially increase. Figure 3.15 shows a prediction of the average number of days exceeding 37.8 °C (100 °F) in the June-July-August (JJA) season 25 years, 50 years, and 90 years into the future under the SRES A2 scenario for Houston, TX, the closest station to Galveston, TX, with available data. The algorithm used for this prediction exploits current observations as well as predictions of the JJA average temperature from 17 of the climate models contained in the WGNE-CMIP3 database prepared for the IPCC Fourth Assessment Report. Twenty-five years from now, the probability of a week (although not necessarily continuous) of 37.8 °C temperatures in this region is greater than 50 percent. Fifty years from now, the overall heating is such that the probability of three weeks of 37.8 °C temperatures is greater than 50 percent. Note that results obtained under either the B1 or A1B forcing scenarios would be statistically indistinguishable from these results until well after the mid-century mark.

Climate models predict that the extreme temperature events could change more than the average climate over the course of the next century (IPCC, 2007). One way of quantifying this is to consider 20-year return values of the annual maximum of the daily average temperature. The 20-year return value is that value that is exceeded by a random variable once every 20 years on average over a long period of time. Such an event is truly rare, occurring only three or four times over the course of a typical human lifetime. Generalized

extreme value theory provides a robust statistical framework to perform these calculations (Zwiers and Kharin, 1998; Wehner, 2005). Figure 3.16 shows the predicted change in this quantity at the end of 21st century under the SRES A1B scenario from a mean model constructed from 10 models from the WGNE-CMIP3[1] database. Over the Gulf States region, this extreme value change is about 1°C greater than the change in the average temperature. Another way to put this in perspective is to consider the frequency with which currently considered rare events will be encountered in the future. Figure 3.17 shows the number of times in a 20-year period that the 1990-1999 return value would be reached near the end of the century. The purple shaded regions exceed 10 times; hence, currently considered rare events are likely to happen every other year or more frequently.

3.1.7 Changes in Specific Temperature Maxima Affecting Transportation

Transportation analysts have identified several specific attributes of temperature change of concern in transportation planning. Changes in annual days above 32.2 °C (90 °F) and maximum high temperature, for example, will impact the ability to construct and maintain transportation facilities. Concrete loses strength if it is set at air temperatures greater than 32.2 °C and the ability of construction workers and maintenance staff to perform their duties is severely curtailed at temperatures above 32.2 °C degrees. In order to properly design for the thermal expansion of concrete and steel elements of transportation facilities, knowledge of the maximum expected temperatures is required.

Since global climate models are integrated at spatial scales around 200 km, a linear regression analysis was used to downscale relationships between the three variables of greatest concern at the localized scale of a weather station to the transportation sector. Historical data from the USHCN for eight observation stations in the Gulf Coast study area were analyzed to determine highest temperature of record, mean number of days at minimum temperature 32.2 °C or higher, and mean daily temperature. Table 3.10 shows the reported observations for the eight weather stations for days above 32.2 °C and the associated annual and July mean daily temperatures.

Based on the relationship established in the regression analysis of the historical data, changes in mean and extreme temperatures were calculated for the study area relevant to the temperatures in 2050 and 2100, as predicted by the global climate models used in this study. The analysis focused on the relationship between mean daily temperature, output from the climate models at 200-km scales, and the desired values downscaled to local spatial scales: number of days above 32.2 °C and the highest temperature of record. Comparisons were made to each of the annual mean daily temperatures and mean daily temperatures for the month of July to determine which relationship better provided the desired forecast variables.

---

[1] Working Group on Numerical Experimentation Coupled Model Intercomparison Project phase 3.

A linear regression of days above 32.2 °C (90 °F) as an independent variable for the stations shown was undertaken for each of the annual mean daily and the July mean daily temperatures as the dependent variables. The regression of observed days above 32.2 °C versus annual mean daily temperature showed that for each rise by 0.6 °C (1 °F) in annual mean daily temperature there is an associated 3.9-day increase in the annual days above 32.2 °C. However, the data for New Orleans falls outside the trend line for this relationship.[2] The regression of days above 32.2 °C versus July mean daily temperature showed that for each rise by 0.6 °C (1 °F) in July mean daily temperature there is an associated 10-day increase in the annual days above 32.2 °C.[3]

The regression of observed high temperature versus annual mean daily temperature suggested that for each rise by 0.6 °C (1 °F) in annual mean daily temperature there is an associated 0.3 °C (0.6° F) rise in high temperature. However, this relationship only has an R-squared of 0.10, largely because the data for New Orleans falls outside the trend line. The regression of high temperature versus July mean daily temperature showed that for each rise by 0.6 °C (1 °F) in July mean daily temperature there is an associated 1.2 °C (2 °F) rise in the high temperature.[4]

The mean daily temperature for the study area is 27.6 °C (81.7 °F). Based on the relationships established above, this implies that the existing high temperature should be approximately 40.6 °C (105 °F). For each additional 0.6 °C (1° F) degree increase in July mean daily temperature that is forecasted by the GCMs, this high temperature can be expected to increase by 1.2 °C (2 °F). Using the relationship developed, this implies that the baseline/historical number of days above 32.2 °C (90 °F) is approximately 77 days. For each additional increase of 0.6 °C (1 °F) in July mean daily temperature that is forecasted by the GCMs, the number of days above 32.2 °C (90 °F) can be expected to increase approximately 10 days..

Airport runway length in the United States is generally calculated based on the mean maximum temperature (that is, the average of the daily high temperatures) during the hottest month of the year during the prior 30-year record. August is the month with the highest monthly mean maximum temperature in the Gulf Coast study area. Mean maximum temperature is reported by NOAA for 283 NOAA stations across the United States, six of which are located in the study area. The average mean maximum temperature for the hottest month of the year from these six stations is 33.1 °C (91.6 °F). To verify this, we determined the 30-year mean maximum temperature data (1972 to 2002) from the Carbon Dioxide Information Analysis Center (CDIAC), which encompasses 12 reporting stations located in the study area. CDIAC data provides station elevation data as well as latitude and longitude data. The average mean maximum temperature from the 12 CDIAC

---

[2] As a result, this relationship only has an R-squared of 0.27.

[3] With an R-squared of 0.61 if New Orleans is included and 0.77 if New Orleans is excluded from the analysis.

[4] The R-squared associated with this data is 0.42 if New Orleans is included and 0.89 if New Orleans is excluded from the analysis.

stations is 33.0 °C (91.4 °F) (table 3.11). The airport section in the subsequent chapter deals more specifically with this dataset in an analysis of how runway length may be impacted by changes in temperature during the next 50 to 100 years.

3.1.8 Increasing Daily Precipitation Extremes

As mentioned above, current generation climate models are limited in their ability to simulate individual storms by a lack of horizontal resolution. From a simple theoretical argument (Allen and Ingram, 2003), it is expected that extreme precipitation events should become more intense as the climate warms. The IPCC (2007) concluded that the frequency of heavy precipitation events had increased over most areas during the past century and that a continued increase in heavy precipitation events is very likely during the 21st century. The largest rainfall rates occur when a column of air is completely saturated and precipitates out nearly completely. The Clausius-Claperyon relationship dictates that as the air temperature increases, the atmosphere has the ability to hold more water vapor. Hence, under a warmer climate, it is very likely that specific humidity will increase both on average and in extreme saturation conditions. Extreme-value analysis of model output for daily precipitation in the Gulf States region, similar to the analysis discussed above with daily surface air temperatures, reveals a predicted increase of around 10 percent in the 20-year return value of the annual maximum of daily averaged precipitation, as shown in figure 3.18. The coarse horizontal resolution of the climate models used in this analysis results in an underestimation of extreme precipitation events (Wehner, 2005). Furthermore, these models lack the resolution to simulate tropical cyclones, a further source of extreme precipitation events. However, these deficiencies likely cause the prediction errors to be conservative, and it is likely that daily mean precipitation levels that are currently rare will become more commonplace in the future.

■ 3.2 Hurricanes and Less Intense Tropical Storms

Tropical cyclones (called hurricanes in the Atlantic and Gulf Coast regions) pose a severe risk to natural systems, personal property, and public infrastructure in the Gulf Coast region, and this risk will likely be exacerbated as the temperature of atmosphere and sea surface increase. Whereas loss of life from hurricanes has decreased in recent decades, property losses due to rapid population growth and economic development of coastal areas has increased (Herbert et al., 1997; Pielke and Pielke, 1997; Pielke and Landsea, 1998). Hurricanes have their greatest impact at the coastal margin where they make landfall and sustain their greatest strength. Severe beach erosion, surge overwash, inland flooding, and windfall casualties are exacted on both cultural and natural resources. Transportation facilities – roads, rails, pipelines, airports, ports – in coastal counties will likely be subjected to increasing hurricane intensity in the coming decades. Changes in Atlantic Basin hurricane formation and the behavior of hurricanes that make landfall in the Gulf Coast region have important implications for transportation planning, design, and maintenance in the short and long term.

3.2.1 Assessing Trends in Historical Hurricane Frequency and Intensity

Understanding hurricane frequency and landfall patterns is an important process in calculating insurance liabilities and rates for coastal communities as well as forecasting future risk under a changing climate. Several studies have shown that landfalling hurricanes are more or less frequent for given coastal reaches of the United States (see figure 3.19) and within given decades over the recorded history of North Atlantic storms (Simpson and Lawrence, 1971; Ho et al., 1987; Neumann, 1991; Jarrell et al., 1992; Gray et al., 1997; Pielke and Pielke, 1997; Neumann et al., 1999; Vickery et al., 2000). While different methods have been employed to calculate landfall probabilities at the state and county levels, there is general agreement that south Florida, the Carolinas, and the western Gulf Coast are most frequently impacted by major hurricanes (figure 3.19).

Studies of multidecadal hurricane variability and cycles have been complicated by the relatively short period of available and reliable data. Landfall counts of tropical storms and hurricanes at Grand Isle, LA, produced with a hurricane simulation model, HURASIM, (Doyle and Girod, 1997) (appendix E) for five-year periods from 1951 through 2005 show periods of greater and lesser hurricane history with short- and long-term variability (figure 3.20). If there is any pattern, historical records exhibit episodic hurricane activity rather than trends toward more frequent or stronger hurricanes, despite the most recent period of intense hurricane activity. While the long-term frequency trend of named storms within the Atlantic Basin has remained fairly constant, interannual variability is prominent particularly among major hurricanes (Gray, 1990; Landsea et al., 1992; Gray et al., 1997; Goldenberg et al., 2001; Bell and Chelliah, 2006). Hurricane spawning patterns have been linked to regional oscillation cycles, Atlantic thermohaline circulation, and African West Sahel rainfall patterns that have improved our understanding and forecasting of hurricane activity in the North Atlantic Basin (Gray et al., 1997; Landsea et al., 1999).

Increased tropical storm activity is likely to accompany global warming as a function of higher sea surface temperatures, which have been observed globally (figure 3.21). The kinetic energy of tropical storms and hurricanes is fueled from the heat exchange in warm tropical waters. An increase in sea surface temperature (SST) from global climate change is likely to increase the probability of higher sustained winds per tropical storm circulation (Emanuel, 1987; Holland, 1997; Knutson et al., 1998). Sea surface temperature has increased significantly in the main hurricane development region of the North Atlantic during the past century (Bell et al., 2007) (figure 3.22) as well as in the Gulf of Mexico (Smith and Reynolds, 2004) (figure 3.23).

Many scientists have evaluated the relationships between 20th-century warming and hurricane intensity, with some suggesting that the incidence of intense hurricanes over the past decade for the Atlantic basin could signal the beginning of an El Nino-Southern Oscillation (ENSO) related cycle of increased hurricane activity (Gray, 1984; O'Brien et al., 1996; Saunders et al., 2000). Henderson-Sellers et al. (1998) found no discernible trends in global hurricane trends with respect to number, intensity, or location during the past century. More contemporary analysis of the upswing in intense hurricane activity since the 1990s demonstrates that the proportion of intense, more destructive hurricanes

has increased in some ocean basins, including the North Atlantic, concomitant with rising sea surface temperature (Emanuel, 2005; Hoyos et al., 2006; Mann and Emanuel, 2006; Trenberth and Shea, 2006; Webster et al., 2005). Some studies conclude that the increase in recent decades is due to the combination of natural cyclical events (such as the North Atlantic Oscillation) and human-induced increases in sea surface temperature (Elsner, 2006).

Ocean currents that regulate heat content also appear to play an important role in the intensity of hurricanes when atmospheric conditions are favorable (Shay, 2006). In the Gulf of Mexico, the Loop Current is a heat conveyor that can build a heat reservoir spanning 200-300 km in diameter and 80-150 m in depth that is generally oriented towards the central Gulf Coast (figure 3.24) (Jaimes et al., 2006). Satellite-based and *in situ* measurements support the hypothesis that the warm water brought into the Gulf of Mexico by the Loop Current played an important role in the rapid intensification of Hurricanes Katrina, Rita, and Wilma (Jaimes et al., 2006).

Santer et al. (2006) used 22 climate models to study the possible causes of increased SST changes in the Atlantic and Pacific tropical cyclogenesis region, where SST increased from 0.32 °C to 0.67 °C (0.57 – 1.21 °F) over the 20th century. Their analysis suggests that century-timescale SST changes of this magnitude cannot be explained solely by unforced variability of the climate system. In experiments in which forcing factors are varied individually rather than jointly, human-caused changes in greenhouse gases are the main driver of the 20th-century SST increases in both tropical cyclogenesis regions. Ouuchi et al. (2006) used an atmospheric general circulation model at 20-km horizontal resolution to directly simulate the relationship between the tropical storm cycle and SST. This hurricane resolving model produced seasonal tropical storm statistics under present day conditions and was capable of hurricane force winds. When driven with the SST anomalies taken from A1B scenario experiments, the model produced fewer tropical storms everywhere except the North Atlantic Basin, where an increase was predicted. Tropical storms were more intense on average in all basins in these modeling experiments.

These results and those from similar studies suggest that as radiative forcing and SST continue to increase, hurricanes will be more likely to form in the Atlantic and Pacific Basins and more likely to intensify in their destructive capacity. In its Fourth Assessment Report, the IPCC (2007) concludes that:

- There is observational evidence for an increase of intense tropical cyclone activity in the North Atlantic since about 1970, correlated with increases of tropical sea surface temperatures;

- Multidecadal variability and the quality of the tropical cyclone records prior to the beginning of routine satellite observations in about 1970 complicate the detection of long-term trends in tropical cyclone activity; and

- There is no clear trend in the annual numbers of tropical cyclones.

3.2.2 Gulf Coast Hurricane History

Gulf coast ecosystems are exposed to varying degrees of hurricane disturbance as influenced by storm frequency, periodicity, and duration. Figure 3.25 shows that tropical storm landfall across the Gulf of Mexico Basin increases geometrically from west to east. Because most storms spawn in tropical waters in the eastern Atlantic there is a greater probability for eastern landmasses on the same latitude to incur tropical storms (Elsner, 1999). Temporal patterns of the past century reveal periods of relatively frequent hurricanes as well as inactive periods for most of the Gulf Coast region. The relatively calm period of record for hurricanes from the 1950s through the 1970s has some hurricane specialists purporting an increase in North Atlantic storms over the past decade related to ENSO oscillations and general warming trends (Elsner and Kara, 1999). Palynological and geological studies offer another means to reconstruct the regional history of hurricane activity over several centuries coincident with species changes and sedimentary overwash indicative of surge heights and storm intensity. One study of lake sediments in coastal Alabama suggests that major hurricanes of a Category 4 or 5 struck the Alabama coast with a frequency of about 600 years during the past three millennia (Liu and Fearn, 1993).

3.2.3 HURASIM: Model Application

HURASIM is a spatial simulation model of hurricane structure and circulation for reconstructing estimated windforce and vectors of past hurricanes. The model uses historical tracking and meteorological data of dated North Atlantic tropical storms from 1851 to present. A description of the HURASIM model is presented in appendix E.

The HURASIM model was applied in a hindcast mode to reconstruct hurricane windfields across the Gulf Coast region from Galveston, TX, to Pensacola, FL, on a 10-km grid basis for the period of record from 1851 to 2003. The model calculated windspeed and direction for every 15 minutes of storm movement retaining only wind events of 30 mph or greater for all proximal storms and grid cells within the study region. Storm tracking for calendar years 2004 and 2005 have not been added to the Hurricane Database (HURDAT) dataset as yet and, therefore, have been omitted from this analysis despite record storm activity that may be associated with multidecadal cycles and/or current global warming trends.

3.2.4 Historical Storm Frequency Across the Northern Gulf Coast
   Study Region

HURASIM model results were categorized by storm class based on the commonly used Saffir-Simpson scale over a 153-year period from 1851 to 2003 to gain an historical perspective of recurrence potential and spatial distribution of storm events along the northern Gulf Coast between Galveston, TX, and Pensacola, FL. Table 3.12 outlines the Saffir-Simpson scale for categorizing storms by intensity associated with range of windspeed. Storms on the Saffir-Simpson scale also have been ascribed typical storm surge levels based on observations during the 20th century. For example, NOAA states that

storm surge during landfall of a Category 1 hurricane is "generally 4 to 5 feet above normal," and a Category 3 hurricane storm surge is "generally 9 to 12 feet above normal" (NOAA, 2007). In the Gulf Coast region, however, storm surge is highly variable for a given class of storm on the Saffir-Simpson scale in the Gulf Coast region. For example, Hurricane Camille, a Category 5 hurricane at landfall, had a peak storm surge in coastal Mississippi of 7.6 m (25 ft), while the storm surge associated with Hurricane Katrina (a Category 3 hurricane at landfall) had peak storm surge of 8.5 m (28 ft) (Graumann et al., 2005).

Figure 3.26 shows the frequency patterns of storm events with Category 1, 2, and 3 winds or higher across the study region. Results show that storm frequency by storm class is highest for southeastern coastal Louisiana than elsewhere and lowest in inland locations, decreasing with increasing latitude. Secondary locations with high hurricane incidence include Galveston, TX, and the Mississippi coast. Coastal reaches west of Galveston, TX, the chenier plain of southwest Louisiana, and northwest Florida have experienced low to moderate hurricane frequency respectively. The highest frequency of Category 3 storm winds or greater for the entire region are seven storms over the 153-year period, equivalent to four to five storms per century. Based on the historical perspective alone, transportation planners should expect at least one major hurricane of Category 3 or greater to strike the northern Gulf Coast every 20 years. Over the same 20 years, planners can expect another Category 2 hurricane and two Category 1 hurricanes for a combined incidence rate of at least one hurricane every five years. While this rate is indicative of the worst-case grid location coastwide and over the entire historical record, the chance for storm track convergence elsewhere within the region is expected to be similar. However, storm frequency may be influenced by multidecadal variability such that some sites may experience higher incidence depending on the timeframe and whether it spans periods of on and off cycles.

3.2.5 Temporal and Spatial Analysis of Hurricane Landfall

The northern Gulf Coast exhibits spatially disjunct patterns of storm strikes related to the landfall tracks and storm categories (figure 3.27). Of storms exceeding Category 3-level winds between 1851 and 2003, the HURASIM model counted a maximum of seven storms equal to a recurrence interval of one major hurricane every 22 years for southeastern Louisiana. Hurricane tracking records are available from 1851 to present, but data accuracy was greatly improved at the turn of the century with expanded and instrumented weather stations and since 1944 when aircraft reconnaissance of tropical storms was instituted. HURASIM model output was analyzed by segmented time periods to determine short-term return frequencies of tropical storms to account for cyclical behavior and data accuracy for successive intervals of 15, 30, and 50 years of the longer 153-year record from 1851 to 2003. Data analysis focuses on the maximum potential return interval of storms by category according to the Saffir-Simpson scale. Given the prospect of questionable data accuracy of storm history and multidecadal storm cycling, it was deemed prudent to report storm frequencies for different time intervals to establish upward bounds of storm recurrence probabilities for catastrophe planning and assessment akin to worst-case

scenarios. Shorter time windows are likely to exhibit a wide range of storm recurrence probabilities (both high and low) relative to longer periods.

The shorter the period of observation, the greater the probability of inflating the calculated return interval. Figure 3.28 shows the storm frequency for 15-, 30-, and 50-year intervals for Category 1 storms or greater for the most active grid location across the study area. The most active time period historically for all time intervals was the latter 19th century, despite concerns of data accuracy for this period. These data show a potential maximum of storm incidence of three to five hurricanes every 10 years, nearly twice the strike frequency for the entire 153-year record. The lowest incidence of hurricane activity within the Gulf Coast study region for all time intervals spans the 1970s and 1980s with two to three hurricanes for every 10 years. These historical hurricane return intervals provide an expected range of .2 and .5 probability that a hurricane may strike a given coastal county within the study region that can be used to guide coastal planning and preparation. Recent hurricane studies spurred by the upswing in hurricane activity of the 1990s and early 21st century reveal the highly variable and cyclical nature of hurricane activity in the Northern Gulf of Mexico, as well as the need for reliable datasets that can be used to quantify long-term trends and relationships with sea surface temperature (Goldenberg et al., 2001).

3.2.6 Patterns of Hurricane Wind Direction

The HURASIM model outputs wind direction during storm landfall, which often relates to storm impact based on exposure to direct wind force. Road signs, for example, may be more prone to damage or destruction depending on their orientation to circulating storm winds. Because most storms approach the coast from the Gulf of Mexico on a northerly track, approaching storm winds are easterly and northeasterly on account of the counterclockwise rotation of North Atlantic tropical storms. Figure 3.29 displays simulated wind rows and direction of wind force derived for one of the most active grid cell locations in the study region at Grand Isle, LA, for tropical storm and hurricane conditions over the 153-year period of record. The concentration of wind rows is westerly and southerly for tropical storm events in accordance with prevailing storm approach from the south. Hurricane-force winds and direction at Grand Isle demonstrate a distinct shift to southwesterly and southeasterly directions as a result of major hurricanes passing to the east. As hurricanes pass inland of a given site, yet sustain their strength, backside winds in the opposite direction can occur. The length of each wind row is a function of the total number of 15-minute intervals of storm track interpolation and passage extracted from the HURASIM model. Longer wind rows are indicative of more frequent occurrences. Wind row data and polargrams have been generated for each grid cell within the Gulf Coast study region so that local and regional characterization of wind direction can be determined.

3.2.7 Modeling Climate Change Effects on Tropical Cyclones into the 21st Century

Early theoretical work on hurricanes suggested an increase of about 10 percent in wind speed for a 2 °C (4 °F) increase in tropical sea surface temperature (Emanuel, 1987). A 2004 study from the Geophysical Fluid Dynamics Laboratory in Princeton, New Jersey, that utilized a mesoscale model, downscaled from coupled global climate model runs, indicated the possibility of a 5 percent increase in the wind speeds of hurricanes by 2080 (cf. IPCC, 2001). To explore how climate change could affect 21st century hurricane intensity, windspeeds of hurricanes during 1904 to 2000 were modeled and then projected to increase from 5 to 20 percent over the equivalent forecast period of 2004 to 2100. Storm tracking for calendar years 2004 and 2005 have not been added to the HURDAT (NOAA/NCDC) dataset as yet and, therefore, have been omitted from this analysis despite record storm activity in 2005 that may be associated with multidecadal cycles and/or current global warming trends. Future storm intensities were calculated by multiplying the historical wind reconstructions with the proportional increase based on the forecast year relative to a ramping increase to 5, 10, 15, and 20 percent by the year 2100. The theoretical and empirical limits of maximum hurricane intensity appear to be highly correlated with SSTs (Miller, 1958; Emanuel, 1986, 1988; Holland, 1997). While climatologists debate the weight of contributing factors, including SST, modeling and recent empirical evidence suggest that a 10 percent or more increase in potential intensity is plausible under warming conditions predicted for the 21st century (Emanuel, 1987; Camp and Montgomery, 2001; Knutson and Tuleya, 2004).

Due to the differences in multidecadal hurricane activity over the 20th century, it was appropriate to evaluate the potential increase in storm frequency relative to the period of record. Figure 3.30 shows the potential increase in storm frequency by years 2050 and 2100 under a climate change scenario that supposes increased ramping of hurricane intensity concomitant with warming sea surface temperatures projected at 5, 10, 15, and 20 percent over the 21st century. Results show that an increase of one to two hurricanes above the historical frequency can be expected by year 2050 and up to four added hurricanes by year 2100. The potential gain of four hurricanes over the next century from a 20 percent increase in storm intensities nearly doubles the strike probability of the historical record. Not only will hurricane incidence increase under these assumptions, but individual storms will be stronger such that more catastrophic storms are likely to develop regardless of landfall location. These models and simulated data provide transportation planners with discrete and generalized probabilities of potential hurricane impact based on past and future climate.

■ 3.3 Sea Level Rise and Subsidence

Changes in climate during ice ages and warming periods have affected sea levels and coastal extent, as evidenced from geologic records. Currently, global sea level is on the

rise and is likely to accelerate with continued fossil fuel consumption from modernization and population growth (IPCC, 2001, 2007). As sea level rises, coastal shorelines will retreat, and low-lying areas will tend to be inundated more frequently, if not permanently, by the advancing sea. Subsidence (or sinking) of the land surface already is contributing to the flooding of transportation infrastructure in many Gulf Coast counties. In order to assess the vulnerability of transportation systems to inundation due to sea level rise, an integrated assessment of all important influences on coastal flooding must be considered. Relative sea level rise (RSLR) is the combined effect of an increase in ocean volume resulting from thermal expansion, the melting of land ice ("eustatic" sea level rise), and the projected changes in land surface elevation at a given location.

In this section, global sea level trends are first reviewed, including a comparison of IPCC findings in the Third and Fourth Assessments. This is followed by an examination of sea level rise and subsidence in the study region. The application of two different models to project RSLR in the region is then discussed, and a summary of the modeled range of projected RSLR to 2100 is presented.

3.3.1 Historical and Projected Global Sea Level Trends

Sea level has risen more than 120 m since the peak of the last ice age (about 20,000 B.P.) and over the 20th century by 1-2 mm/year (Douglas, 1991, 1997; Gornitz, 1995; IPCC, 2001). The rate of global sea level rise since 1963 is estimated at 1.8 mm/year (IPCC, 2007). More recent analysis of satellite altimetry data for the period from 1993 to 2003 shows a global average rate of sea level rise of about 3.1 (2.4-3.8) mm per year. Whether the faster rate since 1993 reflects decadal variability or a long-term acceleration over the 20th-century rate is unclear. There is high confidence, however, that the rate of observed sea level rise was greater in the 20th century compared to the 19th century (IPCC, 2007).

The rate of sea level rise in the world ocean basins varied significantly during the 20th century. Sea level rise during the 21st century is projected to have substantial geographical variability as well. The historical rate of sea level rise calculated from tide gauge records, and satellite altimetry is much higher in the Gulf of Mexico than in many other ocean basins (see IPCC, 2007, Working Group I, page 412).

The IPCC Third Assessment Report (TAR) (2001) projected an increase of 0.09-0.88 m in average global sea level by year 2100 with a mid-range estimate of 0.45 m. The range of projected sea level rise through 2100 is slightly lower and narrower in the IPCC Fourth Assessment Report (AR4) (see table 3.1). The midpoint of the projections in sea level rise differs by roughly 10 percent, and the ranges in the two assessment reports would have been similar if they had treated uncertainties in the same way (IPCC, 2007). As noted earlier, the IPCC 2007 sea level rise projections do not include rapid dynamical changes in ice flow from Greenland or Antarctica. If realized, some of the model-based projections could more than double the rate of sea level rise over the past century.

3.3.2 Tide Records, Sea Level Trends, and Subsidence Rates along the Central Gulf Coast

Changes in mean water level at a given coastal location are affected by a combination of changes in sea level in an ocean basin and by local factors such as land subsidence. Gulf Coastal Plain environments, particularly in the central and western parts of the Gulf Coast study area, are prone to high rates of land surface subsidence attributed to soil decomposition and compaction, deep fluid extraction (Morton et al., 2001, 2002; White and Morton, 1997), and the lack of sediment deposition. For example, the Mississippi River delta region demonstrates relative sea level rates of 10 mm/year, tenfold greater than current eustatic sea level rise (Penland and Ramsay, 1990; Gornitz, 1995). Cahoon et al. (1998) measured subsidence rates for several Gulf Coast sites ranging from a low of 2.7 mm/year in the Big Bend region of northwest Florida up to 23.9 mm/year for coastal Louisiana. Some of the forces driving shallow subsidence apparently included seasonal changes in water levels and a periodic occurrences of major storms.

The National Ocean Service (NOS), a division of NOAA, validates and reposits historical water level records at primary tide stations along the coasts and Great Lakes of the United States. Historic data from tide stations located within the Gulf Coast study region have been downloaded from the NOS web site at <http://tidesandcurrents.noaa.gov> in graphical and digital formats to be used in model simulations for projecting future sea level rise. Three tide stations at Pensacola, FL, Grand Isle, LA, and Galveston, TX, comprise the most reliable long-term tide records corresponding with the eastern, central, and western coverage of the study area (figure 3.31). The mean sea level trend for these gauges shows Grand Isle, LA, with the highest rate at 9.85 mm/year, followed by Galveston, TX, at 6.5 mm/year, and Pensacola, FL, at the lowest rate of 2.14 mm/year. These trend values are indicative of the high rates of local subsidence in Louisiana and Texas relative to the more stable geology underlying the Florida Panhandle. Multiple studies have extracted subsidence rates from these and other tide gauges within the Gulf Coast sector with some variability in rate estimates and methodology that mostly reaffirm regional patterns of generally high or low subsidence trends (Swanson and Thurlow, 1973; Penland and Ramsay, 1990; Zervas, 2001; Shinkle and Dokka, 2004).

Long-term tide gauge records are among the most reliable measures of local and regional subsidence. However, tide records also include the long-term trend of eustatic sea level change, which over the last century has been estimated at 1.7-1.8 mm/year on a global basis (Douglas, 1991, 1997, 2001; IPCC, 2001, 2007; Holgate and Woodworth, 2004). Accounting for historical eustatic change in accord with the global average equates to regional subsidence rates of 8.05 mm/year for Grand Isle, LA, and the Mississippi River deltaic plain; 4.7 mm/year for Galveston, TX, and the chenier plain; and 0.34 mm/year for Pensacola, FL, and Mississippi/Alabama Sound of the central Gulf Coast. The high subsidence rate of the Mississippi River Delta region at Grand Isle, LA, is more than four times greater than the historical eustatic trend of the last century and will account for a relative rise in sea level approaching 0.81 m by the year 2100, apart from future eustatic changes. Some areas within the coastal zone of Louisiana have subsidence rates exceeding

20 mm/year, demonstrating the potential range and variability within a subregion (Shinkle and Dokka, 2004).

Subsidence rates across a broad region like the Gulf Coast are highly variable on a local scale even within a representative coastal landform such as the Mississippi River deltaic plain or chenier plain. Many factors contribute to the rate and process of subsidence at a given locale by natural compaction, dewatering, and subsurface mineral extractions. Releveling surveys of benchmark monuments and well heads provide additional evidence and rates of rapid subsidence (Morton et al., 2001, 2002; Shinkle and Dokka, 2004). An extensive releveling project of the Lower Mississippi River coastal plain of first-order benchmarks along major highway corridors provides an expansive network of measured subsidence rates (Shinkle and Dokka, 2004). Oil and gas extractions in coastal Louisiana and southeastern Texas have accelerated local subsidence and wetland loss concomitant with production (Morton et al., 2001, 2002). Releveling projects in large cities such as New Orleans and Houston-Galveston have demonstrated high subsidence rates related to sediment dewatering and groundwater pumping, increasing the vulnerability to local flooding (Gabrysch, 1984; Zilkowski and Reese, 1986; Gabrysch and Coplin, 1990; Holzschuh, 1991; Paine, 1993; Galloway et al., 1999; Burkett et al., 2002).

3.3.3 Sea Level Rise Scenarios for the Central Gulf Coast Region

Two different sea level rise models were used to assess the range of sea level change that could be expected in the study area during the next 50 to 100 years. The Sea Level Rise Rectification Program (SLRRP) (see appendix F) is a model developed by the U.S. Geological Survey to explore the combined effects of future sea level change and local subsidence on coastal flooding patterns. CoastClim is a commercially available model that allows users to select GCM and emissions scenarios to predict sea level change within GCM grid cells over oceans. Table 3.13 outlines the selection list of GCM models that were available for use with SLRRP and the CoastClim models at the time of this study.

SLRRP projects future sea level rise for select tide gauge locations by rectifying the historical tide record of monthly means for the period of record and adding the predicted global mean eustatic sea level change obtained from IPCC (2001).[5] The tidal data input for the SLRRP model is composed of mean monthly water levels, which captures both short-term seasonal deviations and long-term trends of sea level change. Monthly values are derived from averaged hourly recordings for each month. A mean sea level trend is calculated for each tide gauge station, which includes both the local subsidence rate of

---

[5] The sea level rise estimates from the IPCC Fourth Assessment Report were not available when the sea level rise simulations were run for this study. The projected range of sea level change in the IPCC Fourth Assessment Report (2007) has an upper limit that is slightly lower and a lower limit that is slightly greater than the projections contained in the IPCC Third Assessment Report (2001). The IPCC Fourth Assessment Report also indicates, however, that the rate of historical sea level rise was greater in the Gulf of Mexico than in most other ocean basins, so the global average rate may tend to underestimate the rate of change in the study area.

vertical land movement and the eustatic rate of global sea level change for the period of record. Data records are given in stage heights for different tidal datums such as mean low water, mean tide level, and mean high water, which were rectified to the North American Vertical Datum of 1988 (NAVD88) to readily compare with land-based elevations of roads and other transportation infrastructure. Monthly extremes data also were used in this study to show that daily highs within a month can exceed the monthly average by as much 0.284 m and 0.196 m for Galveston, TX, and Pensacola, FL, respectively. (SLRRP model procedures and inputs are explained in further detail in appendix F.)

The SLRRP model indicates that surface elevations between 47.8 cm and 119.6 cm (NAVD88) will be inundated by sea level rise through 2050, dependent on geographic location, emissions scenario, and GCM forecast. The SLRRP model suggests that surface elevations between 70.1 cm and 199.6 cm (NAVD88) will be inundated by sea level rise through 2100, again dependent on geographic location, emissions scenario, and GCM forecast. Table 3.14 provides SLRRP model results showing the mean land surface elevations (cm, NAVD88) subject to coastal flooding for Galveston, TX, Grand Isle, LA, and Pensacola, FL, by 2050 and 2100 based on averaged output for all seven GCM models for the A1F1, B1, A1B, and A2 emissions scenarios.

The CoastClim V.1. model is another database tool for extracting predicted sea level for a given location, GCM, and emissions scenario much like the SLRRP model. CoastClim has a global database to predict regional patterns of sea level change associated with grid cell output of inclusive GCM models. CoastClim's user-friendly interface allows the user to select the region of interest from a global map. With a mouse click on the shoreline map, CoastClim picks the closest GCM grid cell and extracts a normalized index of regional sea level change relative to the global mean sea level. The normalized index is derived as a ratio or scaling factor for the average pattern of sea level change for the region or grid cell resolution divided by the global mean sea level change for the forecast period of 2071 to 2100. Table 3.15 shows the equivalent normalized index for each of seven GCM model selections for Galveston, TX, Grande Isle, LA, and Pensacola, FL. The different models display a variable range of grid cell resolution and projected sea level response above and below the global mean from 0.88 to 1.04 for the northern Gulf Coast region. The user also can select from six SRES emissions scenarios (A1B, A1F1, A1T, A2, B1, and B2) to run for a given GCM application. CoastClim displays the predicted outcome in relative sea level rise above zero in tabular and graphical format from 1990 to 2100.

CoastClim was used to generate predicted outcomes for seven different GCM models, six SRES scenarios, and three greenhouse gas forcing conditions of low, mid, and high for a total of 126 individual sea level rise curves for the 21st century. Results indicate that sea level rise will vary with both the selected model and emissions scenario. The high emissions A1F1 outcome for all GCM models predicts the highest rates of sea level change among SRES options, with a minimum eustatic sea level rise of 0.67 m by 2100, maximum potential rise of 1.55 m, and a mid-range around 1 m depending on model selection. The CoastClim model shows that relative sea level will rise between 12.68 cm and 75.42 cm by 2050, dependent on-site location, emissions scenario, and GCM forecast. By 2100, CoastClim predicts a potential sea level rise between 23.64 cm and 172.06 cm depending on-site location, emission scenario, and GCM forecast. Table 3.16 displays the CoastClim

model results of the mean predicted sea level rise (cm) for the Gulf Coast region by 2050 and 2100 under high, mid-, and low IPCC (2001) scenarios based on combined output for all seven GCM models for the A1F1, B1, A1B, and A2 emissions scenarios. However, these same eustatic rates are captured in the SLRRP model but rectified to a geodetic datum and local tidal conditions that more accurately reflect the potential for coastal flooding.

■ 3.4 Storm Surge

Storm surge is a wave of water that is pushed onshore by the force of the winds in the right quadrant of hurricane approach that can often inundate shoreline and inland areas up to many miles, length, and width. The added wave energy from advancing storms combines with normal tides to create the hurricane storm tide, which increases mean water levels to record heights, usually inundating roadways and flooding homes and businesses. The level of surge in a particular area is determined by the slope of the offshore continental shelf and hurricane intensity. The stronger the hurricane and the shallower the offshore water, the higher the surge will be. This advancing surge combines with the normal tides to create the hurricane storm tide, which can increase the mean water level 15 ft or more. In addition, wind-driven waves are superimposed on the storm tide. This rise in water level can cause severe flooding in coastal areas, particularly when the storm tide coincides with the normal high tides.

3.4.1 Predicting Storm Surge with the SLOSH Model

NOAA's National Weather Service forecasters model storm surge using the SLOSH (Sea, Lake, and Overland Surges from Hurricanes) model. NOAA and the Federal Emergency Management Agency (FEMA) use SLOSH to predict potential height of storm surge so as to evaluate which coastal areas are most threatened and must evacuate during an advancing storm. The SLOSH model is a computerized model run by NOAA's National Hurricane Center (NHC) to estimate storm surge heights and winds resulting from historical, hypothetical, or predicted hurricanes by taking into account storm barometric pressure, size, forward speed, track, and wind force. The model accounts for astronomical tides by specifying an initial tide level but does not include rainfall amounts, riverflow, or wind-driven waves. SLOSH also considers the approach or angle of hurricane landfall, which can effectively enhance surge height of westerly and northwesterly approaching storms along the northern Gulf Coast. Graphical output from the model displays color-coded storm surge heights for a particular area in feet above the model's reference level, the National Geodetic Vertical Datum (NGVD), which is the elevation reference for most maps. Emergency managers use output data and maps from SLOSH to determine which areas must be evacuated for storm surge.

Modeling, theory, and recent empirical evidence suggest that hurricane intensity is likely to increase in the Gulf Coast region (see prior section on hurricanes). Even if hurricanes do

not become more intense, however, sea level rise alone will increase the propensity for flooding that will occur when hurricanes make landfall in the Gulf Coast region. To assess the combined potential effects of hurricanes and sea level rise on the Gulf Coast transportation sector, a database of storm surge heights for Category 3 and 5 hurricanes was developed by using NOAA's SLOSH model for all coastal counties (extending inland from coastal counties along the Gulf of Mexico to those counties incorporating I-10) for the study area. Resulting surge elevations were overlaid on ArcView™ representations of each study area, enabling views of the study area in its entirety and minimum graphic representations at the county/parish level.

The NHC developed the SLOSH model to predict storm surge potential from tropical cyclones for comprehensive hurricane evacuation planning. The SLOSH models requires grid-based configurations of near-shore bathymetry and topography on a basin level. The NHC has defined 38 basins in the Atlantic and Pacific Oceans of which there are 14 subbasins that define the offshore and onshore geomorphology of the Gulf Coast shoreline from the Florida Keys to the Laguna Madre of Texas. SLOSH model simulations were performed for a merged suite of SLOSH basins (n=7) that covers the central Gulf Coast between Galveston, TX, and Mobile, AL, (table 3.17). SLOSH output were compiled for 28 simulation trials to extract surge levels for varying storm intensities (Categories 2-5) and landfall approaches. A sample simulation of surge height predictions are shown based on combined output for storms of Category 2, 3, 4, and 5 approaching the eastern half of the study area (Louisiana, Mississippi, and Alabama) on different azimuths (figure 3.32). Storm intensity, speed, and direction produces different storm surge predictions. Model simulation trials conducted for the SLOSH basin that covers New Orleans involved calibration and validation checks with historical storms and flood data.

Study area SLOSH applications involved the collection, synthesis, and integration of various geospatial information and baseline data for the central Gulf Coast region relevant to storm surge model implementation and predictions, with the following objectives:

- To derive a database of storm surge heights for Category 3 and 5 hurricanes by using NOAA's SLOSH model for all coastal counties (extending inland from coastal counties along the Gulf of Mexico to those counties incorporating I-10), for the study area spanning Galveston, TX, to Mobile, AL;

- To overlay the resulting surge elevations on ArcView™ representations of each study area, enabling views of the study area in its entirety and minimum graphic representations at the county level;

- To add topographic contours at 1-m intervals to the study area datasets; and

- To color code storm surge heights based on surge elevation in meters.

The integration of SLOSH output with local geospatial data will be particularly useful in phase II of the study, which will involve an assessment of transportation impacts for a particular county or Metropolitan Planning Organization (MPO) within the study area.

3.4.2 Future Sea Level Rise and Storm Surge Height

Sea level rise can be incorporated into surge height predictions from SLOSH simulations for future years by elevating surge levels in proportion to the amount of rise for any given scenario (figure 3.33). Sea level change will be particularly important in influencing this coastal area, since the land already is subject to flooding with supranormal tides and surge and rainfall events of even smaller, less powerful, tropical storms. Improved spatial detail and vertical accuracy of coastal elevations will greatly enhance predictions of the spatial extent of flooding from projected sea level rise and storm surges. Lidar imagery used in this project for coastal Louisiana offers distinct advantages for modeling purposes and graphical representation over other available Digital Elevation Model (DEM) data sources such as the National Elevation Dataset (figure 3.34). Also, it is expected that storm surges superimposed on higher mean sea levels will tend to exacerbate coastal erosion and land loss. During Hurricanes Rita and Katrina, for example, 562 km^2 (217 mi^2) of land in coastal Louisiana was converted to open water (Barras, 2006), and the Chandeleur Island chain was reduced in size by roughly 85 percent (USGS, 2007). The implications of the loss of these natural storm buffers on transportation infrastructure have not been quantified.

Surge analyses were conducted for the Gulf Coast study area by reviewing historical tide records and simulated hurricane scenarios based on the NOAA SLOSH model. Highest tide records for over 70 coastal tide stations were obtained from historical records within the study area, with the highest recorded surge of 6.2 m (20.42 ft) (NAVD88) at Bay St. Louis, MS, in the wake of a northerly approaching Category 5 storm, Hurricane Camille (1969). After Hurricane Katrina (2005), high watermark surveys in New Orleans proper and east along the Gulf Coast in Mississippi revealed storm surge heights approaching 8.5 m (28 ft) mean sea level (m.s.l.). Simulated storm surge from NOAA SLOSH model runs across the central Gulf Coast region demonstrate a 6.7-7.3-m (22-24-ft) potential surge with major hurricanes of Category 3 or greater without considering a future sea level rise effect. Storm approach from the east on a northwesterly track can elevate storm surge 0.3-1.0 m (1-3 ft) in comparison to a storm of equal strength approaching on a northeasterly track. The combined conditions of a slow churning Category 5 hurricane making landfall on a westerly track along the central Gulf Coast under climate change and elevated sea levels indicate that transportation assets and facilities at or below 9 m (30 ft) m.s.l. are subject to direct impacts of projected storm surge.

■ 3.5 Other Aspects of Climate Change with Implications for Gulf Coast Transportation

Temperature, precipitation, runoff, sea level rise, and tropical storms are not the only components of Gulf Coast climate that have the potential to change as the temperature of the atmosphere and the sea surface increase. Changes in wind and wave regime, cloudiness, and convective activity could possibly be affected by climate change and would have implications for some modes of transportation in the Gulf Coast region.

3.5.1 Wind and Wave Regime

There have been very few long-term assessments of near surface winds in the United States. Groisman and Barker (2002) found a decline in near surface winds of about -5 percent during the second half of the 20th century for the United States, but they suggest that a stepwise increase in the number of wind-reporting stations noticeably reduced the variance of the regionally averaged time series. They note that most reporting stations are located near airports and other developed areas. They did not attribute the decrease to climate change or land use change. Warming trends can be expected to generate more frequent calm weather conditions typical of summer months and generally characterized by lower winds than more windy conditions typical of cold-season months (Groisman et al., 2004).

Few studies have been made of potential changes in prevailing ocean wave heights and directions as a consequence of climate change, even though such changes can be expected (Schubert et al., 1998; McLean et al., 2001). In the North Atlantic, a multidecadal trend of increased wave height has been observed, but the cause is poorly understood (Guley and Hasse, 1999; Mclean et al., 2001). Wolf (2003) attributes the increasing North Atlantic wave height in recent decades to the positive phase of the North Atlantic Oscillation, which appears to have intensified commensurate with the slow warming of the tropical ocean (Hoerling et al., 2001; Wang et al., 2004). Changes in wave regime will not likely be uniform among ocean basins, however, and no published assessments have focused specifically on how climate change may affect wind and wave regime in the Gulf of Mexico. One 3-year study of wave and wind climatologies for the Gulf of Mexico (Teague et al., 1997) indicates that wave heights and wind speeds increase from east to west across the Gulf. This particular study, which is based on TOPEX/POSEIDEN satellite altimetry and moored surface buoy data, also indicates seasonality with the highest wind speeds and wave heights in the fall and winter.

Scenarios of future changes in seasonal wave heights constructed by using climate model projections for the northeastern Atlantic indicated increases in both winter and fall seasonal means in the 21st century under three forcing scenarios (Wang et al., 2004). The IPCC (2007) concludes that an increase in peak winds associated with hurricanes will accompany an increase in tropical storm intensity. Increasing average summer wave heights along the U.S. Atlantic coastline are attributed to a progressive increase in hurricane activity between 1975 and 2005 (Komar and Allan, 2007). Wave heights greater than 3 m increased by 0.7 to 1.8 m during the study period, with hourly averaged wave heights during major hurricanes increasing significantly from about 7 m to more than 10 m since 1995 (Komar and Allan, 2007). A more recent study of wave heights in the central Gulf of Mexico between 1978 and 2005 suggests a slight increase, but the trend is not statistically significant (Komar and Allan, 2008) (figure 3.35).

If tropical storm windspeed increases as anticipated (see section 3.2.8), this will tend to have a positive effect on mean wave height during the coming decades. Wave heights in coastal bays also will tend to increase due to the combined erosional effects of sea level

rise and storms on coastal barrier islands and wetlands (Stone and McBride, 1998; Stone et al., 2003).

3.5.2 Humidity and Cloudiness

As the climate warms, the amount of moisture in the atmosphere is expected to rise much faster than the total precipitation amount (Trenberth et al., 2003). The IPCC (2007) has concluded that tropospheric water vapor increased over the global oceans by 1.2 ± 0.3 percent per decade from 1988 to 2004, consistent in pattern and amount with changes in SST and a fairly constant relative humidity. Several studies have reported an increase in the near surface specific humidity (the mass of water vapor per unit mass of moist air) over the United States during the second half of the past century (Sun et al., 2000; Ross and Elliot, 1996). Sun et al. (2000) found that during 1948 to 1993, the mean annual specific humidity under clear skies steadily increased at a mean rate of 7.4 percent per 100 years.

Gaffen and Ross (1999) analyzed annual and seasonal dewpoint temperature, specific humidity, and relative humidity at 188 first-order weather stations in the United States for the period from 1961 to 1995. (Relative humidity is a measure of comfort based on temperature and specific humidity.) Coastal stations in the southeastern United States were moister than inland stations at comparable latitude, and stations in the eastern half of the country had specific humidity values about twice those at interior western stations. This dataset also shows increases in specific humidity of several percent per decade and increases in dewpoint of several tenths of a degree per decade over most of the country in winter, spring, and summer, with nighttime humidity trends larger than daytime trends (Gaffen and Ross, 1999). In the southeastern United States, specific humidity increased 2 to 3 percent per decade between 1973 and 1993 (Ross and Elliot, 1996), and this trend is expected to continue.

3.5.3 Convective Activity

Sun et al. (2001) documented a significant increase in total, low, cumulonimbus, and stratocumulus cloudiness across the United States during 1948 to 1993. The largest changes in the frequency of cumulonimbus cloudiness occurred in the intermediate seasons, especially in the spring. The increase in the frequency of cumulonimbus cloud development is consistent with the nationwide increase in the intensity of heavy and very heavy precipitation observed by Karl and Knight (1998) and Groisman et al. (2004). Cumulonimbus clouds are commonly associated with afternoon thunderstorms in the Gulf Coast region. The historical and projected increase in summer minimum temperatures for the study area suggest an increase in the probability of severe convective weather (Dessens, 1995, Groisman et al., 2004).

■ 3.6 Conclusions

The empirical climate record of the past century, in addition to climate change scenarios, was examined to assess the past and future temperature and hydrology of the central Gulf Coast region. The empirical record of the region shows an annual temperature pattern with high values in the 1920s-1940s, with a drop in annual temperatures in late 1950s, which persisted through the 1970s. Annual temperatures then began to climb over the past three decades but still have not reached the highs of previous decades. The timing of the increase in Gulf Coast temperatures is consistent with the global "climate shift" since the late 1970s (Karl et al., 2000 and Lanzante, 2006) when the rate of temperature change increased in most land areas.

Annual precipitation in the study area shows a suggestion toward increasing values, with some climate divisions, especially those in Mississippi and Alabama, having significant long-term trends. There also is a modeled long-term trend of increasing annual runoff regionwide. Over the entire record since 1919, there was an increase in rainfall that, combined with relatively cool temperatures, led to an estimated 36 percent increase in runoff. Modeled future water balance, however, suggests that runoff is expected to either decline slightly or remain relatively unchanged, depending upon the balance of precipitation and evaporation. Moisture deficits and drought appear likely to increase across the study area, though model results are mixed. These findings are consistent with the IPCC (2007), which concludes that it is very likely that heat waves, heat extremes, and heavy precipitation events over land will increase during this century and that the number of dry days (or spacing between rainfall events) will increase. Even in mid-latitude regions where mean precipitation is expected to decrease, precipitation intensity is expected to increase (IPCC, 2007).

Changes in rainfall beyond the study area can play an important role in the hydrology of the coastal zone. Weather patterns over the Mississippi River basin, which drains 41 percent of the United States, and other major drainages contribute to the total runoff in the Gulf Coast region. Several recent modeling efforts suggest an increase in average annual runoff in the eastern half of the Mississippi River watershed, while drainage west of the Mississippi and along the southern tier of states is generally predicted to decrease (Milly et al., 2005; IPCC, 2007). In the case of the Mississippi River, drainage to the coast is not presently a major factor in terms of flooding of infrastructure, because the river is levied and only a small portion of its flow reaches the marshes and shallow waters of the Louisiana coastal zone. Drainage of the Mississippi River and other rivers to the coast, however, is important in maintaining coastal soil moisture and water quality. The decline of approximately 150,000 acres of coastal marsh in southern Louisiana in 2000 was attributed to extreme drought, high salinities, heat and evaporation, and low river discharge (State of Louisiana, 2000).

As stated earlier, climate models currently lack the spatial and temporal detail needed to make confident projections or forecasts for a number of variables, especially on small spatial scales, so plausible "scenarios" are often used to provide input to decision making. Output from an ensemble of 21 general circulation models (GCMs) run with the three

emissions scenarios indicate a wide range of possible changes in temperature and precipitation out to the year 2050. The models agree to a warmer Gulf Coast region of about 1.5 °C ± 1 °C, with the greatest increase in temperature occurring in the summer. Based on historical trends and model projections, we conclude that it is very likely that in the future the number of very hot days will substantially increase across the study area. Due to the non-normality of temperature distributions over the five Gulf States, extreme high temperatures could be about 1°C greater than the change in the average temperature simulated by the GCMs.

Scenarios of future precipitation are more convoluted, with indications of increases or decreases by the various models, but the models lean slightly toward a decrease in annual rainfall across the Gulf Coast. However, by compounding changing seasonal precipitation with increasing temperatures, average runoff is likely to remain the same or decrease, while deficits (or droughts) are more likely to become more severe.

Each of the climate model and emissions scenarios analyzed in this report represent plausible future world conditions. As stated earlier, GCMs currently lack the spatial and temporal detail needed to make projections or forecasts, so plausible "scenarios" are often used to provide input to decision making. These models also lack the capacity for simulating small-scale phenomena such as thunderstorms, tornadoes, hail, and lightning. However, climate models do an excellent job of simulating temperature means and extremes. Hourly and daily precipitation and runoff extremes are much more difficult to simulate due to horizontal resolution constraints. However, based on observational and modeling studies the IPCC (2007) and numerous independent climate researchers have concluded that more intense precipitation events are very likely during this century over continental land masses in the Northern Hemisphere.

Recent empirical evidence suggests a trend towards more intense hurricanes formed in the North Atlantic Basin, and this trend is likely to intensify during the next century (IPCC, 2007). In the Gulf region, there is presently no compelling evidence to suggest that the number or paths of tropical storms have changed or are likely to change in the future. Convective activity, heavy precipitation events, and cloudiness all appear likely to increase in the Gulf Coast region as the climate warms.

Change in the rate of sea level rise is dependent on a host of interacting factors that are best evaluated on decadal to centennial time scales. Two complimentary modeling approaches were applied in this study to assess the potential rise in sea level and coastal submergence over the next century. Both models were used to estimate RSLR by 2050 and 2100 under a range of greenhouse gas emissions scenarios. Both models account for eustatic sea level change as estimated by the global climate models and also incorporate values for land subsidence in the region based on the historical record. One model, CoastClim, produces results that are closer to a simple measure of future sea level change under the scenarios of future climate. A similar model, SLRRP, also incorporates values for high and low tidal variation attributed to astronomical and meteorological causes, which are pulled from the historical record. The SLRRP model is rectified to the NAVD88 that is commonly used by surveyors to calculate the elevations of roads, bridges, levees, and other infrastructure. The tide data used in the SLRRP model is based on a monthly average of the mean high tide

(called mean high higher water) for each day of the month. The SLRRP results capture seasonal variability and interannual trends in relative sea level change, while the CoastClim results do not.

The three long-term tide gauge locations analyzed in this study represent three subregions of the study area: Galveston, TX (the chenier plain); Grand Isle, LA (the Mississippi River deltaic plain); and Pensacola, FL (Mississippi/Alabama Sound). For each of these gauges, we examined potential range of relative sea level rise through 2050 and 2100 using the SRES B1, A1B, A2, and A1F1 emissions scenarios based on the combined output of 7 GCMs (table 3.14). Results for the year 2100 generated with CoastClim range from 24 cm (0.8 ft) in Pensacola to 167 cm (5.5 ft) in Grand Isle. Results for the year 2100 from SLRRP, which as noted above accounts for historical tidal variation, are somewhat higher: predicted relative sea level ranges from 70 cm (2.3 ft, NAVD88) in Pensacola to 199 cm (6.5 ft, NAVD88) in Grand Isle.

Storm surge simulations accomplished basin-specific surge height predictions for a combination of storm categories, track speeds, and angled approach on landfall that can be summarized by worst-case conditions to exceed 6 to 9 m (20 to 30 ft) along the central Gulf Coast. Storm attributes and meteorological conditions at the time of actual landfall of any storm or hurricane will dictate actual surge heights. Transportation officials and planners within the defined study area can expect that transportation facilities and infrastructure at or below 9 m of elevation along the coast are subject to direct and indirect surge impacts. Sea level rise of 1 to 2 m (3-6 ft) along this coast could effectively raise the cautionary height of these surge predictions to 10 m (33 ft) or more by the end of the next century.

Changes in climate can have widespread effects on physical and biological systems of low-lying, sedimentary coasts. However, the large and growing pressures of development are responsible for most of the current stresses on Gulf Coast natural resources, which include: water quality and sediment pollution, increased flooding, loss of barrier islands and wetlands, and other factors that are altering the resilience of coastal ecosystems (U.S. Environmental Protection Agency, 1999). Human alterations to freshwater inflows through upstream dams and impoundments, dredging of natural rivers and engineered waterways, and flood-control levees also have affected the amount of sediment delivered to the Gulf coastal zone. Roughly 80 percent of U.S. coastal wetland losses have occurred in the Gulf Coast region since 1940, and predictions of future population growth portend increasing pressure on Gulf Coast communities and their environment. Sea level rise will generally increase marine transgression on coastal shorelines (Pethick, 2001) and the frequency of barrier island overwash during storms, with effects most severe in coastal systems that already are stressed and deteriorating. An increase in tropical storm intensity or a decrease in fresh water and sediment delivery to the coast would tend to amplify the effects of sea level rise on Gulf Coast landforms.

Our assessment of historical and potential future changes in Gulf Coast climate section draws on publications, analyses of instrumental records, and models that simulate how climate may change in the future. Model results, climatic trends during the past century, and climate theory all suggest that extrapolation of the 20th-century temperature record

would likely underestimate the range of change that could occur in the next few decades. The global near-surface air temperature increase of the past 100 years is approaching levels not observed in the past several hundred years (IPCC, 2001); nor do current climate models span the range of responses consistent with recent warming trends (Allen and Ingram, 2002). Regional "surprises" are increasingly possible in the complex, nonlinear Earth climate system (Groisman et al., 2004), which is characterized by thresholds in physical processes that are not completely understood or incorporated into climate model simulations; e.g., interactive chemistry, interactive land and ocean carbon emissions, etc. While there is still considerable uncertainty about the *rates* of change that can be expected (Karl and Trenberth, 2003), there is a fairly strong consensus regarding the direction of change for most of the climate variables that affect transportation in the Gulf Coast region. Key findings from this analysis and other published studies for the study region include:

Warming Temperatures – An ensemble of GCMs indicate that the average annual temperature is likely to increase by 1-2 °C (2-4 °F) in the region by 2050. Extreme high temperatures also are expected to increase, and within 50 years the probability of experiencing 21 days a year with temperatures of 37.8 °C (100 °F) is greater than 50 percent.

Changes in Precipitation Patterns – While average annual rainfall may increase or decrease slightly, the intensity of individual rainfall events is likely to increase during the 21st century. It is possible that average soil moisture and runoff could decline, however, due to increasing temperature, evapotranspiration rates, and spacing between rainfall events.

Rising Sea Levels – Relative sea level is likely to rise between 1 and 6 ft by the end of the 21st century, depending upon model assumption and geographic location. The highest rate of relative sea level rise will very likely be in the central and western parts of the study area (Louisiana and East Texas) where subsidence rates are highest.

Storm Activity – Hurricanes are more likely to form and increase in their destructive potential as the sea surface temperature of the Atlantic and Gulf of Mexico continue to increase. Rising relative sea level will exacerbate exposure to storm surge and flooding. Depending on the trajectory and scale of individual storms, facilities at or below 9 m (30 ft) could be subject to direct storm surge impacts.

■ 3.7 References

Ahijevych, D.A., R.E. Carbone, and C.A. Davis, 2003: Regional Scale Aspects of the Diurnal Precipitation Cycle. Preprints, *31st International Conference on Radar Meteorology,* Seattle, Washington, American Meteorological Society, 349-352B.

Allen, R.G., 2003: *REF-ET User's Guide.* University of Idaho Kimberly Research Stations: Kimberly, Idaho.

Allen, R.G., L.S. Pereira, D. Raes, and M. Smith, 1998: *Crop Evapotranspiration-Guidelines for Computing Crop Water Requirements.* FAO Irrigation and Drainage Paper 56, Food and Agriculture Organization, Rome.

Allen, M.R. and W.J. Ingram, 2002: Constraints on future changes in climate and the hydrologic cycle. *Nature*, 419:224-232.

Bell, G.D., and M. Chelliah, 2006: Leading tropical modes associated with interannual and multidecadal fluctuations in North Atlantic hurricane activity, *Journal of Climatology*, 19, 590– 612.

Bell, G.D., E. Blake, C.W. Landsea, M. Chelliah, R. Pasch, K.C. Mo, and S.B. Goldenberg, 2007: Tropical Cyclones: Atlantic Basin. In: "Chapter 4: The Tropics", from the *State of the Climate in 2006*, A. Arguez (ed.). *Bulletin of the American Meteorological Society* 88:S1-S135.

Benjamin, J., L.K. Shay, E. Uhlhorn, T.M. Cook, J. Brewster, G. Halliwell, and P.G. Black, 2006: Influence of Loop Current ocean heat content on Hurricanes Katrina, Rita, and Wilma. In: *27th Conference on Hurricanes and Tropical Meteorology*, Paper C3.4, American Meteriological Society, 24-28 April 2006, Monterey, California. 4 pages.

Burkett, V.B., D.B. Zilkowski, and D.A. Hart, 2002: Sea Level Rise and Subsidence: Implications for Flooding in New Orleans, Louisiana. In: Prince, K.R., Galloway, D.L. (Eds.) *Subsidence Interest Group Conference, Proceedings of the Technical Meeting*, Galveston, Texas, 27-29 November 2001. USGS Water Resources Division Open-File Report Series 03-308, U.S. Geological Survey, Austin, Texas.

Cahoon, D.R., J.W. Day, Jr., D. Reed, and R. Young, 1998: Global climate change and sea level rise: estimating the potential for submergence of coastal wetlands. In: *Vulnerability of coastal wetlands in the Southeastern United States: climate change research results, 1992-1997.* [G.R. Guntenspergen and B.A. Vairin, eds.] U.S. Geological Survey Biological Resources Division Biological Science Report, USGS/BRD/BSR-1998-0002, pp 21-34.

Christopherson, R.W., 2000: *Geosystems*. Prentice-Hall, Upper Saddle River, New Jersey.

Dessens, J., 1995: Severe convective weather in the context of a nighttime global warming. *Geophysical Research Letters,* **22,** 1241–1244.

Dingman, S.L., 2002: *Physical Hydrology, 2nd Ed.* Prentice Hall, Upper Saddle River, New Jersey.

Douglas, B.C., 1991: Global sea level rise. *Journal of Geophysical Research* 96: 6981-92.

Douglas, B.C., 1997: Global sea rise: A redetermination. *Surveys in Geophysics*, Volume 18, pages 279-292.

Douglas, B.C., 2001: Sea level change in the era of the recording tide gauge. In: *Sea level Rise: History and Consequences*, International Geophysics Series, Volume 75, edited by B. Douglas, M. Kearney, and S. Leatherman, Chapter 3, pages 37-64. Academic Press, San Diego, California.

Easterling, D.R., T.R. Karl, E.H. Mason, P.Y. Hughes, D.P. Bowman, R.C. Daniels, and T.A. Boden (Eds.), *United States Historical Climatology Network (U.S. HCN) Monthly.*

Elsner, J.B., 2006: Evidence in support of the climate change-Atlantic hurricane hypothesis. *Geophysical Research Letters* 33: L16705.

Emanuel, K., 1987: The dependence of hurricane intensity on climate. *Nature* 326: 483-485.

Emanuel, K., 2005: Increasing destructiveness of tropical cyclones over the past 30 years. *Nature* 436: 686-688.

Fontenot, R., 2004: *An Evaluation of Reference Evapotranspiration Models in Louisiana.* M.N.S. Thesis, Department of Geography and Anthropology, Louisiana State University.

Gabrysch, R.K., 1984: *Ground-water withdrawals and land-surface subsidence in the Houston-Galveston region, Texas, 1906-1980.* Texas Department of Water Resources Report 287, Austin, Texas, 64 pages.

Gabrysch, R.K., and L.S. Coplin, 1990: *Land-surface subsidence resulting from ground-water withdrawals in the Houston-Galveston Region, Texas, through 1987.* U.S. Geological Survey, Report of Investigations No. 90-01, 53 pages.

Gaffen, D.J., and R.J. Ross, 1999: Climatology and trends in U.S. surface humidity and temperature, *Journal of Climate* 12:

Galloway, D., D.R. Jones, and S.E. Ingebritsen, 1999: *Land Subsidence in the United States.* U.S. Geological Survey Circular 1182.

Gornitz, V., 1995: Sea level rise: a review of recent past and near-future trends. *Earth Surface Processes and Landforms* 20:7-20.

Goldenberg, S.B., Landsea, C.W., Mestas-Nunez, A.M., and Gray, W.M., 2001: The recent increase in Atlantic hurricane activity: Causes and implications. *Science* 293: 474-479.

Graumann, A., T. Houston, J. Lawrimore, D. Levinson, N. Lott, S. McCown, S. Stephens and D. Wuertz, 2005. *Hurricane Katrina – a climatological perspective.* October 2005, Updated August 2006. Technical Report 2005-01. 28 pages. NOAA National Climate Data Center, available at http://www.ncdc.noaa.gov/oa/reports/tech-report-200501z.pdf.

Groisman, P.Y., R.W. Knight, T.R. Karl, D.R. Easterling, B. Sun, and J.H. Lawrimore, 2004: Contemporary changes of the hydrological cycle over the contiguous United States: Trends derived from in situ observations. *Journal of Hydrometeorology,* 5**,** 64-85.

Groisman, P.Y., and H.P. Barker, 2002: Homogeneous blended wind data over the contiguous United States. Preprints, *13th Conference on Applied Climatology,* Portland, Oregon, American Metrological Society, J114–J117.

Guley, S.K., and L. Hasse, 1999: Changes in wind waves in the North Atlantic over the last 30 years. *International Journal of Climatology*, 19, 1,091-1,117.

Guttman, N.B., and Quayle, R.G., 1996: A Historical Perspective of U.S. Climate Divisions. *Bulletin of the American Meteorological Society,* 77: 293-303.

Hanson, R.L., 1991: *Evapotranspiration and Droughts*, in Paulson, R.W., Chase, E.B., Roberts, R.S., and Moody, D.W., Compilers, National Water Summary 1988-89-Hydrologic Events and Floods and Droughts: U.S. Geological Survey Water-Supply Paper 2375, pages 99-104.

Hoerling, M.P., J.W. Hurrell, X. Taiyi, 2001: Tropical origins for recent North Atlantic climate change. *Science* 292: 90-92.

Holgate, S.J., and P.L. Woodworth, 2004: Evidence for enhanced coastal sea level rise during the 1990s. *Geophysical Research Letters*, Volume 31: L07305.

Holzschuh, J.C., 1991: *Land subsidence in Houston, Texas U.S.A.: Field-trip guidebook for the Fourth International Symposium on Land Subsidence*, May 12-17, 1991, Houston, Texas, 22 pages.

Hoyos, C.D., P.A. Agudelo, P.J. Webster, J.A. Curry, 2006: Deconvolution of the Factors Contributing to the Increase in Global Hurricane Intensity. *Science* 312: 94-97.

IPCC (Intergovernmental Panel on Climate Change), 1996: *Climate Change 1995: Impacts, Adaptations and Mitigation of Climate Change: Scientific-Technical Analyses*. Cambridge University Press, New York, New York, 880 pages.

IPCC, 2001: *Climate Change 2001: Impacts, Adaptation, and Vulnerability*. J.J. McCarthy, O.F. Canziani, N.A. Leary, et al. (Eds.). Contribution of Working Group II to the Third Assessment Report of the Intergovernmental Panel on Climate Change. New York, New York: Cambridge University Press. 944 pages. (Available on-line at http://www.ipcc.ch/).

IPCC, 2007: *Climate Change 2007: The Physical Science Basis, Summary for Policy-Makers*. Contribution of Working Group I to the Fourth Assessment Report of the Intergovernmental Panel on Climate Change. Geneva, Switzerland, 21 pages.

Jensen, D.T., G.H. Hargreaves, B. Temesgen, and R.G. Allen, 1997: Computation of ETo

under Nonideal Conditions. *Journal of Irrigation and Drainage Engineering* 123(5): 394-400.

Karl, T., R. Knight, and N. Plummer, 1995: Trends in High-Frequency Climate Variability in the Twentieth Century. *Nature* 377: 217-220.

Karl, T.R. C.N. Williams Jr., and F.T. Quinlan, 1990: *United States Historical Climatology Network (HCN) Serial Temperature and Precipitation Data,* ORNL/CDIAC-30, NDP-019/R1, Carbon Dioxide Information and Analysis Center, Oak Ridge National Laboratory, Oak Ridge, Tennessee.

Karl, T.R., and C.W. Williams, Jr., 1987: An Approach to Adjusting Climatological Time Series for Discontinuous Inhomogeneities, *Journal of Applied Meteorology,* Volume 26, 1,744-1,763.

Karl, T.R., C.N. Williams Jr., P.J. Young, and W.M. Wendland, 1986: A Model to Estimate the Time of Observation Bias with Monthly Mean Maximum, Minimum, and Mean Temperatures for the United States, *Journal of Applied Meteorology,* Volume 25, 145-160, 1986.

Karl, T.R., H.F. Diaz, and G. Kukla, 1988: Urbanization: Its Detection and Effect in the United States Climate Record. *Journal of Climate*, 1,099-1,123.

Karl, T.R., and R.W. Knight, 1998: Secular trends of precipitation amount, frequency, and intensity in the United States. *Bulletin of the American Metrological Society,* 79**,** 231-241.

Karl, T.R., R.W. Knight, and B. Baker, 2000: The record breaking global temperatures of 1997 and 1998: evidence for an increase in the rate of global warming? *Geophysical Research Letters*, 27(5), 719-722.

Karl, T.R., and K.E. Trenberth, 2003: Modern global climate change. *Science*, 302 (5651), 1,719-1,723.

Keim, B.D., 1997: Preliminary Analysis of the Temporal Patterns of Heavy Rainfall across the Southeastern United States. *Professional Geographer* 49(1):94-104.

Keim, B.D., A.M. Wilson, C.P. Wake, and T.G. Huntington, 2003: Are there spurious temperature trends in the United States Climate Division database? *Geophysical Research Letters* 30(7):1404, doi:10.1029/2002GL016295, 2003.

Keim, B.D., M.R. Fisher, and A.M. Wilson, 2005: Are there spurious precipitation trends in the United States Climate Division database? *Geophysical Research Letters 32*, L04702, doi:10.1029/2004GL021985, 2005.

Komar, P.D., and J.C. Allan, 2007: Higher Waves Along U.S. East Coast Linked to Hurricanes. *EOS*, Transactions American Geophysical Union, Volume 88, Issue 30, page 301.

Komar, P.D., and J.C. Allan, 2008: Increasing hurricane-generated wave heights along the U.S. east coast and their climate controls. *Journal of Coastal Research*, March 2008, Volume 24, Issue 2.

Lanzante, J.R., T.C. Peterson, F.J. Wentz, and K.Y. Vinnikov, 2006: What do observations indicate about the changes of temperature in the atmosphere and at the surface since the advent of measuring temperatures vertically? In: *Temperature Trends in the Lower Atmosphere*, Edited by T.R. Karl, S.J. Hassol, C.D. Miller and W.L. Murray. U.S. Climate Change Science Program, Synthesis and Assessment Product 1.1, Washington, D.C. pages 47-70.

Liu, K., and M.L. Fearn, 1993: Lake-sediment record of late Holocene hurricane activity from coastal Alabama. *Geology* 21:973-976.

Mann, M.E. and K.A. Emanuel, 2006: Atlantic hurricane trends linked to climate change. *EOS* 87 (24): 233-244.

McLean, R.F., Tsyban, A., Burkett, V., Codignotto, J., Forbes, D., Ittekkot, V., Mimura, N., and R.J. Beamish, 2001: Coastal zones and marine ecosystems. In: *Climate Change: Impacts, Adaptation, and Vulnerability.* Third Assessment Report, Working Group II report of the Intergovernmental Panel on Climate Change (IPCC). IPCC Secretariat, Geneva, Switzerland, pages 343-379.

Milly, P.C.D., K.A. Dunne, and A.V. Vecchia, 2005: Global pattern of trends in streamflow and water availability in a changing climate. *Nature* 438: 347-350.

Morton, R.A., N.A. Buster, and M.D. Krohn, 2002: Subsurface Controls on Historical Subsidence Rates and Associated Wetland Loss in Southcentral Louisiana. *Transactions Gulf Coast Association of Geological Societies.* Volume 52, pages 767-778.

Morton, R.A., N.A. Purcell, and R.L. Peterson, 2001: Field evidence of subsidence and faulting induced by hydrocarbon production in coastal southeast Texas. *Transactions Gulf Coast Association of Geological Society*, Volume 51: 239-248.

Nakicenovic, N., and Swart, R. (Eds.), 2000: *Special Report on Emissions Scenarios*. Cambridge University Press. Cambridge, United Kingdom, 612 pages http://www.grida.no/climate/ipcc/emission/See Special Report on Emissions Scenarios.

NOAA, 2007: *The Saffir Simpson Scale*. http://www.nhc.noa.gov/aboutsshs.shtml.

Nerem, R.S., D.P. Chambers, E.W. Leuliette, G.T. Mitchum, and B.S. Giese, 1999: Variations in Global Mean Sea Level Associated with the 1997-1998 ENSO Event: Implications for Measuring Long-Term Sea Level Change. *Geophysical Research Letters,* 26 (19), 3,005-3,008.

Nicholls, R.J., P.P. Wong, V. Burkett, J. Codignotto, J. Hay, R. McLean, S. Ragoonaden,

and C. Woodroffe, 2007: Coastal Systems and Low-Lying Areas. In: *Climate Change Impacts, Adaptations, and Vulnerability.* Intergovernmental Panel on Climate Change Fourth Assessment Report. IPCC Secretariat, Geneva, Switzerland.

Oouchi, K., Yoshimura, J., Yoshimura, H., Mizuta, R., Kusunoki, S., and A. Noda, 2006: Tropical Cyclone Climatology in a Global-Warming Climate as Simulated in a 20km-Mesh Global Atmospheric Model: Frequency and Wind Intensity Analyses. *Journal of the Meteorological Society of Japan*, 84, 259-276,10.

Parson, E., V. Burkett, K. Fisher-Vanden, D. Keith, L. Mearns, H. Pitcher, C. Rosenzweig, M. Webster, 2007. *Global Change Scenarios: Their Development and Use.* Subreport 2.1B of Synthesis and Assessment Product 2.1 by the U.S. Climate Change Science Program and the Subcommittee on Global Change Research. Department of Energy, Office of Biological & Environmental Research, Washington, D.C., U.S.A., 106 pages.

Paine, J.G., 1993: Subsidence of the Texas coast – Inferences from historical and late Pleistocene sea levels: *Tectonophysics,* Volume 222, pages 445-458.

Penland, S., and K. Ramsey, 1990: Relative sea level rise in Louisiana and the Gulf of Mexico: 1908-1988. *Journal of Coastal Research* 6:323-342.

Pethick, J., 2001: Coastal management and sea-level rise. *Catena*, 42, 307-322.

Quayle, R.G., D.R. Easterling, T.R. Karl, and P.Y. Hughes, 1991: Effects of Recent Thermometer Changes in the Cooperative Station Network, *Bulletin of the American Meteorological Society*, Volume 72, 1,718-1,724.

Ross, R.J., and W.P. Elliott, 1996: Tropospheric water vapor climatology and trends over North America: 1973–93. *Journal of Climate* 9: 3,561–3,574.

Ruosteenoja, K., T.R. Carter, K. Jylha, and H. Tuomenvirta, 2003: *Future Climate in World Regions: An Intercomparison of Model-Based Projections for the New IPCC Emissions Scenarios.* Finnish Environment Institute, Helsinki, 83 pages.

Santer, B.D., T.M.L. Wigley, P.J. Gleckler, C. Bonfils, M.F. Wehner, K. AchutaRao, T.P. Barnett, J.S. Boyle, W. Brüggemann, M. Fiorino, N. Gillett, J.E. Hansen, P.D. Jones, S.A. Klein, G.A. Meehl, S.C.B. Raper, R.W. Reynolds, K.E. Taylor, and W.M. Washington, 2006: Forced and unforced ocean temperature changes in Atlantic and Pacific tropical cyclogenesis regions. *Proceedings of the National Academy of Sciences*, 103: 13,905-13,910.

Scharroo, R., W.H.F. Smith, and J.L. Lillibridge, 2005: Satellite Altimetry and the Intensification of Hurricane Katrina. *Eos*, Volume 86, No. 40, 4 October, page 366.

Shay, L.K., 2006: Positive feedback regimes during tropical cyclone passage. In: *14th Conference on Sea-Air Interactions*, AMS Annual Meeting, 30 January-3 February, Atlanta, Georgia.

Shell International, 2003: *Scenarios: an Explorer's Guide*. Global Business Environment. [Online at: www-static.shell.com/static/royal-en/downloads/scenarios_ explorersguide.pdf.

Shingle, K.D. and R.K. Dokka, 2004: *Rates of vertical displacement at benchmarks in the Lower Mississippi valley and the northern Gulf Coast*. NOAA Technical Report NOS/NGS 50, U.S. Department of Commerce, 135 pages.

Smith, T.M., and R.W. Reynolds, 2004: Improved Extended Reconstruction of SST (1854-1997). *Journal of Climate* 17: 2,466-2,477.

Stone, G.W., and R.A. McBride, 1998: Louisiana barrier islands and their importance in wetland protection: Forecasting shoreline change and subsequent response of wave climate. *Journal of Coastal Research*, 14, 900-14,916.

Stone, G.W., J.P. Morgan, A. Sheremet, and X. Zhang, 2003: *Coastal land loss and wave-surge predictions during hurricanes in Coastal Louisiana: implications for the oil and gas industry*. Coastal Studies Institute, Louisiana State University, 67 pages.

State of Louisiana, 2000: *Brown Marsh Questions and Answers*. Coastal Wetlands Planning, Protection, and Restoration Task Force, Baton Rouge, Louisiana Department of Natural Resources, Fact Sheet #5. [Online at: http://www.brownmarsh.net/factSheets/brown%20marsh%20Q%20and%20A.pdf].

Sun, B., P. Ya. Groisman, R.S. Bradley, and F.T. Keimig, 2000: Temporal changes in the observed relationship between cloud cover and surface air temperature. *Journal of Climate,* 13, 4,341–4,357.

Sun, B., P. Ya. Groisman and I.I. Mokhov, 2001: Recent changes in cloud type frequency and inferred increases in convection over the United States and the former USSR. *Journal of Climate,* 14, 1,864–1,880.

Swanson, R.L., and C.I. Thurlow, 1973: Recent Subsidence Rates along the Texas and Louisiana Coasts as Determined from Tide Measurements. *Journal of Geophysical Research*: Volume 78: 2,665-2,671.

Tebaldi, C., L.O. Mearns, R.L. Smith, and D. Nychka, 2004: Regional Probabilities of Precipitation Change: A Bayesian Analysis of multimodel simulations. *Geophysical Research Letters*, Volume 31.

Tebaldi, C., R.L. Smith, D. Nychka, and L.O. Mearns, 2005: Quantifying Uncertainty in Projections of Regional Climate Change: A Bayesian Approach to the Analysis of Multimodel Ensembles. *Journal of Climate*, Volume 18, Number 10, 1,524-1,540.

Teague, W.J., P.A. Hwang, G.A. Jacobs, E.F. Thompson, and D.W. Wang, 1997: *A three-year climatology of waves and winds in the Gulf of Mexico*. U.S. Naval Research Laboratory, Stennis, Mississippi. NRL/MR/7332--97-8068. 20 pages.

Trenberth, K.E., A. Dai, R.M. Rasmussen, and D.B. Parsons, 2003: The changing character of precipitation. *Bulletin of the American Meteorological Society* 84: 1,205-1,217.

Trenberth, K.E., and D.J. Shea, 2006: Atlantic hurricanes and natural variability in 2005. *Geophysical Research Letters* 33: L12704.

Turc, L., 1961: Evaluation des besoins en eau d'irrigation, evapotranspiration potentielle, formule climatique simplifee et mise a jour. (In French). *Annales Agronomiques* 12(1): 13-49.

Twilley, R.R., E. Barron, H.L. Gholz, M.A. Harwell, R.L. Miller, D.J. Reed, J.B. Rose, E. Siemann, R.G. Welzel, and R.J. Zimmerman, 2001: *Confronting Climate Change in the Gulf Coast Region: Prospects for Sustaining Our Ecological Heritage.* Union of Concerned Scientists, Cambridge, Massachusetts and Ecological Society of America, Washington, D.C., 82 pages.

U.S. Environmental Protection Agency (EPA), 1999: *Ecological Condition of Estuaries in the Gulf of Mexico.* Office of Research and Development, National Health and Environmental Effects Research Laboratory, Gulf Ecology Division, Gulf Breeze, Florida. EPA-620-R-98-004. 80 pages.

U.S. Geological Survey (USGS), 2007. Predicting flooding and coastal hazards. U.S. Geological Survey, Coastal and Marine Geology Program. Sound Waves Monthly Newsletter, June 2007. page 1.

Wang, X.L., F.W. Zweirs, and V.R. Swail, 2004: North Atlantic Ocean Wave Climate Change Scenarios for the Twenty-First Century, *Journal of Climate,* pages 2,368–2,383.

Webster, P.J., G.J. Holland, J.A. Curry, and H. Chang, 2005: Changes in tropical cyclone number, duration, and intensity in a warming environment. *Science* 309: 1,844-1,846.

Wehner, M., 2005: Changes in daily precipitation and surface air temperature extremes in the IPCC AR4 models. *U.S. CLIVAR Variations*, 3, (2005) pages 5-9. Lawrence Berkeley National Laboratory, LBNL-61594.

White, W.A., and R.A. Morton, 1997: Wetland losses related to fault movement and hydrocarbon production, southeastern Texas coast. *Journal of Coastal Research* 13: 1,305-1,320.

Wigley, T.M.L., S.C.B. Raper, M. Hulme, and S. Smith, 2000: *The MAGICC/SCENGEN Climate Scenario Generator: Version 2.4.* Technical Manual, Climatic Research Unit, UEA, Norwich, United Kingdom, 48 pages.

Wilks, D.S., 1993: Comparison of three-parameter probability distributions for representing annual and partial duration precipitation series. *Water Resources Research* 29: 3,543-3,549.

Wolf, J., 2003: Effects of Climate Change on Wave Height at the Coast. *Geophysical Research Abstracts*, European Geophysical Society 5: 13,351.

Zervas, C., 2001: Sea Level Variations of the United States 1854-1999; NOAA Technical Report NOS CO-OPS 36, NOAA, Silver Spring, Maryland, 66 pages.

Zilkoski, D.B., and S.M. Reese, 1986: *Subsidence in the Vicinity of New Orleans as Indicated by Analysis of Geodetic Leveling Data*. NOAA Technical Report NOS 120 NGS 38, National Oceanic and Atmospherics Administration, Rockville, Maryland.

Zwiers, F.W., and V.V. Kharin, 1998: Changes in the extremes of the climate simulated by CCC GCM2 under CO_2 doubling. *Journal of Climate*, 11, 2,200-2,222.

Table 3.1 **Projected global average surface warming and sea level rise at the end of the 21st century (IPCC, 2007). These estimates are assessed from a hierarchy of models that encompass a simple climate model, several Earth models of intermediate complexity (EMIC), and a large number of atmosphere-ocean global circulation models (AOGCM). Sea level projections do not include uncertainties in carbon-cycle feedbacks because a basis in published literature is lacking (IPCC, 2007).**

Case	Temperature Change (°C from 2090-2099 Relative to 1980-1999)		Sea Level Rise (m) from 2090-2099 Relative to 1980-1999)
	Best Estimate	**Likely Range**	**Model-Based Range, Excluding Future Rapid Dynamical Changes in Ice Flow**
Constant Year 2000 Concentrations	0.6	0.3-0.9	NA
B1 Scenario	1.8	1.1-2.9	0.18-0.38
A1T Scenario	2.4	1.4-3.8	0.20-0.45
B2 Scenario	2.4	1.4-3.8	0.20-0.43
A1B Scenario	2.8	1.7-4.4	0.21-0.48
A2 Scenario	3.4	2.0-5.4	0.23-0.51
A1F1 Scenario	4.0	2.4-6.4	0.26-0.59

Table 3.2   United States Historical Climatology Network (USHCN) stations within the seven climate divisions of the central Gulf Coast region.

Climate Division (CD)	USHCN Stations
Texas CD 8	Danevang, Liberty
Louisiana CD 7	Jennings[1]
Louisiana CD 8	Franklin, Lafayette
Louisiana CD 9	Donaldsonville, Houma, New Orleans, Thibodaux
Louisiana CD 6	Amite, Baton Rouge, Covington
Mississippi 10	Pascagoula, Poplarville, Waveland
Alabama CD 8	Fairhope

[1] The Jennings climate record only dates back to the late 1960s. As a result, CD 7 is made up of an average of Liberty, TX, to the west and Lafayette, LA, to the east.

Table 3.3   List of GCMs run with the three SRES emissions scenarios (A1B, A2, and B1) for this study. Not all model runs were available from the IPCC Data Centre for each SRES scenario.

A1B		A2		B1	
Temperature	**Precipitation**	**Temperature**	**Precipitation**	**Temperature**	**Precipitation**
CCCMA	CCCMA.T63	BCCR	BCCR	BCCR	BCCR
CCCMA.T63	CNRM	CCCMA	CNRM	CCCMA	CCCMA.T63
CNRM	CSIRO	CNRM	CSIRO	CCCMA.T63	CNRM
CSIRO	GFDL0	CSIRO	GFDL0	CNRM	CSIRO
GFDL0	GFDL1	GFDL0	GFDL1	CSIRO	GFDL0
GFDL1	GISS.AOM	GFDL1	GISS.ER	GFDL0	GFDL1
GISS.AOM	GISS.EH	GISS.ER	INMCM3	GFDL1	GISS.AOM
GISS.EH	GISS.ER	INMCM3	IPSL	GISS.AOM	GISS.ER
GISS.ER	IAP	IPSL	MIROC.MEDRES	GISS.ER	IAP
IAP	INMCM3	MIROC.MEDRES	ECHAM	IAP	INMCM3
INMCM3	IPSL	ECHO	MRI	INMCM3	IPSL
IPSL	MIROC.HIRES	ECHAM	CCSM3	IPSL	MIROC.HIRES
MIROC.HIRES	MIROC.MEDRES	MRI	PCM	MIROC.HIRES	MIROC.MEDRES
MIROC.MEDRES	ECHAM	CCSM	HADCM3	MIROC.MEDRES	ECHAM
ECHO	MRI	PCM	HADGEM1	ECHO	MRI
ECHAM	CCSM3	HADCM3		ECHAM	CCSM3
MRI	PCM	HADGEM1		MRI	PCM
CCSM	HADCM3			CCSM	HADCM3
PCM				PCM	
HADCM3				HADCM3	
HADGEM1					

Table 3.4 **Scenarios of temperature change (°C) from an ensemble of GCMs for the 5th, 25th, 50th, 75th, and 95th percentiles for the A1B scenario for 2050 relative to 1971-2000 means.**

	5th	25th	50th	75th	95th
Winter	0.18	0.95	1.42	1.89	2.56
Spring	1.22	1.55	1.80	2.04	2.38
Summer	1.24	1.66	1.94	2.23	2.70
Autumn	1.31	1.69	1.93	2.22	2.62

Table 3.5 **Scenarios of precipitation change (percent) from an ensemble of GCMs for the 5th, 25th, 50th, 75th, and 95th percentiles for the A1B scenario for 2050 relative to 1971-2000 means.**

	5th	25th	50th	75th	95th
Winter	-13.30	-5.95	-1.79	2.49	9.01
Spring	-21.07	-11.04	-5.04	1.80	10.17
Summer	-36.10	-17.77	-6.39	6.25	26.24
Autumn	-8.20	0.46	5.97	12.05	21.50

Table 3.6   Scenarios of temperature change (°C) from an ensemble of GCMs for the 5th, 25th, 50th, 75th, and 95th percentiles for the A2 scenario for 2050 relative to 1971-2000 means.

	5th	25th	50th	75th	95th
Winter	0.2	1.0	1.5	2.0	2.9
Spring	0.8	1.3	1.7	2.0	2.6
Summer	1.1	1.5	1.8	2.1	2.5
Autumn	1.0	1.5	1.8	2.1	2.6

Table 3.7   Scenarios of precipitation change (percent) from an ensemble of GCMs for the 5th, 25th, 50th, 75th, and 95th percentiles for the A2 scenario for 2050 relative to 1971-2000 means.

	5th	25th	50th	75th	95th
Winter	-12.7	-5.7	0.4	5.6	13.6
Spring	-22.9	-12.8	-6.0	0.5	10.3
Summer	-31.2	-15.0	-5.2	5.9	21.3
Autumn	-7.3	1.3	7.0	12.7	22.1

Table 3.8 **Scenarios of temperature change (°C) from an ensemble of GCMs for the 5th, 25th, 50th, 75th, and 95th percentiles for the B1 scenario for 2050 relative to 1971-2000 means.**

	5th	25th	50th	75th	95th
Winter	-0.31	0.44	1.02	1.53	2.32
Spring	0.67	1.05	1.32	1.62	2.03
Summer	0.64	1.09	1.35	1.63	2.03
Autumn	0.62	1.04	1.33	1.62	2.07

Table 3.9 **Scenarios of precipitation change (percent) from an ensemble of GCMs for the 5th, 25th, 50th, 75th, and 95th percentiles for the B1 scenario for 2050 relative to 1971-2000 means.**

	5th	25th	50th	75th	95th
Winter	-9.77	-4.37	-0.52	3.36	9.51
Spring	-16.94	-7.96	-2.94	2.41	11.38
Summer	-27.06	-14.16	-3.36	7.43	24.19
Autumn	-7.83	-0.06	5.63	11.13	19.40

Table 3.10   Days above 32.2 °C (90 °F) and mean daily temperature in the study area for datasets running through 2004. The start date varies by location (note the number of years of observed data).

Station	Years of Observed Data	Annual Days Above 90 °F	Normal Mean Daily (°F) Annual	July
Mobile, AL	42	74	66.8	81.5
Baton Rouge, LA	45	84	67.0	81.7
Lake Charles, LA	40	76	67.9	82.6
New Orleans, LA	58	72	68.8	82.7
Meridian, MS	40	80	64.7	81.7
Houston, TX	35	99	68.8	83.6
Port Arthur, TX	44	83	68.6	82.7
Victoria, TX	43	106	70.0	84.2

Table 3.11   Modeled outputs of potential temperature increase (°C [°F]) scenarios for August.

Mid-Term Potential (2050 Scenarios)			Long-Term Potential (2100 Scenarios)			
Temperature Increase by Scenario Percentile: °C (°F)			Temperature Increase by Scenario Percentile: °C (°F)			
Scenario	**5th**	**50th**	**95th**	**Scenario**	**5th**	**50th**	**95th**
A1B	1.6 (2.9)	2.5 (4.5)	**3.4 (6.1)**	**A1B**	3.0 (5.4)	3.9 (7.0)	5.0 (9.0)
B1	**0.9 (1.6)**	1.8 (3.2)	2.6 (4.7)	**B1**	**1.8 (3.2)**	2.7 (4.9)	3.6 (6.5)
A2	1.1 (2.0)	2.3 (4.1)	**3.4 (6.1)**	**A2**	3.3 (5.9)	4.7 (8.5)	**6.0 (10.8)**

Note: Lowest/highest changes in bold.

Table 3.12   Saffir-Simpson Scale for categorizing hurricane intensity and damage potential. Note that maximum sustained wind speed is the only characteristic used for categorizing hurricanes.

Saffir-Simpson Scale and Storm Category	Central Pressure (mbar)	Maximum Sustained Wind Speed (mph)	Damage Potential
1	980	74-95	Minimal
2	965-979	96-110	Moderate
3	945-964	111-130	Extensive
4	920-944	131-155	Extreme
5	< 920	>155	Catastrophic

Table 3.13   GCM model-selection options based on data availability for the USGS SLRRP and CoastClim models for generating future sea level rise projections. There are 3 GCM model datasets shared between SLRRP and CoastClim and a total of 11 GCM models and datasets altogether.

SLRRP GCM Listing	CoastClim GCM Listing
CSIRO_Mk2	CGCM1
CSM 1.3	CGCM2
ECHAM4/OPYC3	CSIRO_Mk2
GFDL_R15_a	GFDL_R15_b
HadCM2	GFDL_R30_c
HadCM3	HadCM2
PCM	HadCM3

Notes: CGMC1, CGCM2: Canadian Global Coupled Model .

CSIRO_Mk2: Commonwealth Scientific and Industrial Research Organisation [Australia] –.

CSM 1.3: Climate Simulation Model (NCAR)

ECHAM4/OPYC3: A coupled global model developed by the Max-Planck-Institute for Meteorology (MPI) and Deutsches Klimarechenzentrum (DKRZ) in Hamburg, Germany

GFDL_R15a, R15b, R30c: Geophysical Fluid Dynamics Laboratory

HADCM2, HADCM3: Hadley Centre Coupled Model.

PCM: Parallel Climate Model – DOE/NCAR

Table 3.14   **USGS SLRRP model results showing the mean land surface elevations (cm [NAVD88]) subject to coastal flooding for the Gulf Coast region by 2050 and 2100 under a high, mid, and low scenario based on combined output for all seven GCM models for the A1F1, B1, A1B, and A2 emissions scenarios.**

Year 2050	Low				Year 2100	Low			
	A1FI	B1	A1B	A2		A1FI	B1	A1B	A2
Galveston, TX	83.0	80.9	83.4	83.4	Galveston, TX	130.7	117.0	124.9	127.0
Grand Isle, LA	107.5	106.0	108.8	106.3	Grand Isle, LA	171.2	159.7	168.7	167.6
Pensacola, FL	48.0	47.8	48.4	53.7	Pensacola, FL	83.9	70.1	78.2	75.2

Year 2050	Mid				Year 2100	Mid			
	A1FI	B1	A1B	A2		A1FI	B1	A1B	A2
Galveston, TX	88.9	86.7	88.7	88.8	Galveston, TX	146.0	129.5	137.1	140.8
Grand Isle, LA	113.6	111.8	114.2	111.8	Grand Isle, LA	185.3	171.4	180.2	181.3
Pensacola, FL	53.9	53.6	53.7	60.0	Pensacola, FL	99.2	82.6	90.3	89.3

Year 2050	High				Year 2100	High			
	A1FI	B1	A1B	A2		A1FI	B1	A1B	A2
Galveston, TX	94.8	92.5	93.9	94.3	Galveston, TX	161.3	142.0	149.3	154.5
Grand Isle, LA	119.6	117.6	119.6	117.3	Grand Isle, LA	199.6	183.1	191.7	195.1
Pensacola, FL	59.8	59.4	58.9	66.3	Pensacola, FL	114.5	95.0	102.5	103.5

Table 3.15   **Regional grid cell counts and normalized indices of sea level rise relative to global mean sea level projections for northern Gulf Coast tide gage locations by different GCM models used in CoastClim simulations.**

CoastClim Models	Gulf Coast Grid Cell Count	Normalized SLR Index		
		Galveston, TX	Grand Isle, LA	Pensacola, FL
CGCM1	5	0.89	0.89	0.89
CGCM2	5	1.04	1.04	0.95
CSIRO_Mk2	3	0.90	0.94	0.94
GFDL_R15_b	2	0.94	0.88	0.89
GFDL_R30_c	6	0.98	1.01	1.01
HadCM2	2	1.02	1.02	1.02
HadCM3	7	1.03	1.00	0.96

Table 3.16   CoastClim model results showing the mean sea level rise (cm) for the Gulf Coast region by 2050 and 2100 under a high, mid, and low scenario based on combined output for all seven GCM models for the A1F1, B1, A1B, and A2 emission scenarios.

Year 2050	Low				Year 2100	Low			
	A1FI	B1	A1B	A2		A1FI	B1	A1B	A2
Galveston, TX	40.5	39.2	40.2	39.6	Galveston, TX	81.8	72.4	76.3	78.6
Grand Isle, LA	60.6	59.3	60.3	59.8	Grand Isle, LA	118.8	109.3	113.3	115.6
Pensacola, FL	14.2	13.0	14.0	14.2	Pensacola, FL	33.6	24.3	28.2	32.0

Year 2050	Mid				Year 2100	Mid			
	A1FI	B1	A1B	A2		A1FI	B1	A1B	A2
Galveston, TX	46.2	44.3	45.8	44.8	Galveston, TX	101.8	84.9	92.2	95.4
Grand Isle, LA	66.4	64.4	66.0	64.9	Grand Isle, LA	138.9	121.8	129.3	132.4
Pensacola, FL	20.0	18.1	19.6	19.8	Pensacola, FL	53.5	36.8	44.1	49.3

Year 2050	High				Year 2100	High			
	A1FI	B1	A1B	A2		A1FI	B1	A1B	A2
Galveston, TX	54.3	51.6	53.8	52.1	Galveston, TX	130	103.7	115.5	119.3
Grand Isle, LA	74.5	71.7	73.9	72.3	Grand Isle, LA	167.3	140.7	152.5	156.4
Pensacola, FL	28.1	25.3	27.5	27.5	Pensacola, FL	81.6	55.6	67.2	73.9

Table 3.17   Seven SLOSH basin codes, name descriptions, and storm categories included in the central Gulf Coast study region and simulation trials from Mobile, AL, to Galveston, TX.

Basin Code	Basin Name	Storm Category
EMOB	Elliptical Mobile Bay	Cat2, Cat3, Cat4, Cat5
NBIX	MS – Gulf Coast	Cat2, Cat3, Cat4, Cat5
MS2	New Orleans	Cat2, Cat3, Cat4, Cat5
LFT	Vermilion Bay	Cat2, Cat3, Cat4, Cat5
EBPT	Elliptical Sabine Lake	Cat2, Cat3, Cat4, Cat5
EGL2	Elliptical Galveston Bay (2002)	Cat2, Cat3, Cat4, Cat5
PSX	Matagorda Bay	Cat2, Cat3, Cat4, Cat5

Table 3.18   SLRRP model parameters and results showing the mean sea level rise projections for the Gulf Coast region by 2050 and 2100 under a high, mid, and low scenario based on combined output for all seven GCM models for the A1F1 emission scenario.

Model Parameters	Scenarios	Louisiana-Texas Chenier Plain	Louisiana Deltaic Plain	Mississippi-Alabama Sound
Tide Gauge		Galveston, TX	Grand Isle, LA	Pensacola, FL
Sea Level Trend (mm/yr)		6.5	9.85	2.14
Subsidence (mm/yr)		4.7	8.05	0.34
Sea Level Rise by 2050 (cm, NAVD88)	High	94.8	119.6	59.8
	Mid	88.9	113.6	53.9
	Low	83.0	107.5	48.0
Sea Level Rise by 2100 (cm, NAVD88)	High	161.3	199.6	114.5
	Mid	146.0	185.3	99.2
	Low	130.7	171.2	83.9

Figure 3.1 CO_2 emissions, SO_2 emissions, and atmospheric CO_2 concentration through 2100 for the six "marker/illustrative" SRES scenarios and the IS92a scenario (a "business as usual" scenario, IPCC [1992]). (Source: IPCC, 2001)
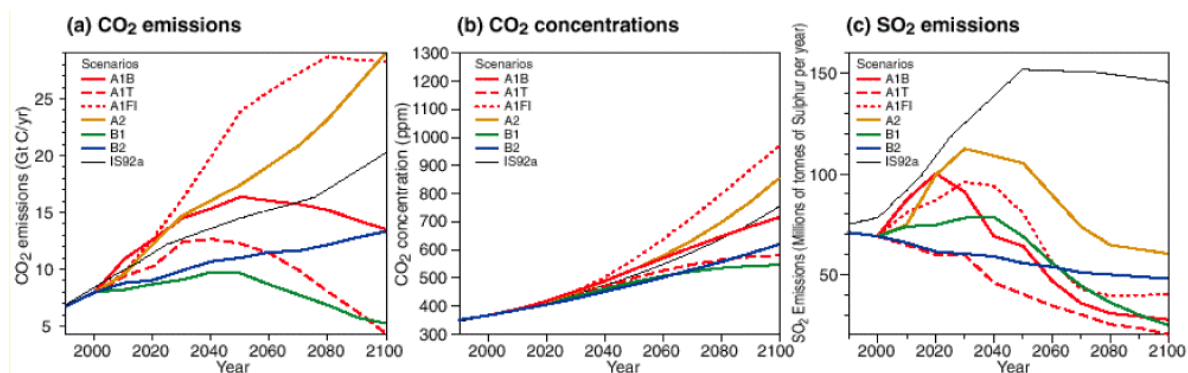
Figure 3.2   United States climate divisions of the central Gulf Coast study area. Empirical trends and variability were analyzed for temperature and precipitation at the Climate Division Dataset-(CDD) level for the climate divisions along the Gulf Coast from Galveston, TX, to Mobile, AL, including Texas Climate Division 8, Louisiana Divisions 6-9, Mississippi Division 10, and Alabama Division 8. These climatic divisions cover the entire central Gulf Coast study area.
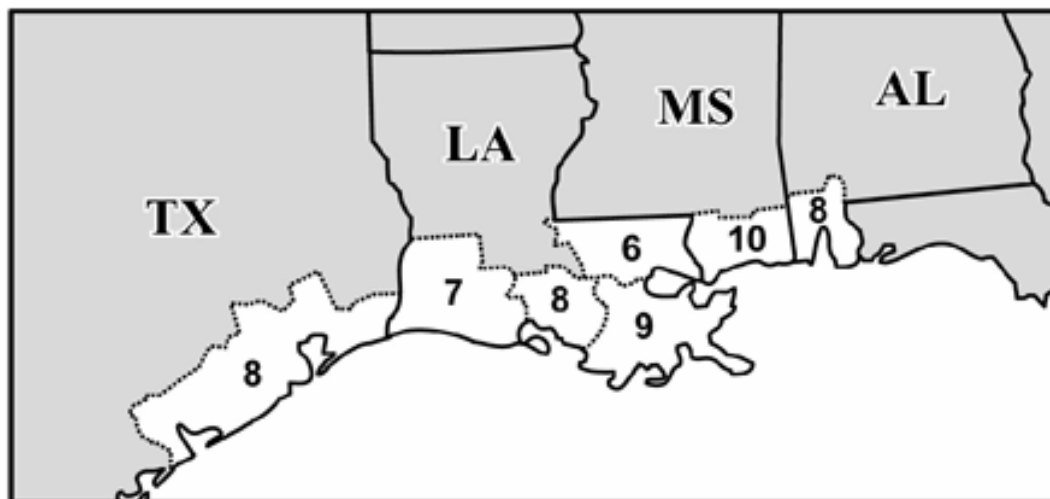
Figure 3.3   Grid area for the GCM temperature and precipitation results presented in section 3.15 of this report, which is a subset of the global grid of a typical GCM output.
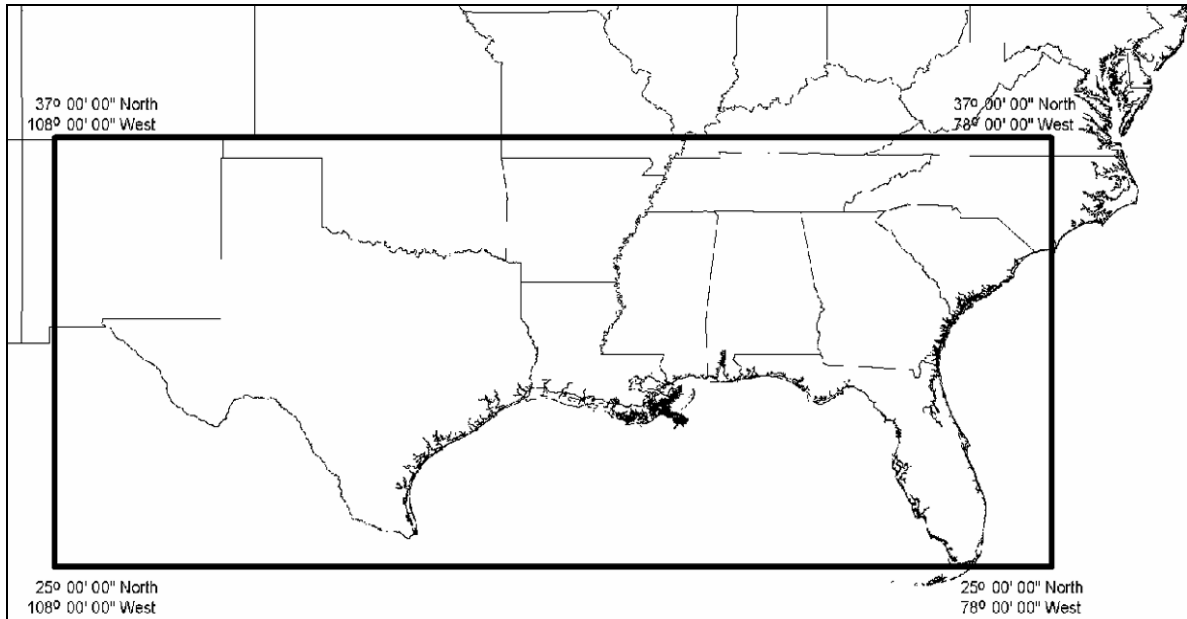
Figure 3.4 **Scatterplot of seasonal temperature and precipitation predictions by an ensemble of GCMs for the Gulf Coast region in 2050 created by using the SRES A1B emissions scenario.**
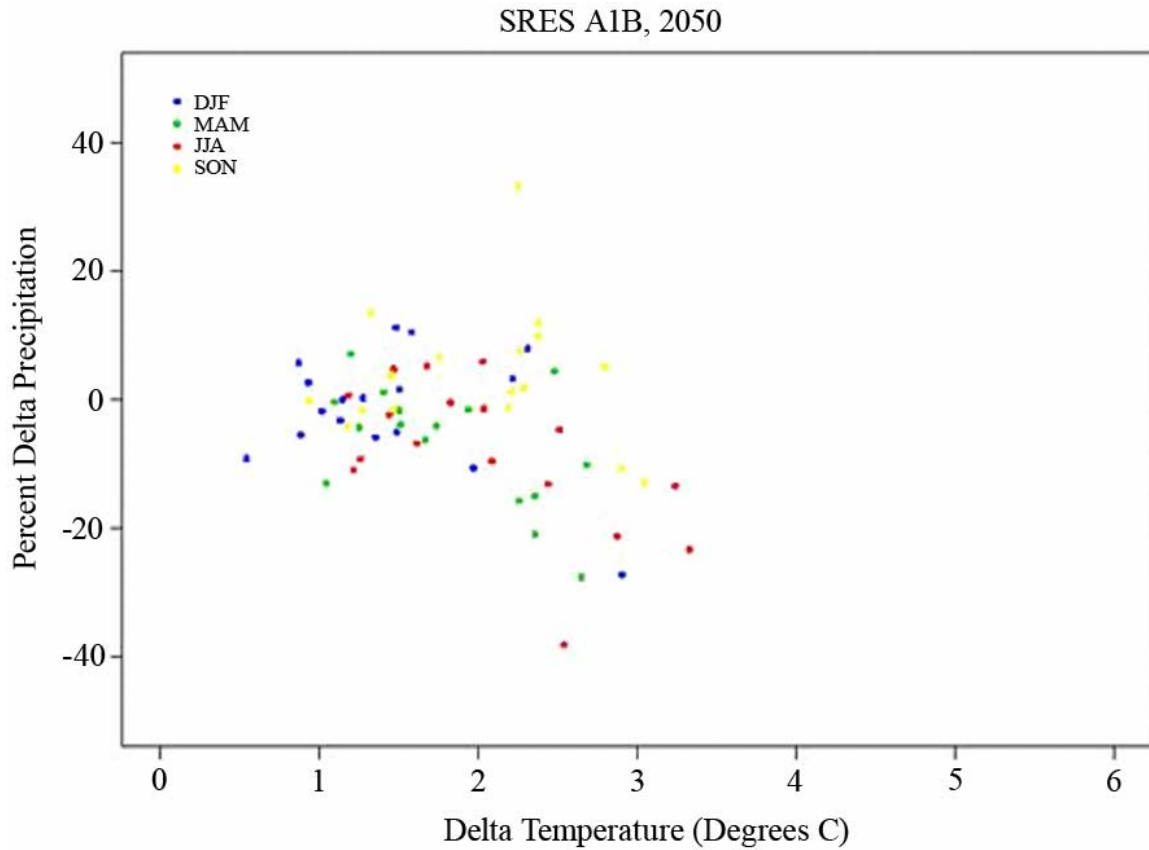
Figure 3.5   Temperature variability from 1905 to 2003 for the seven climate divisions making up the Gulf Coast study area. The level of significance in long-term temperature trend within each division was determined at a≤0.05.
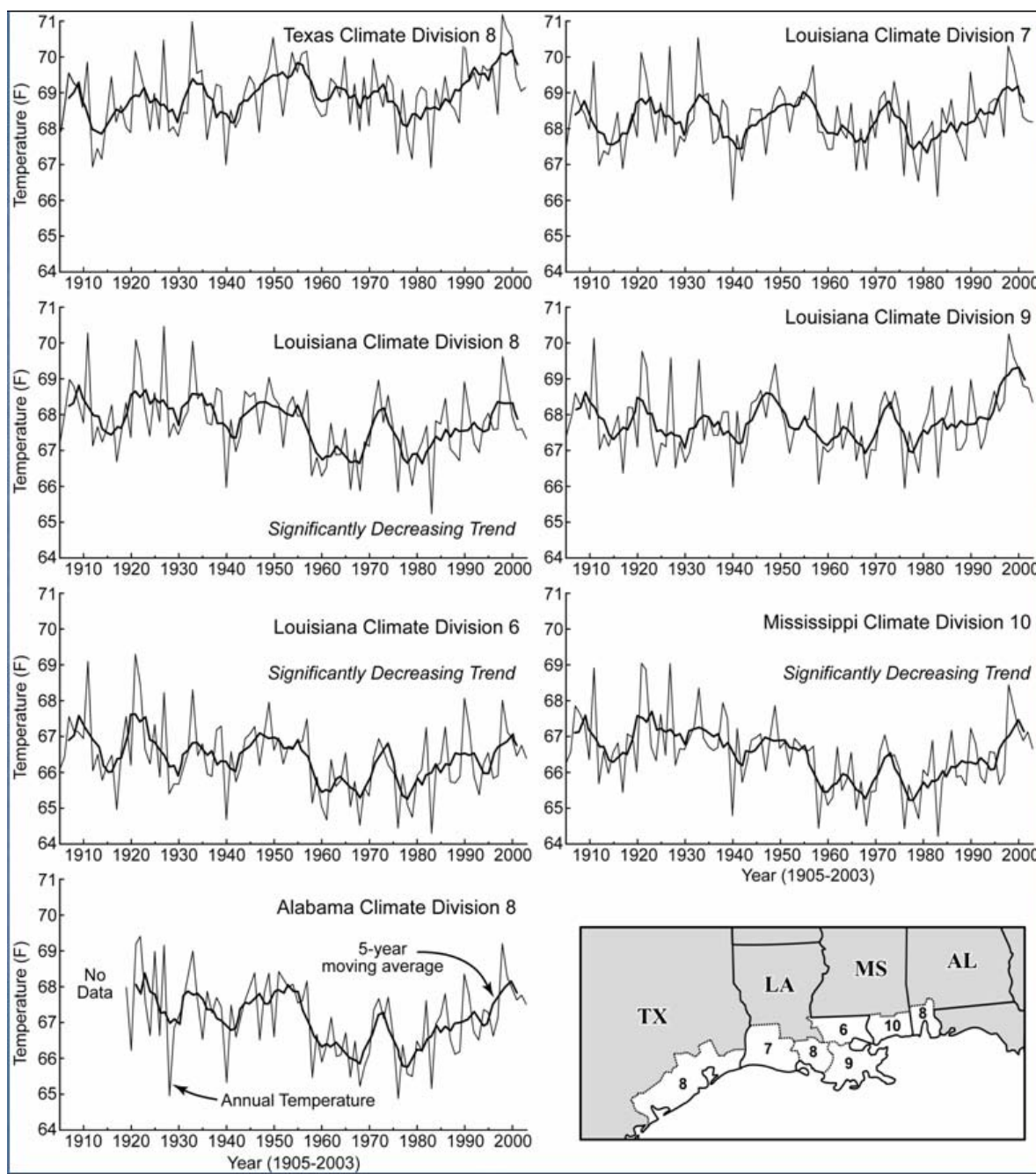
Figure 3.6   Precipitation variability from 1905 to 2003 for the seven climate divisions making up the Gulf Coast study area. The level of significance in long-term precipitation trend within each division was determined at a≤0.05.
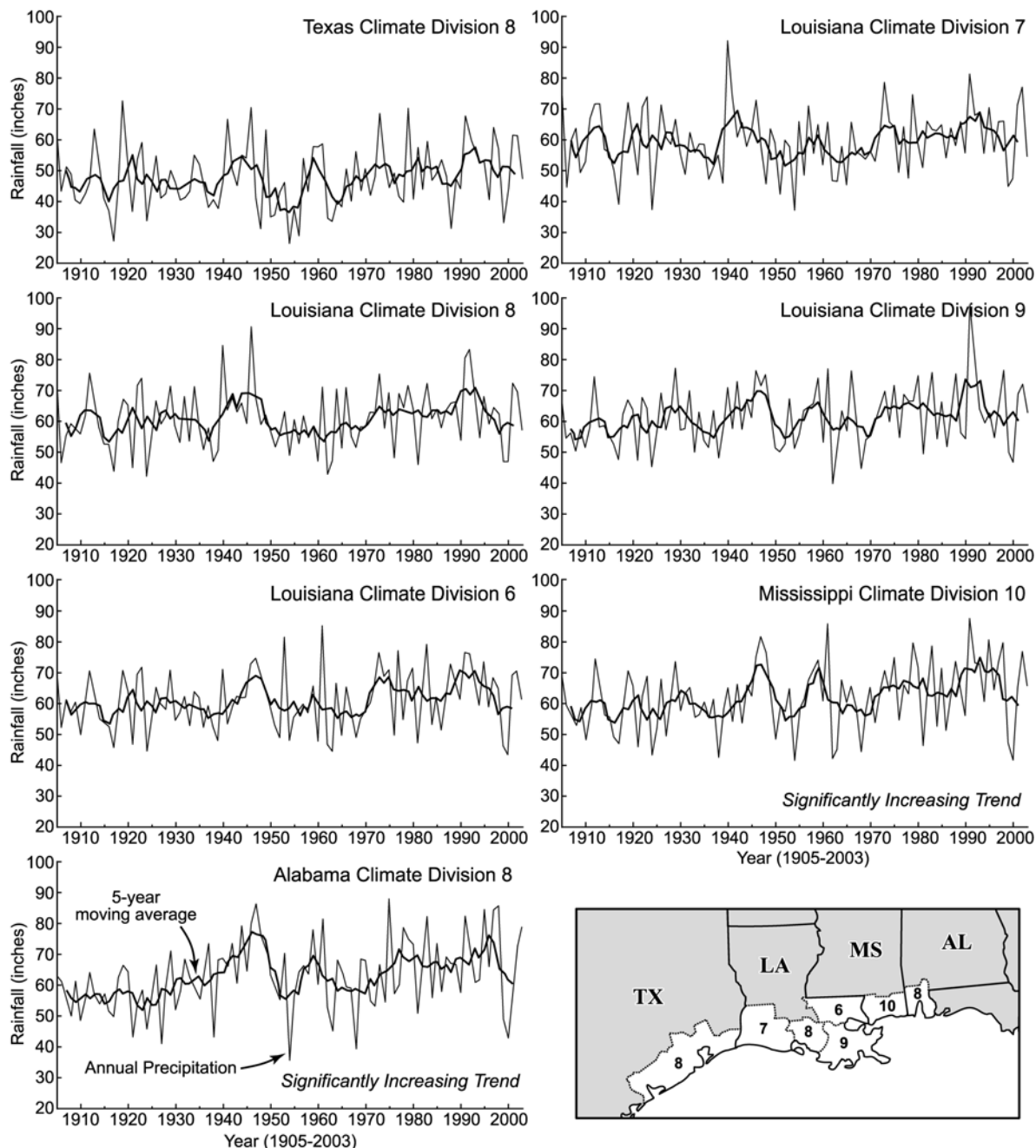
Figure 3.7   Variability and trends in model-derived surplus (runoff) and deficit from 1919 to 2003 for the Gulf Coast study area.
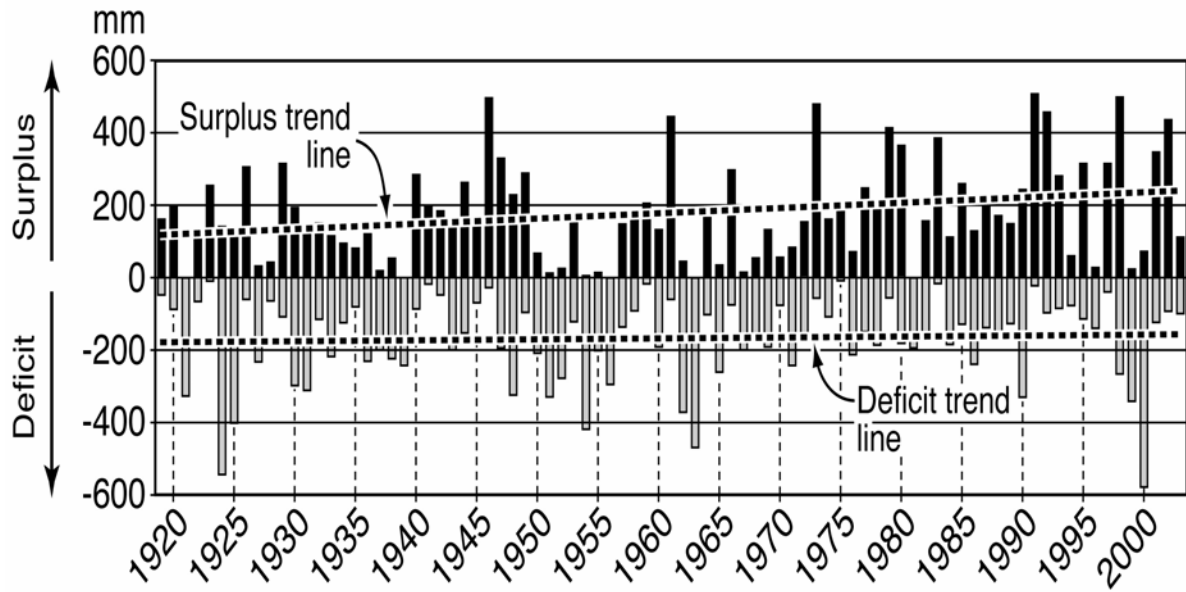
Figure 3.8   Probability density functions for seasonal temperature change in the Gulf Coast study area for 2050 created by using the A1B emissions scenario.
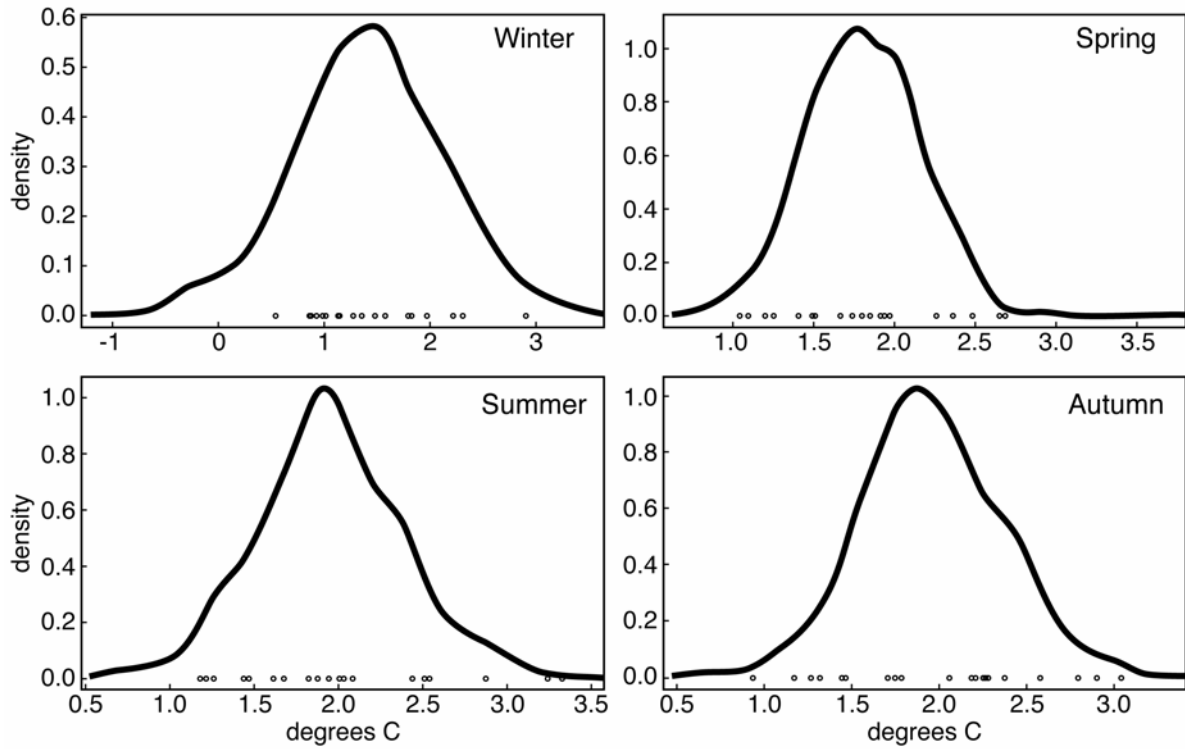
Figure 3.9   Probability density functions for seasonal precipitation change in the Gulf Coast study area for 2050 created by using the A1B emissions scenario.
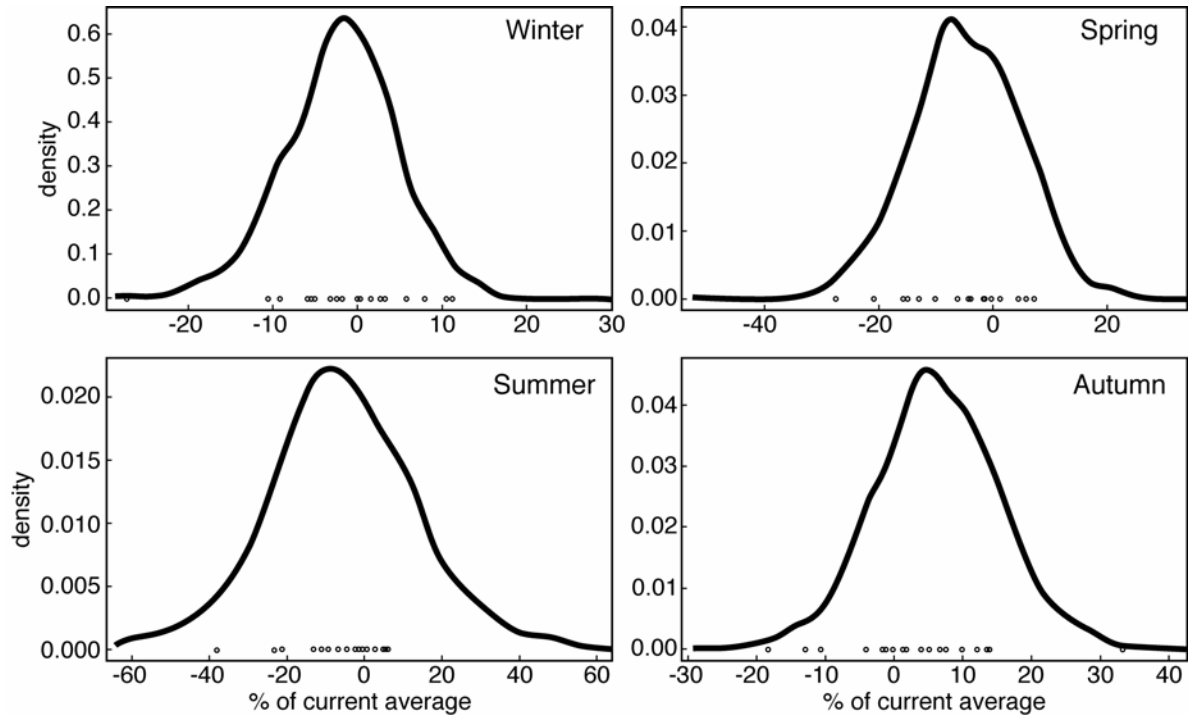
Figure 3.10   Quantile estimates of monthly precipitation for the 2- to 100-year return period generated by using the 1971 to 2000 baseline period relative to GCM output for the A1B emissions scenario at the 5, 50, and 95 percent quartiles.
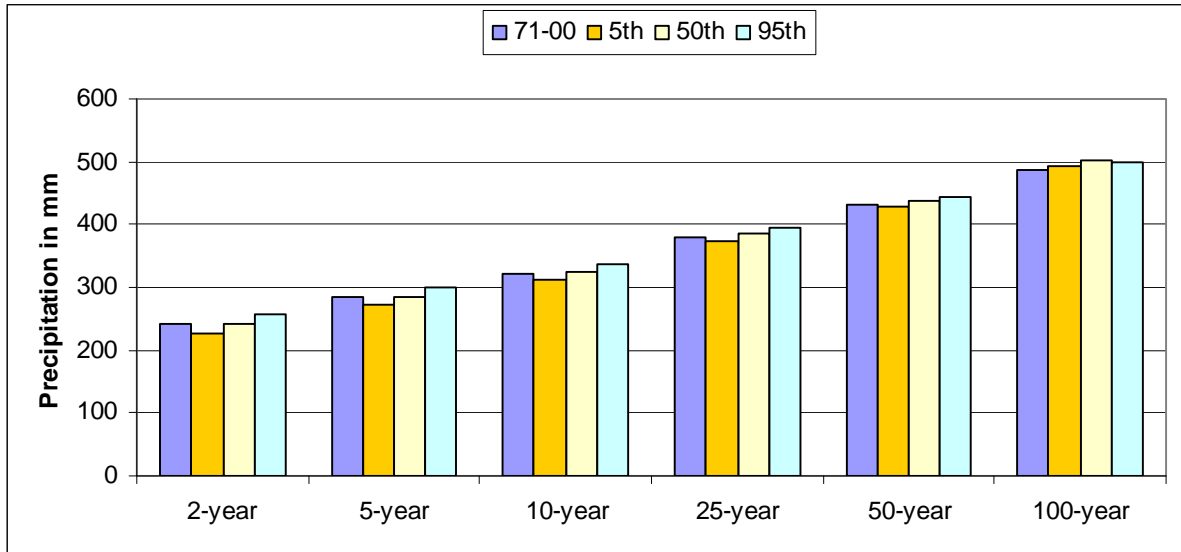
Figure 3.11 Quantile estimates of monthly average runoff for the 2- to 100-year return period generated by using the 1971 to 2000 baseline period relative to GCM output for the A1B emissions scenario at the 5, 50, and 95 percent quartiles.
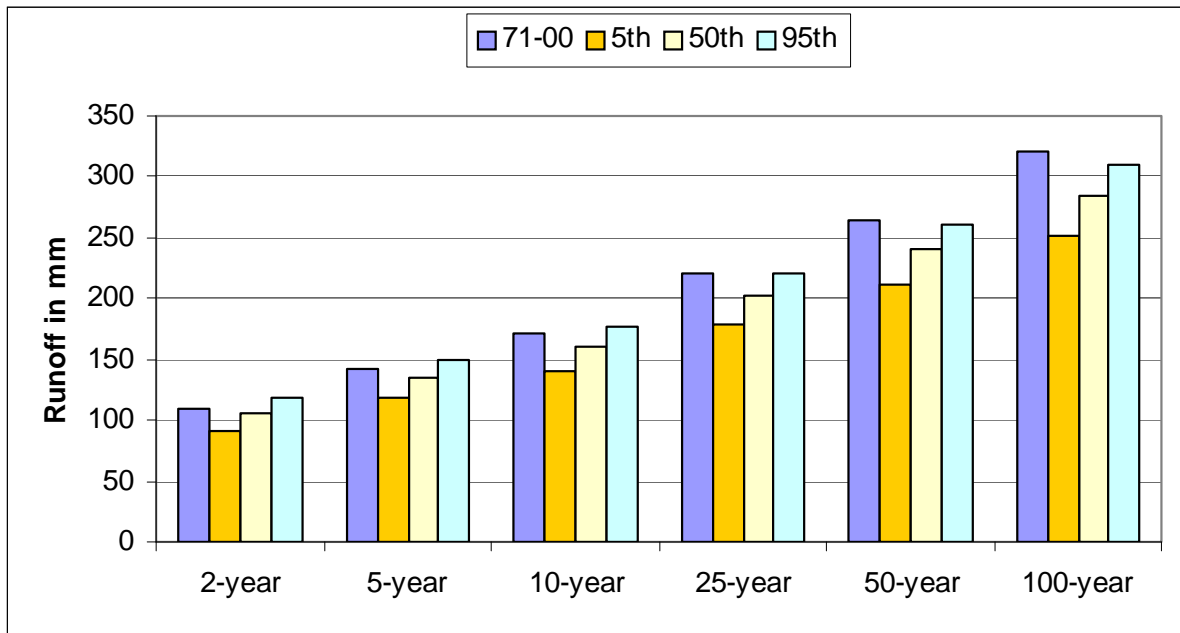
Figure 3.12   Quantile estimates of monthly average deficit for the 2- to 100-year return period generated by using the 1971 to 2000 baseline period relative to GCM output for the A1B emissions scenario at the 5, 50, and 95 percent quartiles.
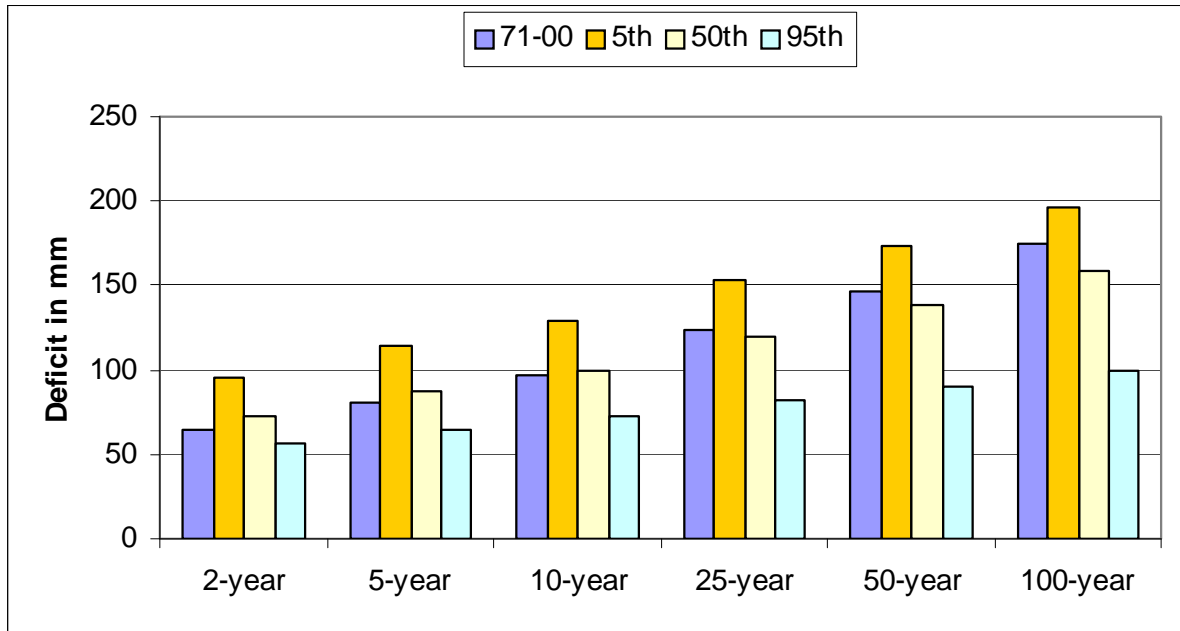
Figure 3.13   The change in the warmest 10 percent of July maximum and minimum temperatures at each station across the entire United States, for 1950-2004. Note that the number of days above the 90th percentile in minimum temperature is rising faster than it is in maximum temperature.
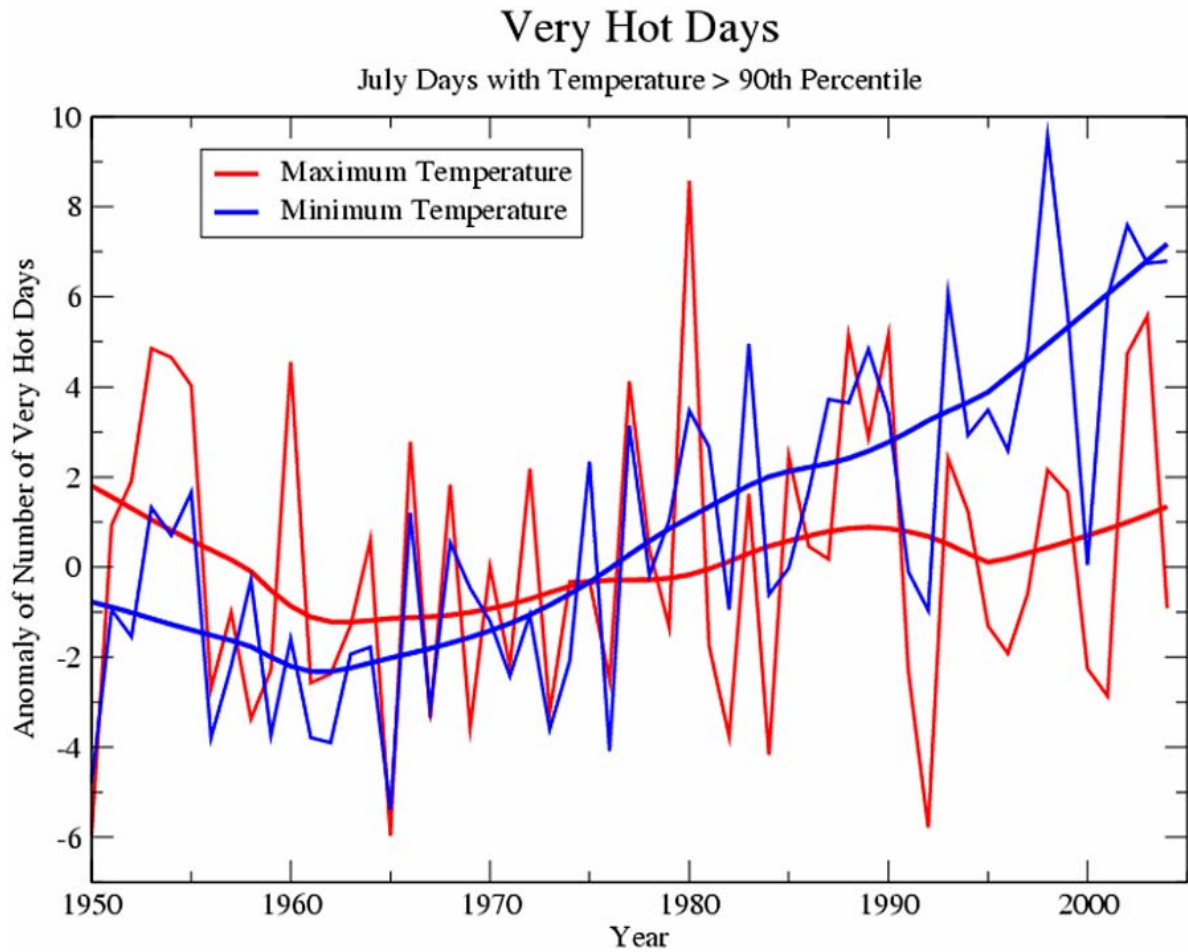
Figure 3.14   Historical time series from stations within 500 km of Dallas, TX, showing anomalies of the number of days above 37.7 °C (100 °F), for 1950-2004.
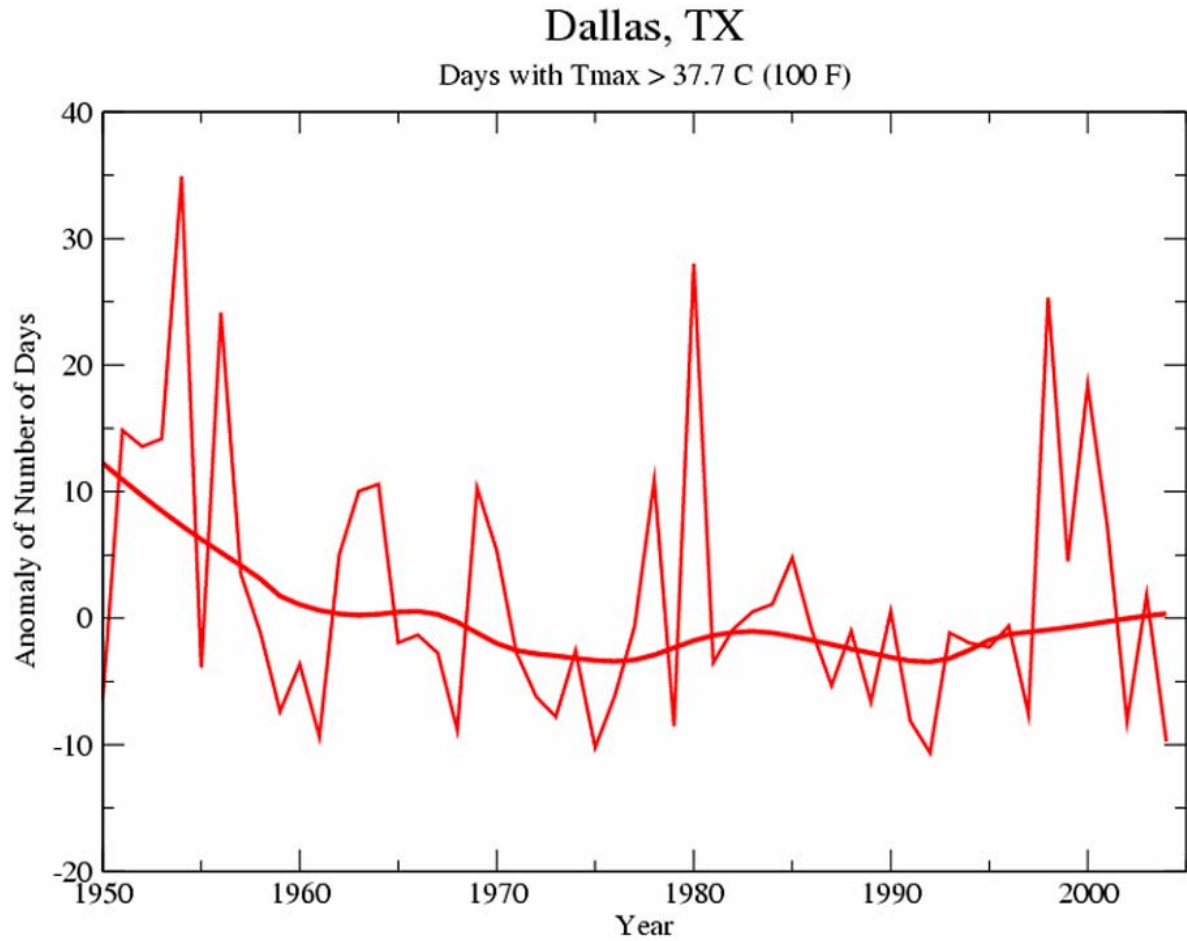
Figure 3.15   The current and future probabilities of having 1 to 20 days during the summer at or above 37.8 °C (100 °F) in or near Houston, TX, under the A2 emissions scenario.
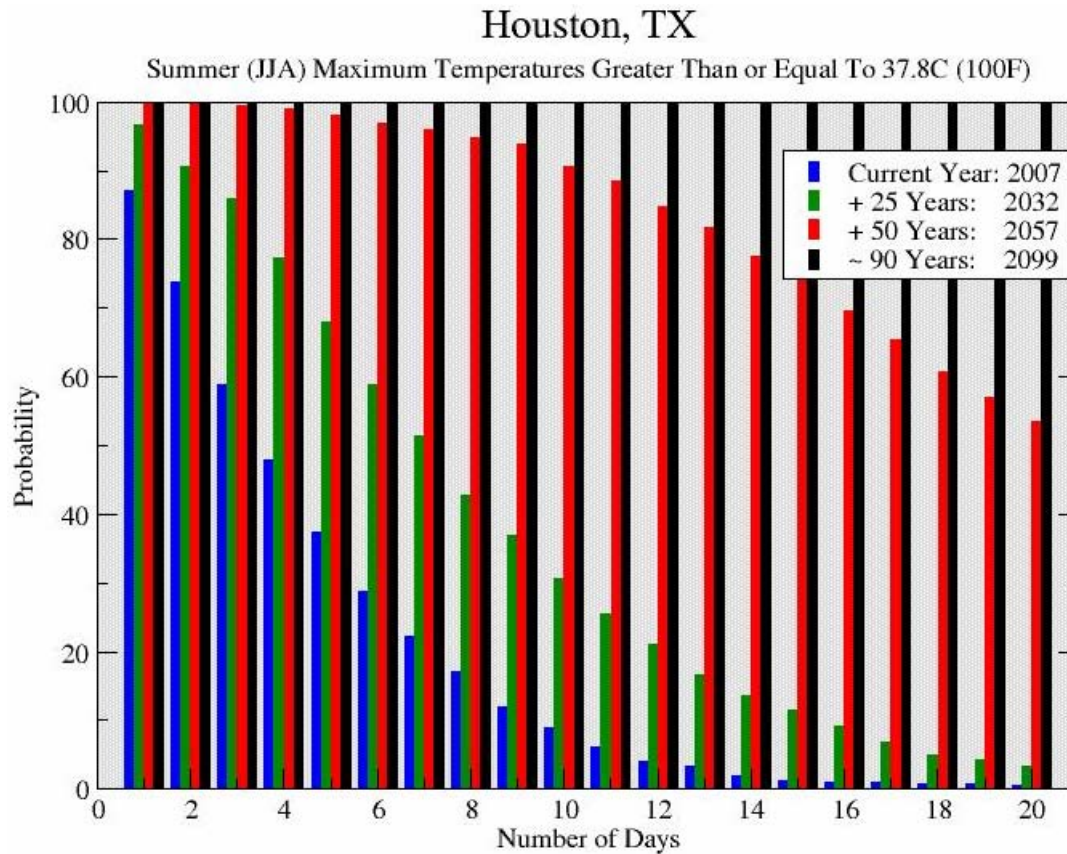
Figure 3.16 Mean model predicted change (°C) of the 20-year return value of the annual maximum daily averaged surface air temperature under the A1B emissions scenario in the Gulf States region. This analysis compares the 1990-1999 period to the 2090-2099 period.
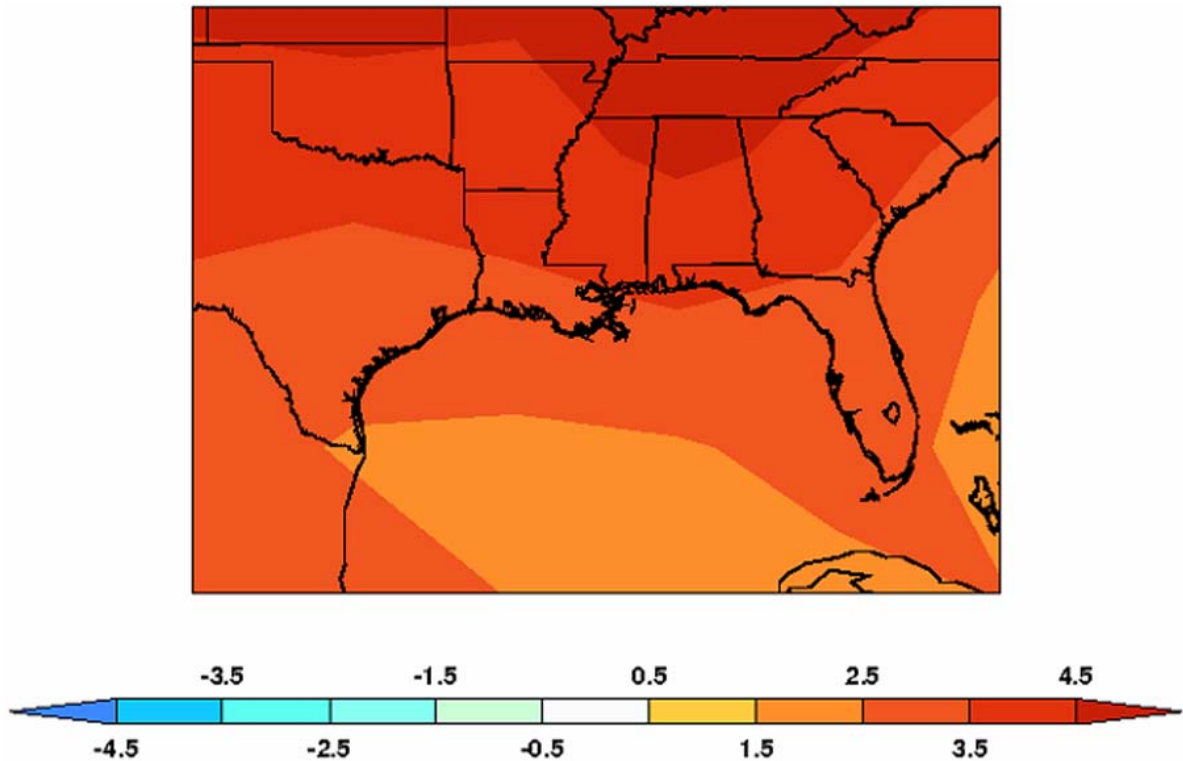
Figure 3.17 **Number of times on average, over a 20-year period, that the 1990-1999 annual maximum daily averaged surface air temperature 20-year return value levels would be reached under the SRES A1B 2090-2099 forcing conditions. Under 1990-1999 forcing conditions, this value is defined to be one.**
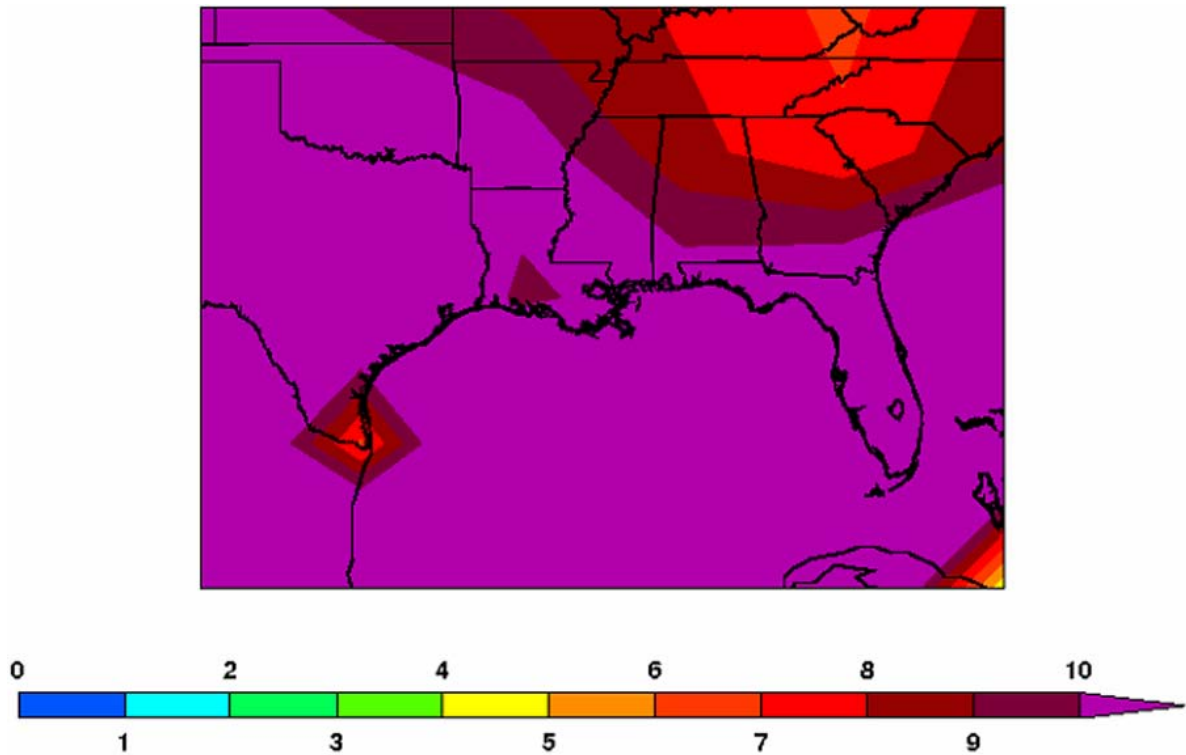
Figure 3.18   Mean model-predicted fractional change of the 20-year return value of the annual maximum daily averaged precipitation under the SRES A1B in the Gulf States region. This analysis compares the 1990-1999 period to the 2090-2099 period.
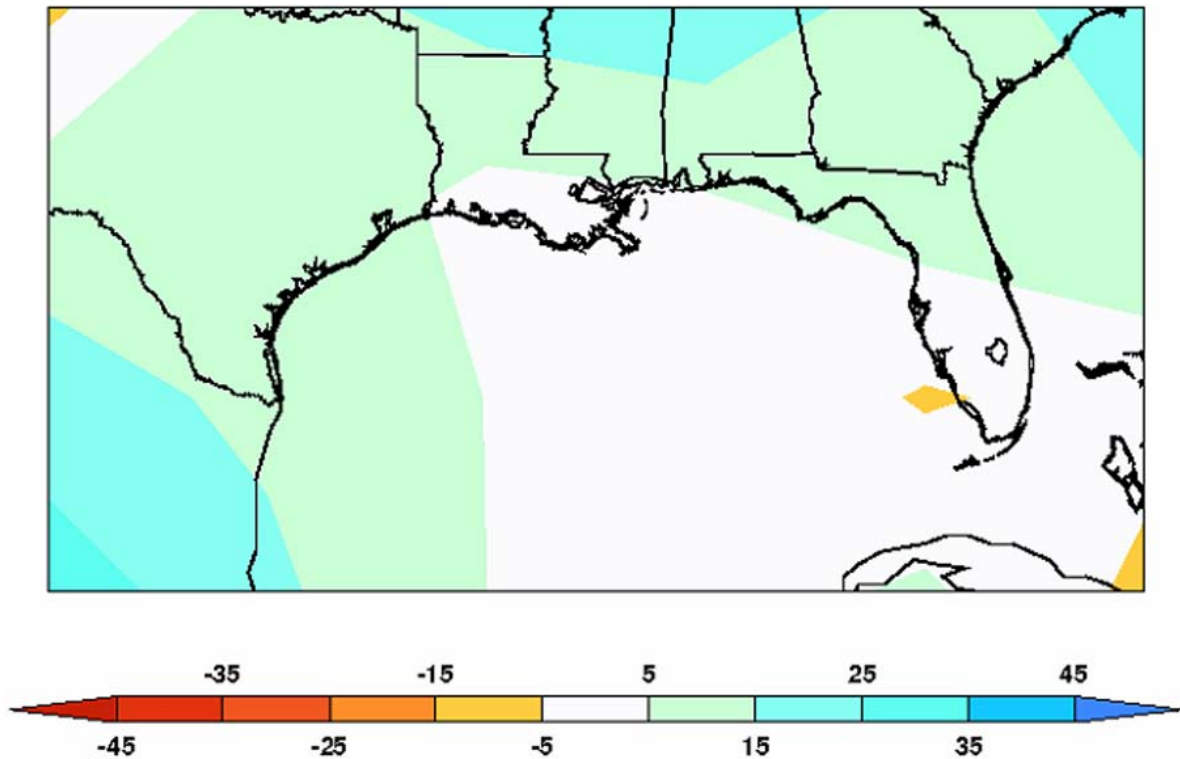
Figure 3.19   Geographic distribution of hurricane landfalls along the Atlantic and Gulf Coast regions of the United States, from 1950 to 2006. (Source: NOAA, National Climate Data Center, Asheville, NC)
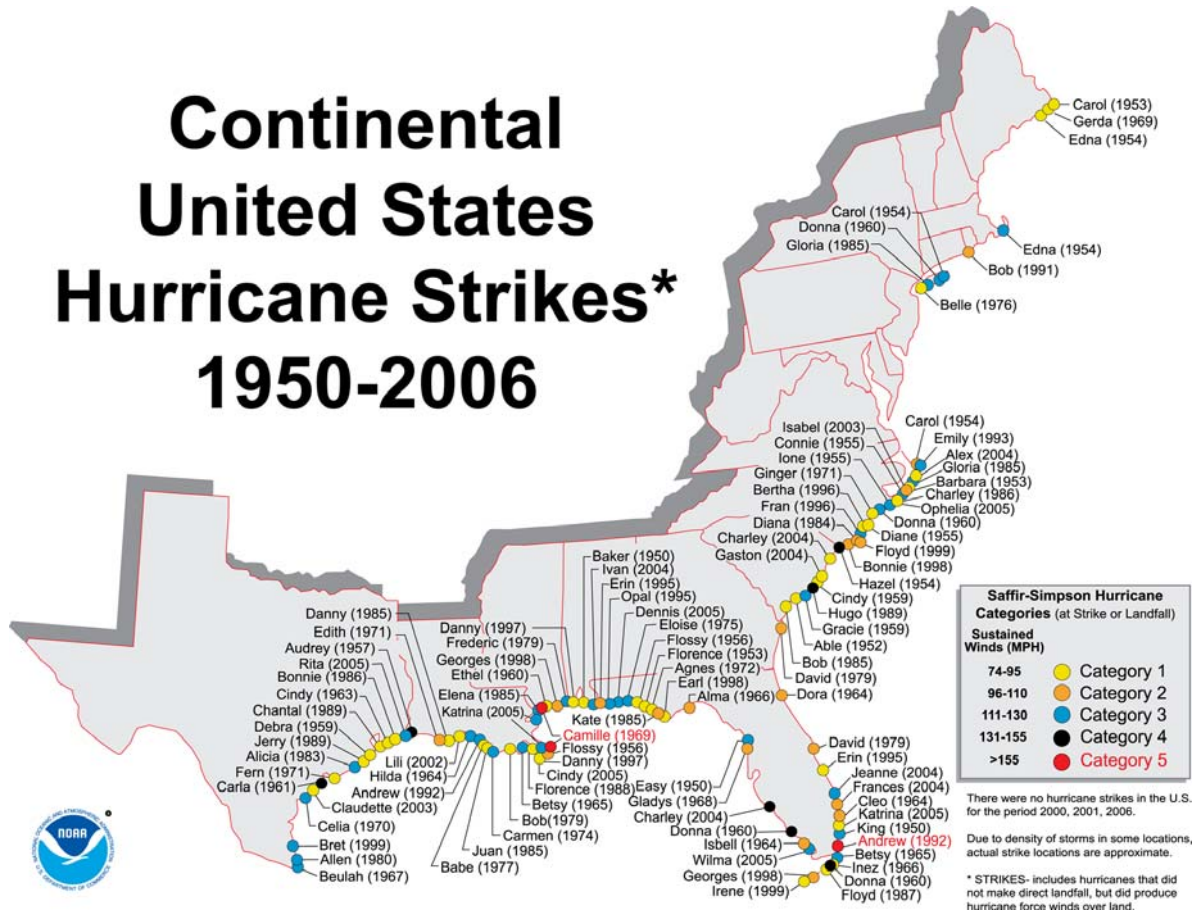
Figure 3.20   Frequency histogram of landfalling storms of tropical storm strength or greater in Grand Isle, LA, summarized on a 5-year basis, for the period 1851-2005. (Source: NOAA National Hurricane Research Division)
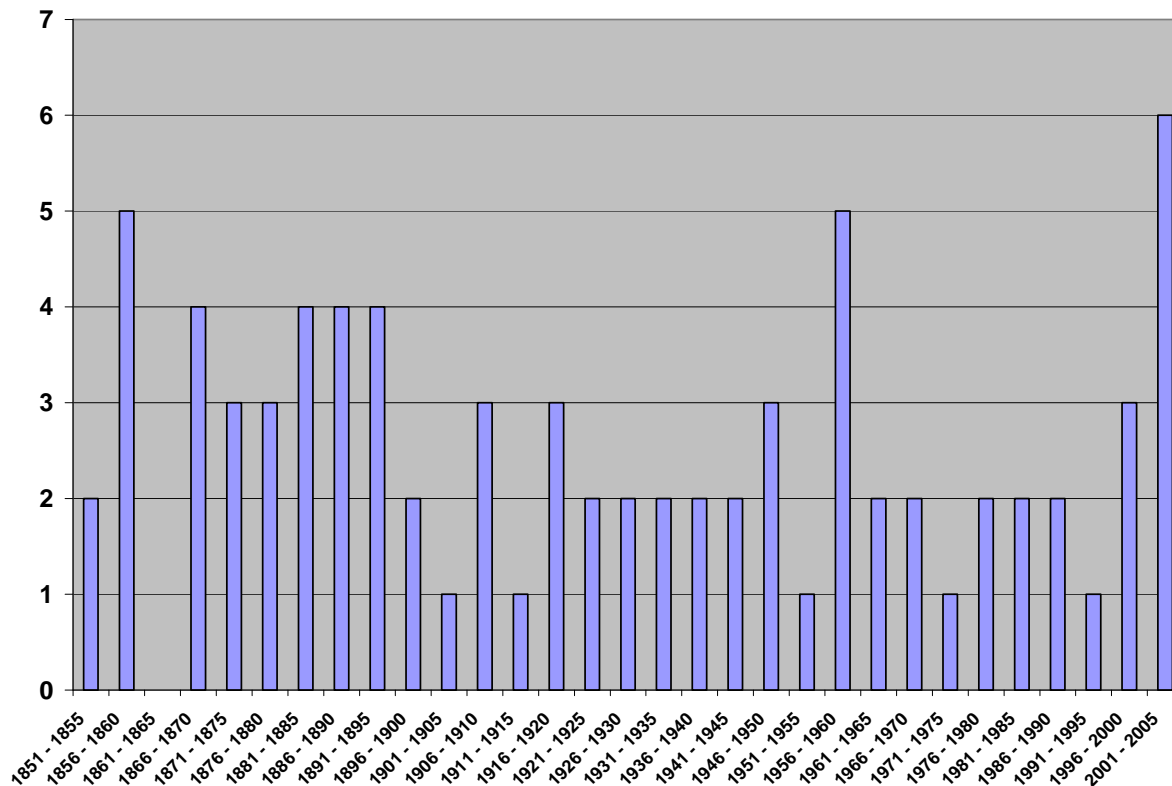
Figure 3.21 Hemispherical and global mean sea surface temperatures for the period of record from 1855 to 2000. (Source: NOAA, National Climate Data Center, Asheville, NC)
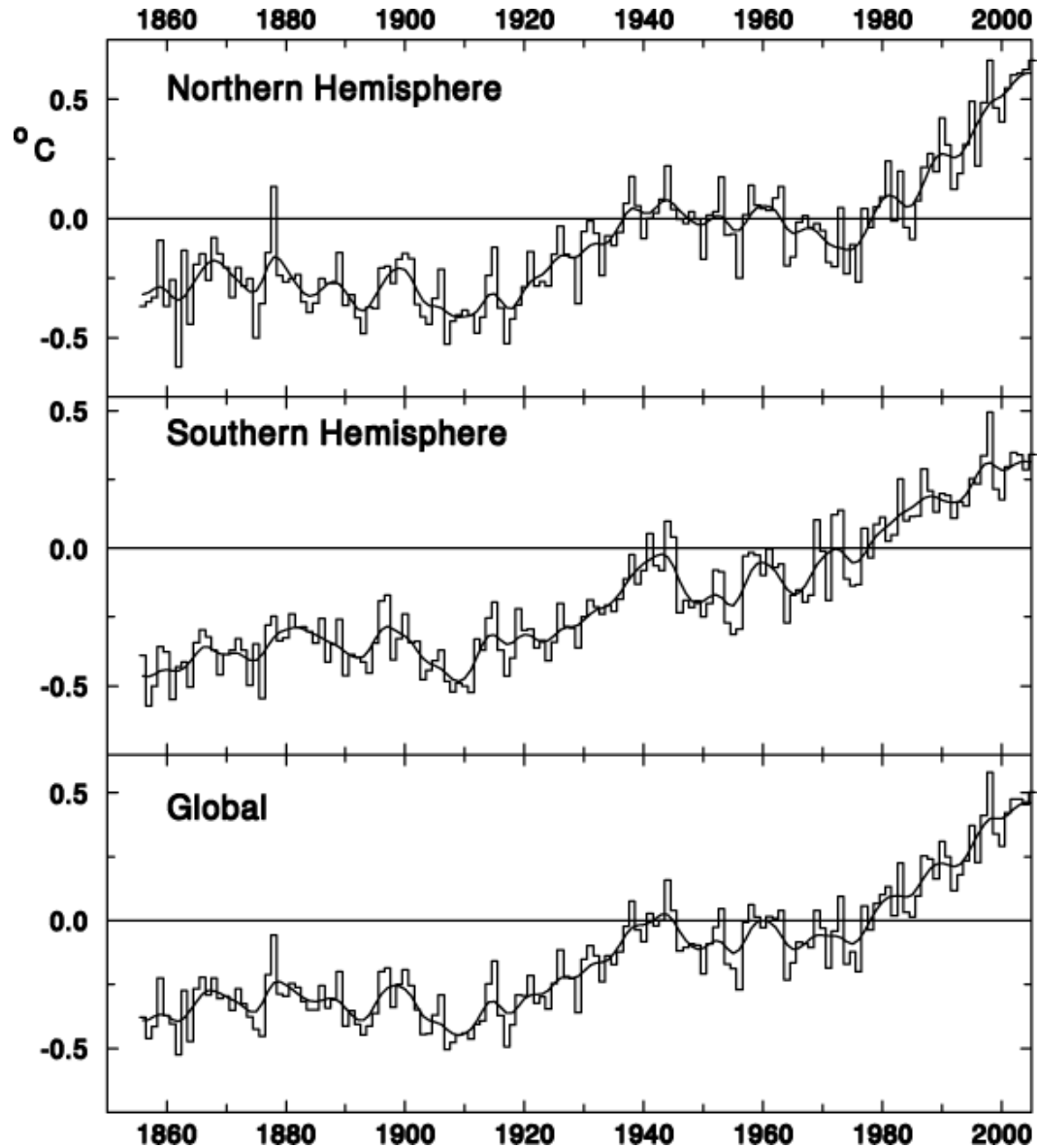
Figure 3.22 Sea surface temperature trend in the main hurricane development region of the North Atlantic during the past century. Red line shows the corresponding 5-yr running mean. Anomalies are departures from the 1971–2000 period monthly means. (Source: Bell et al., 2007)
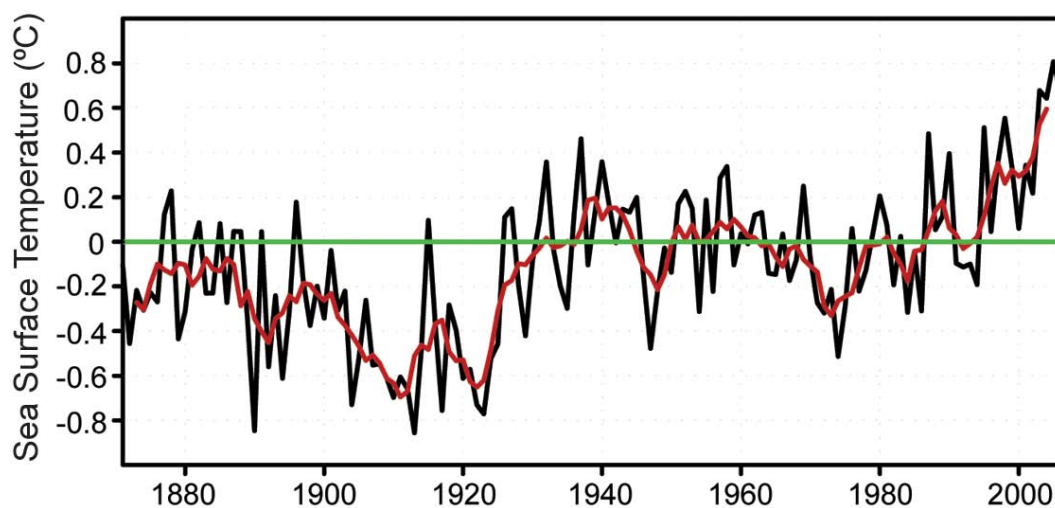
Figure 3.23   Sea surface temperature trends in the Gulf of Mexico region produced by using the ERSST v.2 database. The plot includes the SST anomalies averaged annually, as well as the anomalies determined from the averages for August only and the July-September peak of the hurricane season. (Source: Smith and Reynolds, 2004)
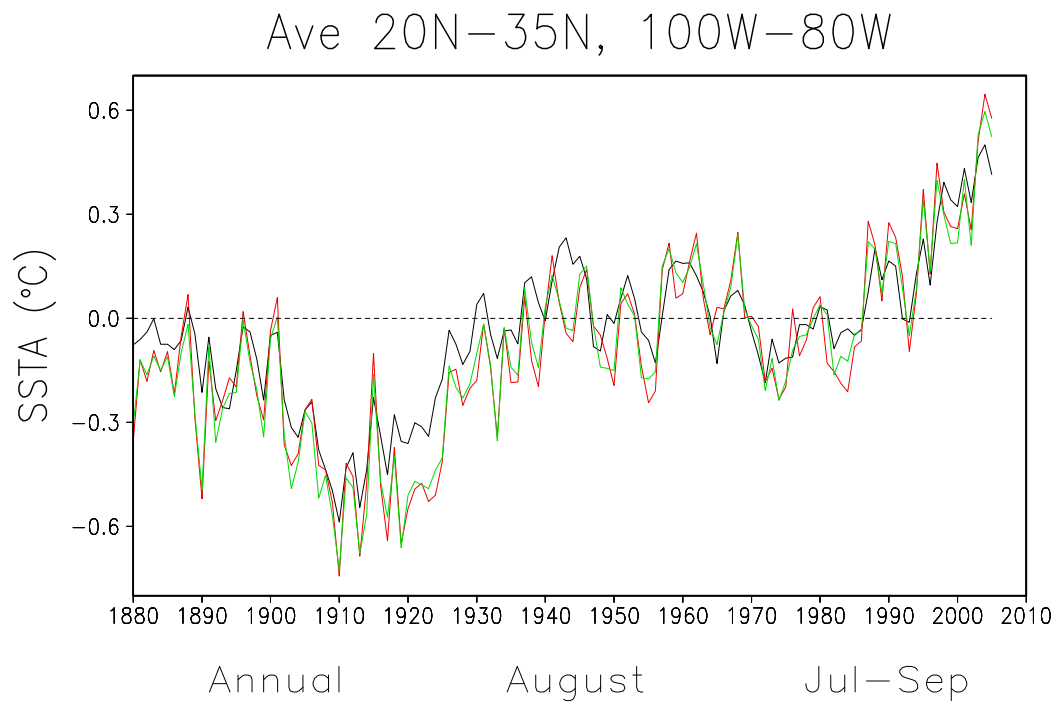
ERSST v.2: Extended Reconstructed Sea Surface Temperatures, version 2.

Figure 3.24 **The location and intensity of Hurricane Katrina at intervals of 6 hours show two intensification events. Circles indicate data from National Hurricane Center advisories showing storm intensity (TS and TD stand for tropical storm and tropical depression, respectively): (a) Intensification is not correlated with sea surface temperature (from POES high-resolution infrared data); (b) In contrast, the intensifications correlate well with highs in the ocean dynamic topography (from Jason 1,TOPEX, Envisat, and GFO sea surface height data). The Loop Current can be seen entering the Gulf south of Cuba and exiting south of Florida; the warm-core ring (WCR) is the prominent high shedding from the Loop Current in the center of the Gulf. (Source: Scharroo et al., 2005)**
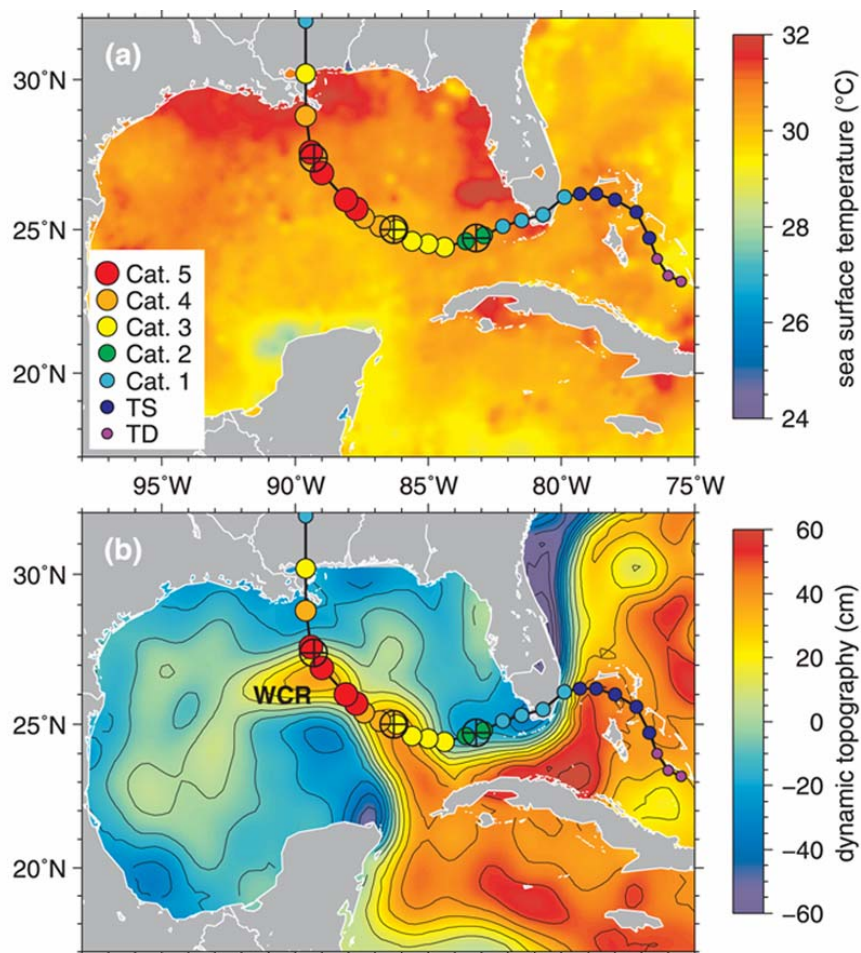
Envisat: An advanced polar-orbiting Earth observation satellite of the European Space Agency that \provides measurements of the atmosphere, ocean, land, and ice

GFO: Satellite program of U.S. Navy GEOSAT Follow-On (GFO) program to maintain continuous ocean observations

Jason-1: NASA satellite monitoring global ocean circulation

POES: Polar Observational Environmental Satellite

TOPEX: TOPEX/Poseidon is a CNES and NASA satellite monitoring ocean surface topography.

Figure 3.25   Frequency histogram of tropical storm events for coastal cities across the Gulf of Mexico region of the United States over the period of record from 1851 to 2006.
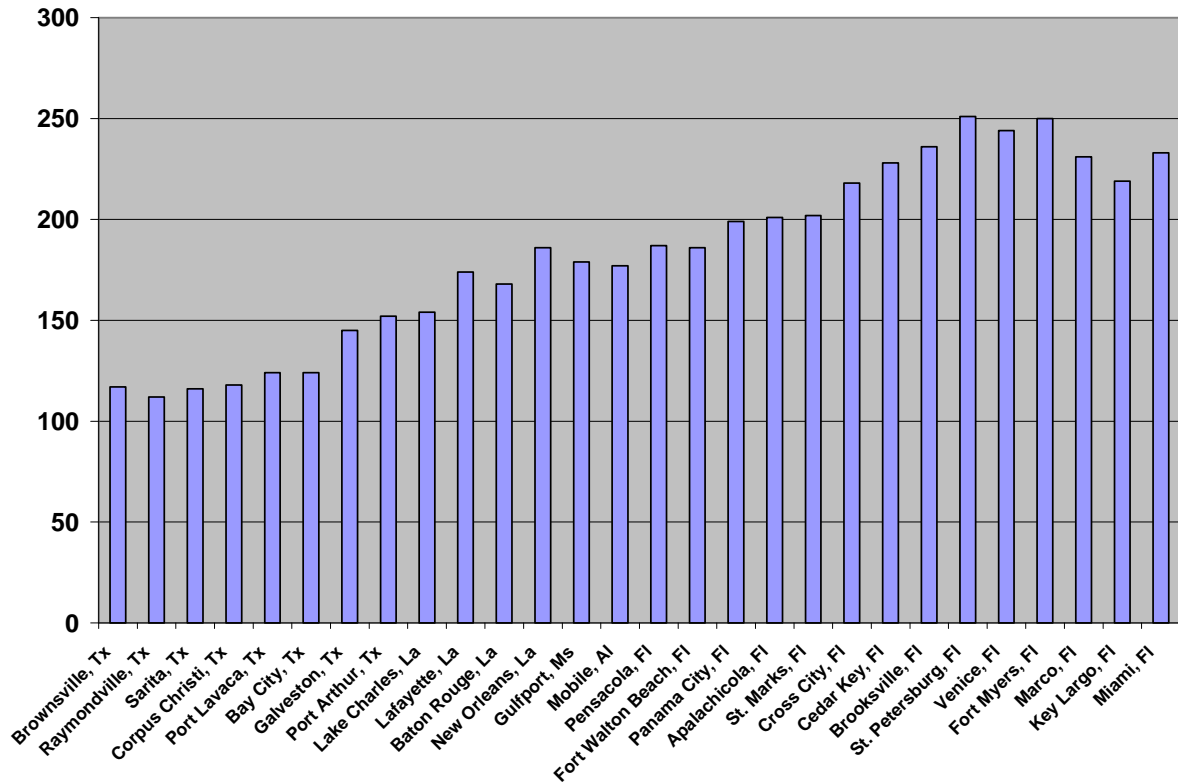
Figure 3.26 Frequency analysis of storm events exhibiting Category 1, 2, and 3 winds or higher across the Gulf Coast study area.
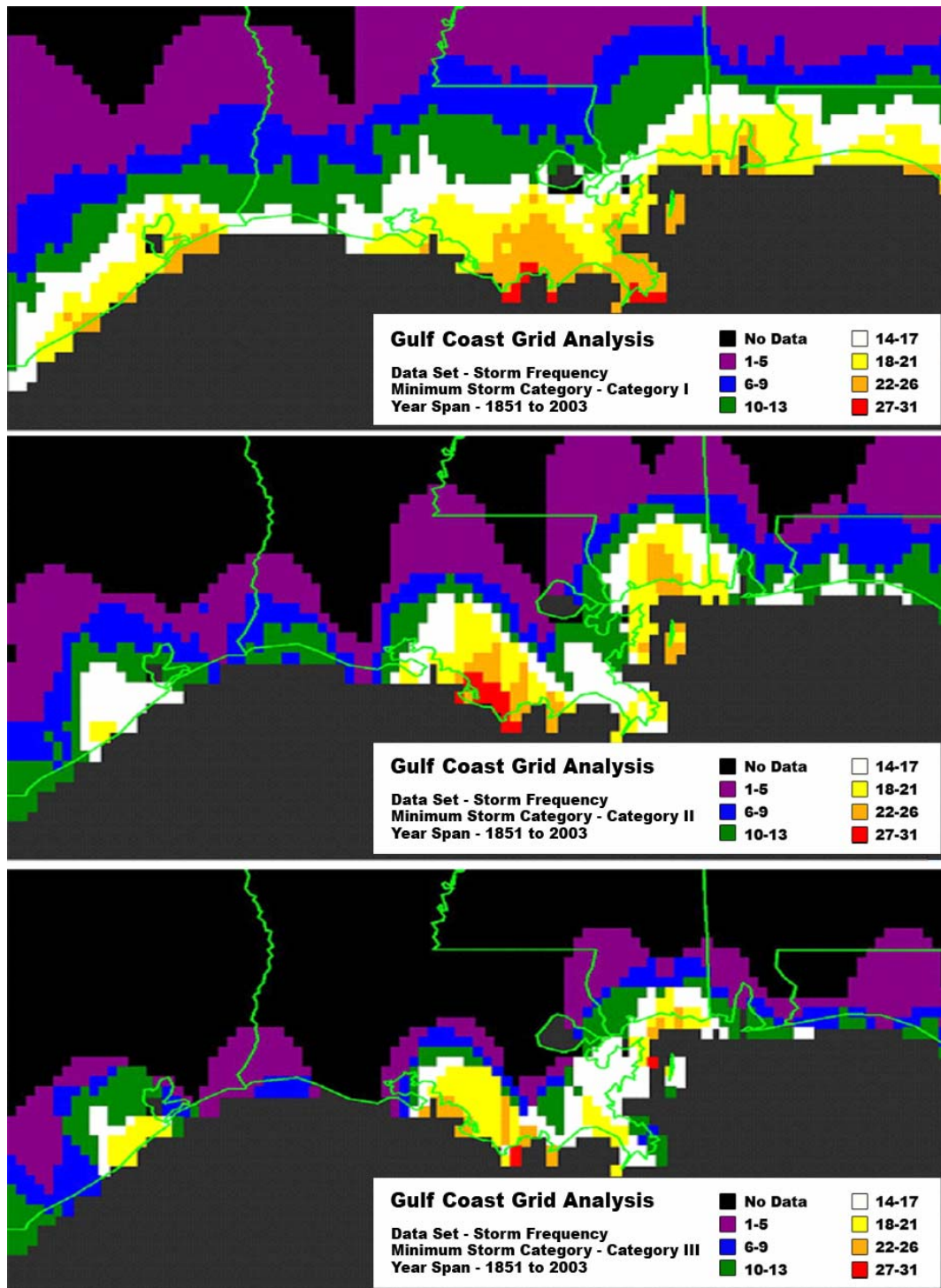
Figure 3.27 Latitudinal gradient of declining storm frequency of Category 1 hurricanes or greater from Grand Isle, LA, inland, illustrating the reduction of storm strength over land away from the coast, for the period 1951-2000.
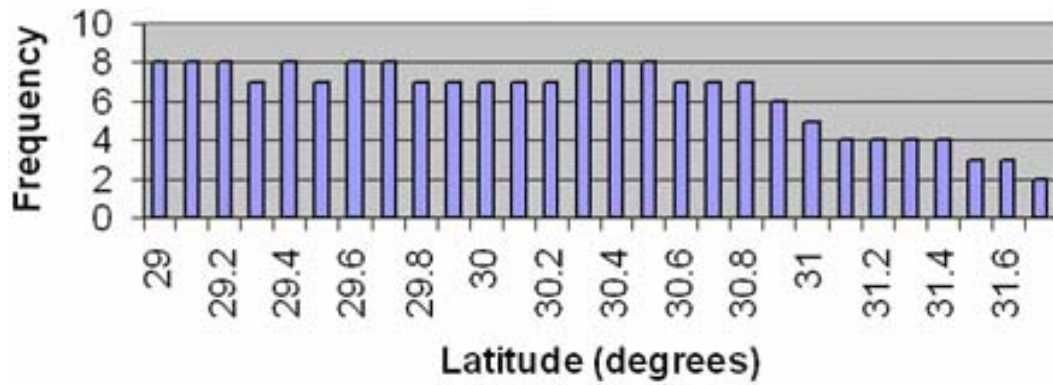
Figure 3.28 Storm frequency variation for 15-, 30-, and 50-year intervals for Category 1 storms or greater for the most active grid location across the Gulf Coast study region.
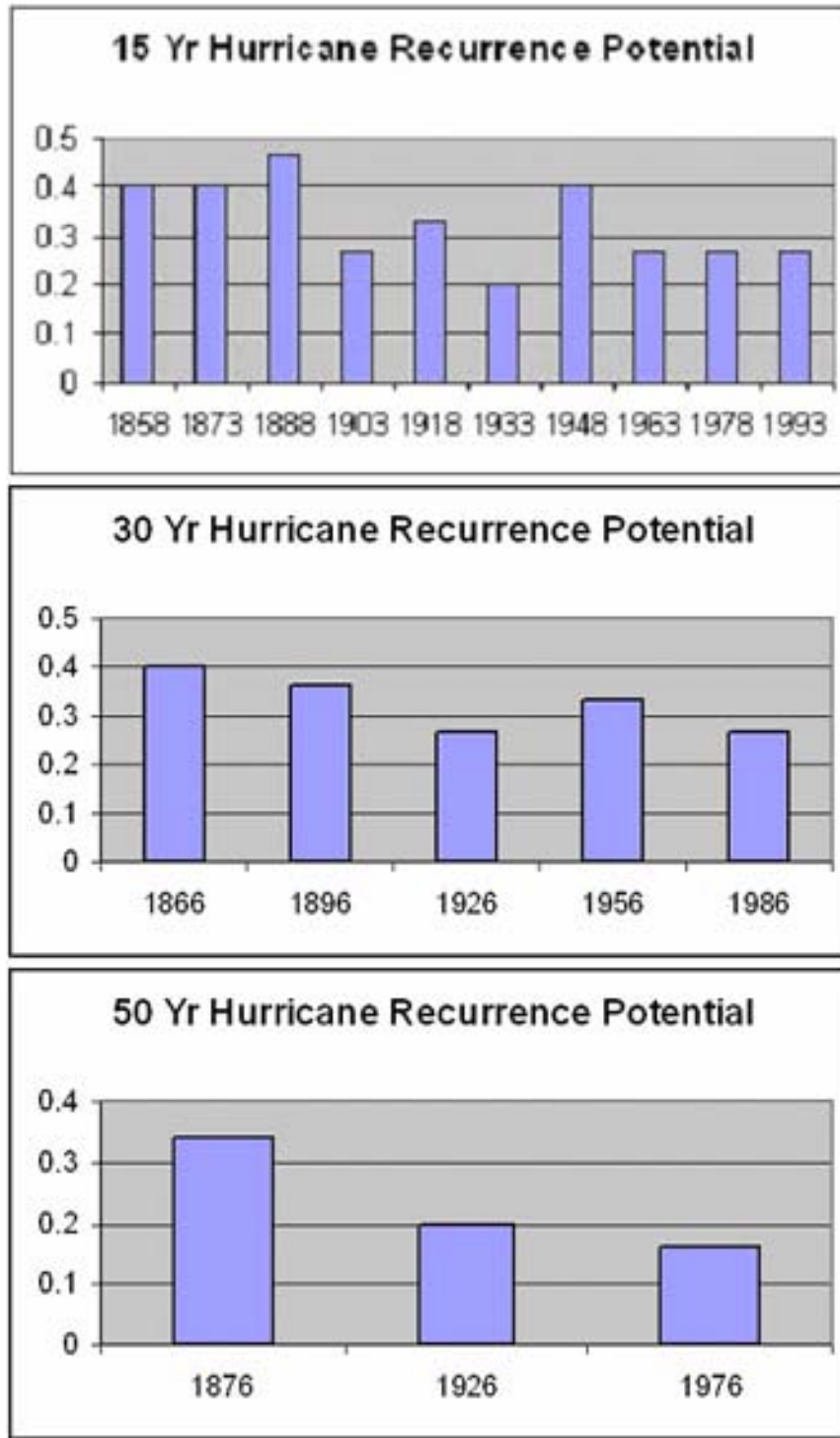
Figure 3.29 Simulated wind rows and direction of wind force derived from the HURASIM model for one of the most active grid cell locations in the study area at Grand Isle, LA, for tropical storm and hurricane conditions over the 153-year period of record, 1851 - 2003.
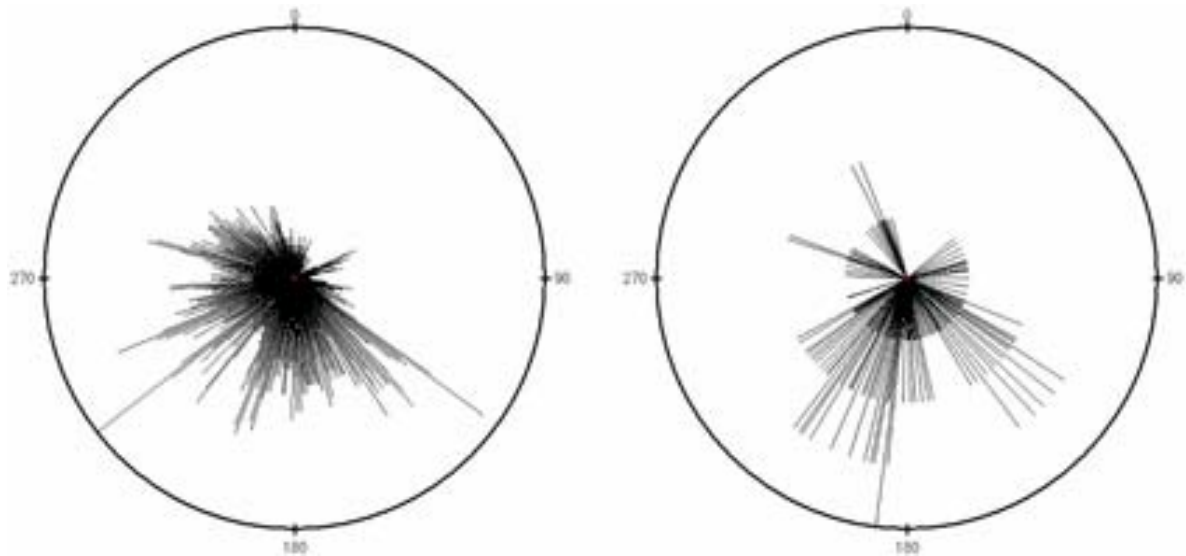
Figure 3.30   Potential increase in the number of hurricanes by the years 2050 and 2100, assuming an increase in hurricane intensity at 5, 10, 15, and 20 percent concomitant with warming sea surface temperatures projected.
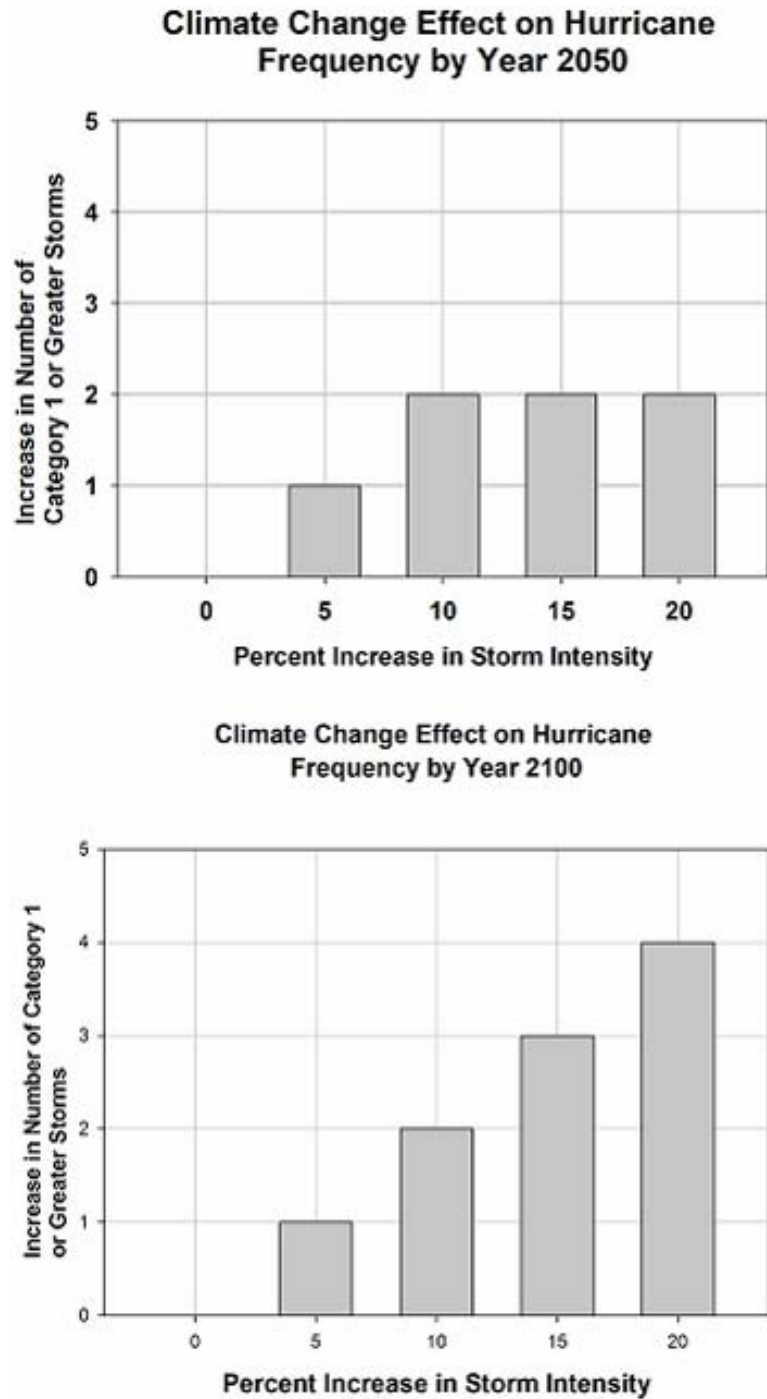
Figure 3.31 **Tide gauge records and mean sea level trend line for three northern Gulf Coast tide stations at Pensacola, FL, Grand Isle, LA, and Galveston, TX, corresponding with the eastern, central, and western coverage of the study area (1900-2000).**
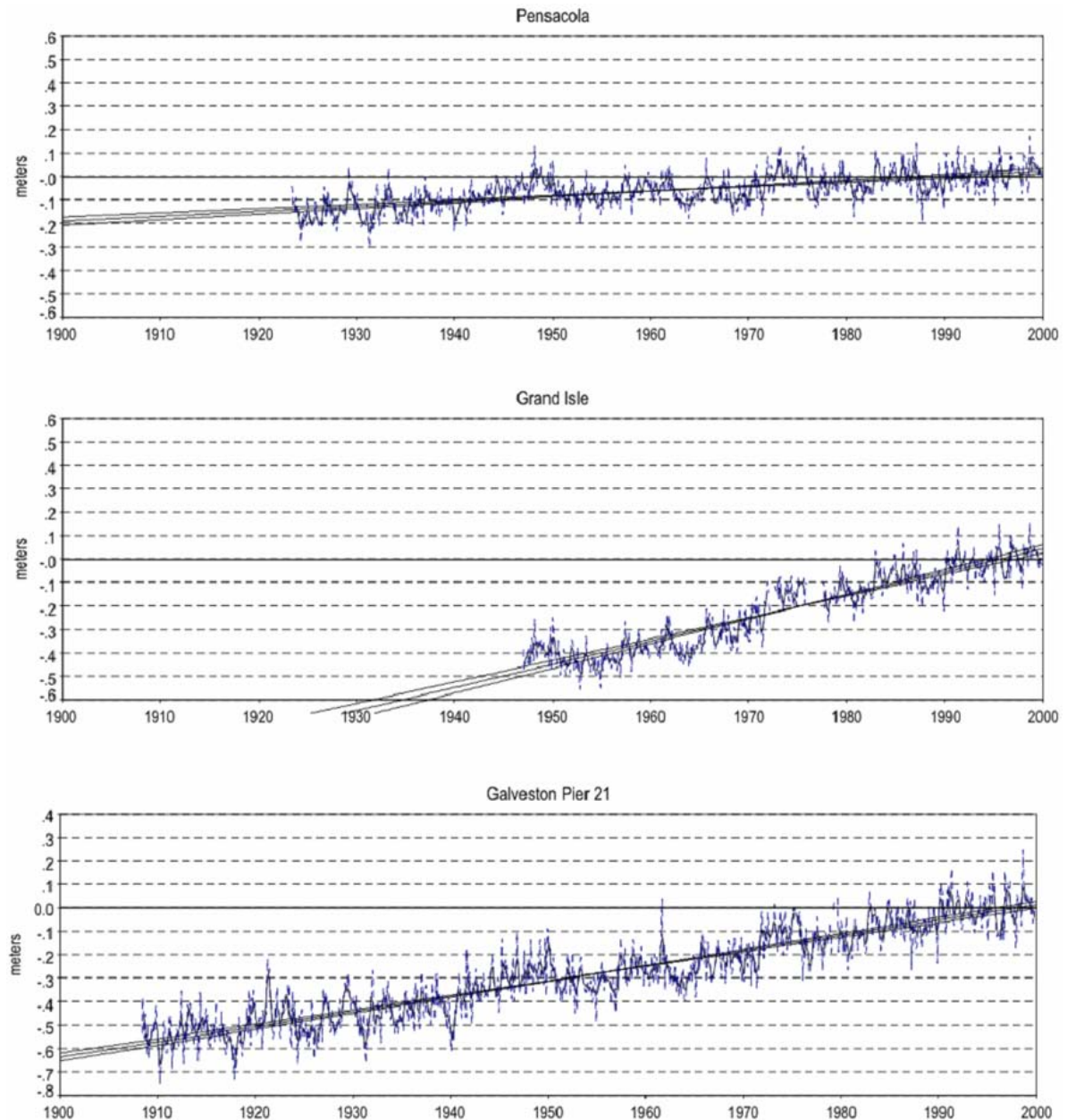
Figure 3.32   Merged results of Category 2 through 5 hurricane surge simulations of a slow-moving storm approaching from the southeast (toward northwest in database), generated by using SLOSH model simulations.
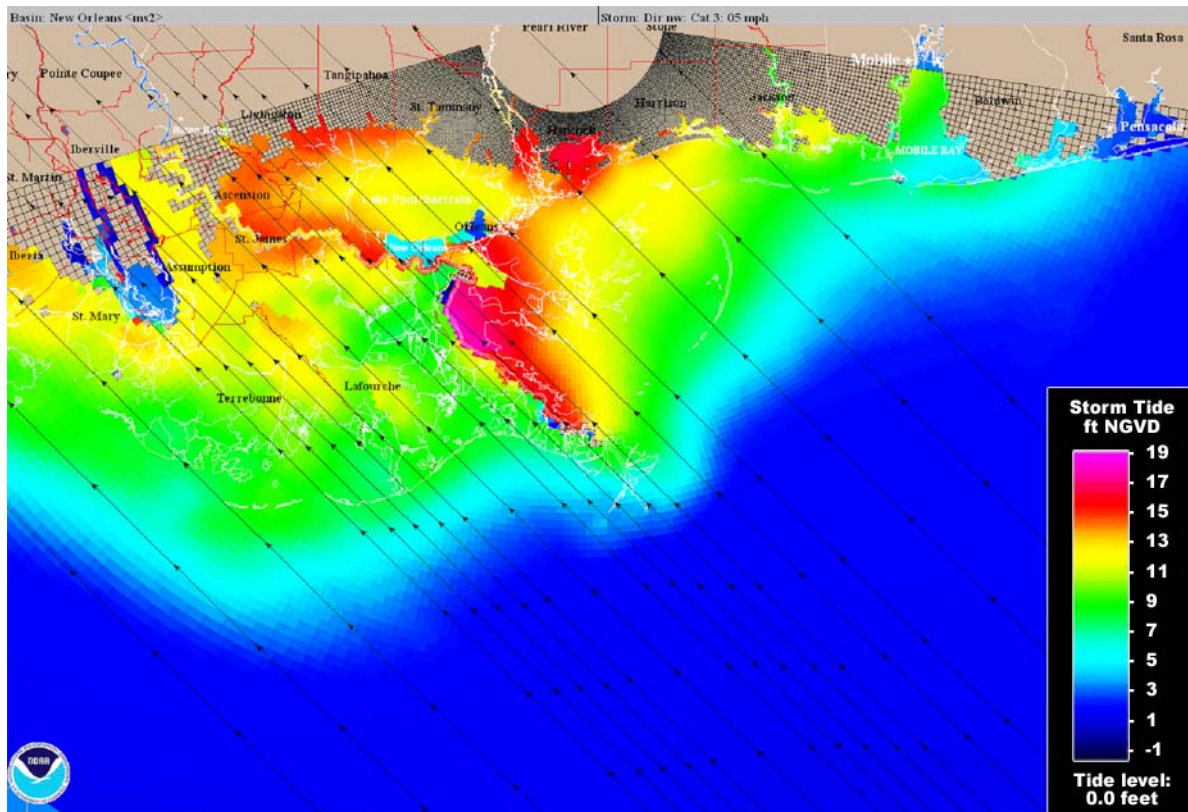
**Figure 3.33   Color schemes illustrate the difference in surge inundation
between a Category 3 and Category 5 storm approaching the
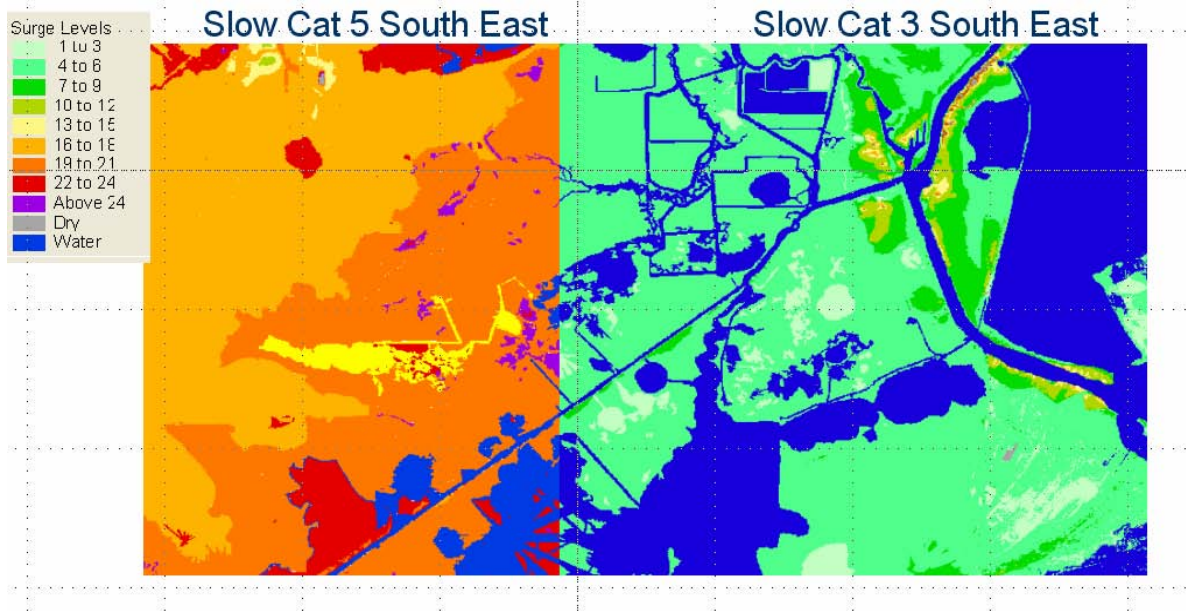southeastern Louisiana coast from the southeast.**

Figure 3.34   Comparison of lidar and National Digital Elevation Data (DEM) for eastern Cameron Parish, LA. The advantages of using a lidar-derived topography are many, particularly as the effects of climate change are likely to be subtle in the short term but significant for this low-lying coast where 1 ft of added flooding will impact a large land area.
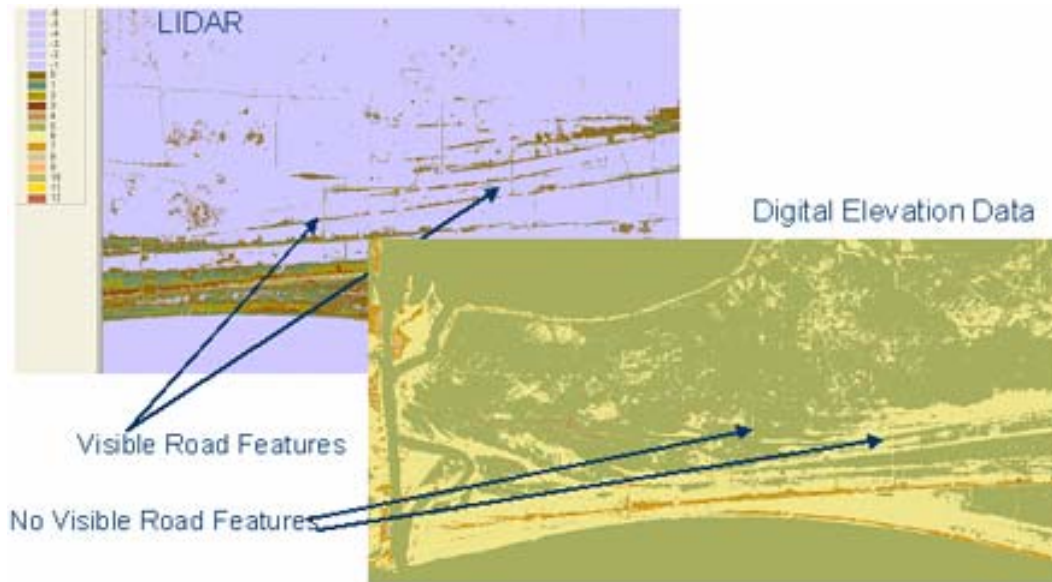
Figure 3.35 Trend in summer wave height (1978-2005) in the mid-Gulf of Mexico. (Figure source: Komar and Allan, 2008; data source: NOAA National Buoy Data Center, Stennis, MS)